Quaternary Science Reviews 29 (2010) 1679–1715

Contents lists available at ScienceDirect

Quaternary Science Reviews

journal homepage: www.elsevier.com/locate/quascirev

Temperature and precipitation history of the Arctic

G.H. Miller [a,*], J. Brigham-Grette [b], R.B. Alley [c], L. Anderson [d], H.A. Bauch [e], M.S.V. Douglas [f], M.E. Edwards [g], S.A. Elias [h], B.P. Finney [i], J.J. Fitzpatrick [d], S.V. Funder [j], T.D. Herbert [k], L.D. Hinzman [l], D.S. Kaufman [m], G.M. MacDonald [n], L. Polyak [o], A. Robock [p], M.C. Serreze [q], J.P. Smol [r], R. Spielhagen [s], J.W.C. White [a], A.P. Wolfe [f], E.W. Wolff [t]

[a] Institute of Arctic and Alpine Research and Department of Geological Sciences, University of Colorado, Boulder, CO 80309-0450, USA
[b] Department of Geosciences, University of Massachusetts, Amherst, MA 01003 USA
[c] Department of Geosciences and Earth and Environmental Systems Institute, Pennsylvania State University, University Park, PA 16802, USA
[d] Earth Surface Processes, U.S. Geological Survey, MS-980, Box 25046, DFC, Denver, CO 80225, USA
[e] Mainz Academy of Sciences, Humanities, and Literature, IFM-GEOMAR, Kiel, Germany
[f] Department of Earth & Atmospheric Sciences, University of Alberta, Edmonton, AB T6G 2E3, Canada
[g] School of Geography, University of Southampton, Highfield, Southampton SO17 1BJ, UK
[h] Geography Department, Royal Holloway, University of London, Egham, Surrey TW20 0EX, UK
[i] Department of Biological Sciences, Idaho State University, Pocatello, ID 83209, USA
[j] Geological Museum, University of Copenhagen, Øster Voldgade 5-7, DK-1350, Copenhagen K, Denmark
[k] Department of Geological Sciences, Brown University, Box 1846, Providence, RI 02912, USA
[l] Water and Environmental Research Center University of Alaska Fairbanks, Box 755860, Fairbanks, AK 99775, USA
[m] School of Earth Sciences and Environmental Sustainability, Northern Arizona University, Flagstaff, AZ 86011-4099, USA
[n] Department of Geography, University of California, Los Angeles, CA 90095, USA
[o] Byrd Polar Research Center, The Ohio State University, 108 Scott Hall, 1090 Carmack Road, Columbus, OH 43210-1002, USA
[p] Department of Environmental Sciences, Rutgers University, 14 College Farm Road, New Brunswich, NJ 08901, USA
[q] Cooperative Institute for Research in Environmental Sciences, NSIDC, University of Colorado, Boulder, CO, USA
[r] Department of Biology, Queen's University, Kingston, Ontario K7L 3N6, Canada
[s] Leibniz Institute for Marine Sciences, IFM-GEOMAR, Wischhofstr. 1-3, D-24148 Kiel, Germany
[t] British Antarctic Survey, High Cross, Madingley Road, Cambridge CB3 0ET, UK

ARTICLE INFO

Article history:
Received 2 May 2009
Received in revised form
20 February 2010
Accepted 1 March 2010

ABSTRACT

As the planet cooled from peak warmth in the early Cenozoic, extensive Northern Hemisphere ice sheets developed by 2.6 Ma ago, leading to changes in the circulation of both the atmosphere and oceans. From ~2.6 to ~1.0 Ma ago, ice sheets came and went about every 41 ka, in pace with cycles in the tilt of Earth's axis, but for the past 700 ka, glacial cycles have been longer, lasting ~100 ka, separated by brief, warm interglaciations, when sea level and ice volumes were close to present. The cause of the shift from 41 ka to 100 ka glacial cycles is still debated. During the penultimate interglaciation, ~130 to ~120 ka ago, solar energy in summer in the Arctic was greater than at any time subsequently. As a consequence, Arctic summers were ~5 °C warmer than at present, and almost all glaciers melted completely except for the Greenland Ice Sheet, and even it was reduced in size substantially from its present extent. With the loss of land ice, sea level was about 5 m higher than present, with the extra melt coming from both Greenland and Antarctica as well as small glaciers. The Last Glacial Maximum (LGM) peaked ~21 ka ago, when mean annual temperatures over parts of the Arctic were as much as 20 °C lower than at present. Ice recession was well underway 16 ka ago, and most of the Northern Hemisphere ice sheets had melted by 6 ka ago. Solar energy reached a summer maximum (9% higher than at present) ~11 ka ago and has been decreasing since then, primarily in response to the precession of the equinoxes. The extra energy elevated early Holocene summer temperatures throughout the Arctic 1–3 °C above 20th century averages, enough to completely melt many small glaciers throughout the Arctic, although the Greenland Ice Sheet was only slightly smaller than at present. Early Holocene summer sea ice limits were substantially smaller than their 20th century average, and the flow of Atlantic water into the Arctic Ocean was substantially greater. As summer solar energy decreased in the second half of the Holocene, glaciers re-established or advanced, sea ice expanded, and the flow of warm Atlantic water into the Arctic Ocean

* Corresponding author. Tel.: +1 303 492 6962.
E-mail address: gmiller@colorado.edu (G.H. Miller).

0277-3791/$ – see front matter
doi:10.1016/j.quascirev.2010.03.001

diminished. Late Holocene cooling reached its nadir during the Little Ice Age (about 1250–1850 AD), when sun-blocking volcanic eruptions and perhaps other causes added to the orbital cooling, allowing most Arctic glaciers to reach their maximum Holocene extent. During the warming of the past century, glaciers have receded throughout the Arctic, terrestrial ecosystems have advanced northward, and perennial Arctic Ocean sea ice has diminished.

Here we review the proxies that allow reconstruction of Quaternary climates and the feedbacks that amplify climate change across the Arctic. We provide an overview of the evolution of climate from the hot-house of the early Cenozoic through its transition to the ice-house of the Quaternary, with special emphasis on the anomalous warmth of the middle Pliocene, early Quaternary warm times, the Mid Pleistocene transition, warm interglaciations of marine isotope stages 11, 5e, and 1, the stage 3 interstadial, and the peak cold of the last glacial maximum.

1. Introduction

Our understanding of the evolution of Arctic climate during the Cenozoic has been increasing rapidly, as access to geological archives improves and new tools become available to unravel climate proxies and to improve both precision and accuracy of geochronologies. However, the Cenozoic history of the Arctic remains broadly incomplete. Although there is some evidence to confirm that the Arctic has cooled from peak warmth in the early Cenozoic to the ice-age times of the Quaternary, firm networks of sites capable of defining the spatial patterns of climate are mostly confined to a few time-windows of the Quaternary. Reconstructing past Arctic climates help to reveal key processes of climate change, including the response to elevated greenhouse-gas concentrations, and provide insights into future climate behavior.

Although the Arctic occupies less than 5% of the Earth's surface, it includes some of the strongest positive feedbacks to climate change (ACIA, 2005a,b). Over the past 65 Ma the Arctic has experienced a greater change in temperature, vegetation, and ocean surface characteristics than has any other Northern Hemisphere latitudinal band (e.g., Sewall and Sloan, 2001; Bice et al., 2006). Quantitative paleoclimate reconstructions suggest that Arctic temperature changes have been 3–4 times the corresponding hemispheric or globally averaged changes over the past 4 Ma (Miller et al., 2010). These changes impact regions outside the Arctic through their proximal influence on the planetary energy balance and circulation of the Northern Hemisphere atmosphere and ocean, and with potential global impacts through changes in sea level, the release of greenhouse gases, and impacts on the ocean's meridional overturning circulation.

Recent instrumental records show that during the past few decades, surface air temperatures throughout much of the Arctic have risen about twice as fast as temperatures in lower latitudes (Delworth and Knutson, 2000; Knutson et al., 2006). The remarkable reduction in Arctic Ocean summer sea ice in 2007 (Fig. 1) outpaced the most recent predictions from available climate models (Stroeve et al., 2008), but it is in concert with widespread reductions in glacier length, increased borehole temperatures, increased coastal erosion, changes in vegetation and wildlife habitats, the northward migration of marine life, the evaporation of

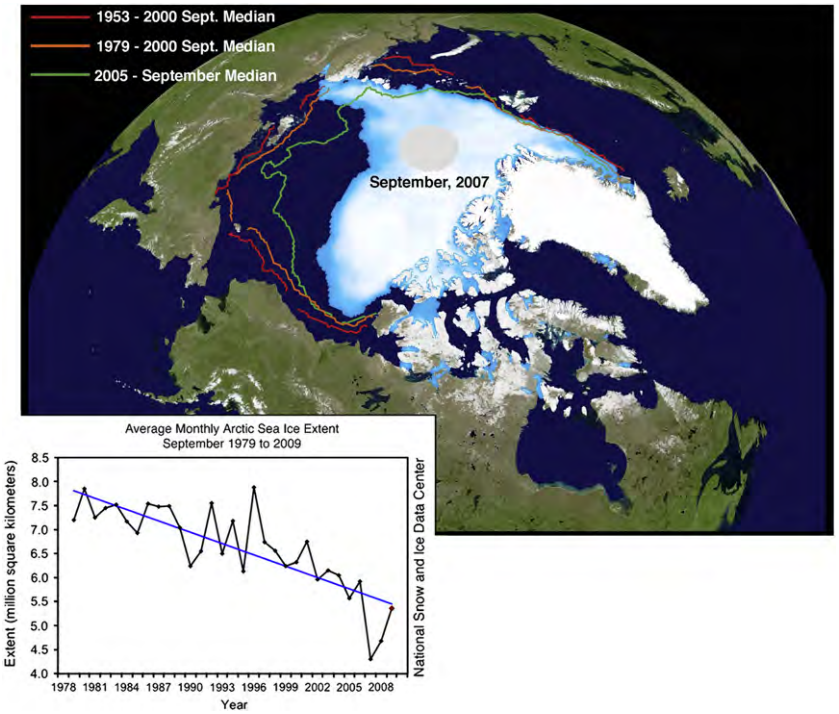

Fig. 1. Median extent of sea ice in September, 2007, compared with averaged intervals during recent decades. Red curve, 1953–2000; orange curve, 1979–2000; green curve, September 2005. Inset: September sea ice area time series from 1979 to 2009 based on satellite imagery (http://nsidc.org/news/press/20091005_minimumpr.html). The reduction in Arctic Ocean summer sea ice in 2007 was greater than that predicted by most recent climate models. [Copyright 2008 American Geophysical Union, reproduced by permission of American Geophysical Union.]

Arctic ponds, and degradation of permafrost. On the basis of the past century's trend of increasing greenhouse gases, climate models forecast continuing warming into the foreseeable future (Fig. 2) and a continuing amplification of temperature change in the Arctic (Serreze and Francis, 2006).

The purpose of this paper is to describe the feedback mechanisms that lead to greater change in Arctic climate than for other latitudinal bands, to identify climate proxies available to reconstruct past climates of the Arctic, to provide a broad overview of Cenozoic climate change leading up to the onset of Northern Hemisphere continental ice sheets, and to review the evidence for changes in temperature and precipitation in the Arctic over the past 3–4 Ma, with a focus on those time intervals with the most extensive paleoclimate datasets.

At the start of the Cenozoic, 65 Ma ago, the planet was ice free; there was no sea ice in the Arctic Ocean, nor was there a Greenland or an Antarctic ice sheet. General cooling through the Cenozoic is attributed mainly to a slow drawdown of greenhouse gases in the atmosphere through the weathering of silicic rocks that exceeded the release of stored carbon through volcanism and reprocessing. At the end of the Pliocene the climate system crossed a threshold that led to the periodic growth and decay of Northern Hemisphere ice sheets. An overview of the evolution of temperature and precipitation over the past 4 Ma offers insights into the positive feedbacks within the Arctic system that result in global impacts. These topics are important in their own right, and they also set the stage for understanding the histories of the Greenland Ice Sheet (Alley et al., 2010) and Arctic Ocean sea ice (Polyak et al., 2010). Because of the great interest in rates of change, a careful consideration of rates of change is reviewed separately by White et al. (2010).

Ages of past events are given as millions of years before present (Ma) or thousands of years before present (ka). For events within the past 40 ka, radiocarbon is the most widely used clock, and radiocarbon ages have been converted to calendar years before present, with present taken to be 1950 AD. Most calibration has been undertaken by the original authors, but in a few cases where the authors have not calibrated their radiocarbon ages we have used Calib 6.0 (http://intcal.qub.ac.uk/calib/calib.html) to make the conversions to keep all events on a common timescale.

2. Feedbacks Influencing Arctic Temperature and Precipitation

The most commonly used measure of climate is the mean surface air temperature (Fig. 3), which is influenced by climate forcings and climate feedbacks. The most important forcings during the Quaternary have been changes in the distribution of solar radiation that resulted from irregularities of Earth's orbit, changes in the frequency of explosive volcanism, changes in atmospheric greenhouse-gas concentrations, and to a lesser extent, small variations in solar irradiance. On longer time scales (tens of millions of years), the long-term increase in the solar constant (a 30% increase in the past 4600 Ma) was important, and the redistribution of continental landmasses caused by plate motions also affected the planetary energy balance, but these forcings are nearly imperceptible on Quaternary timescales.

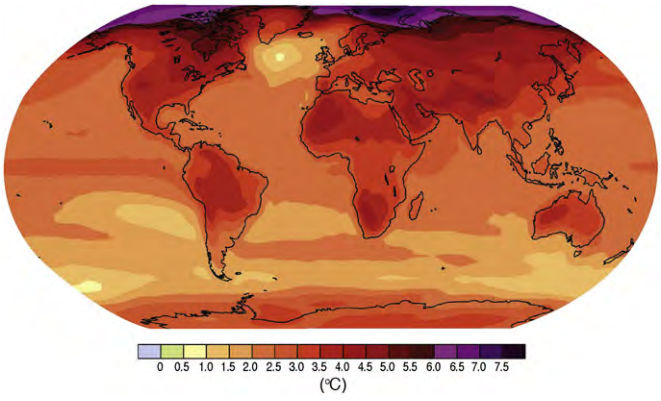

Fig. 2. Projected surface temperature changes for the last decade of the 21st century (2090–2099) relative to the period 1980–1999. The map shows the IPCC multi-Atmosphere–Ocean coupled Global Climate Model average projection for the A1B (balanced emphasis on all energy resources) scenario. The most significant warming is projected to occur in the Arctic (IPCC, 2007; Fig. SPM6).

How much the temperature changes in response to a forcing of a given magnitude (or in response to the net magnitude of a set of forcings in combination) depends on the sum of all of the feedbacks. Feedbacks can act in days or less or endure for millions of years. Changes in planetary temperatures may, for example, have many causes, including a brighter Sun, higher concentration of greenhouse gases in the atmosphere, or less blocking of the Sun by volcanic aerosols. Here we focus primarily on the relatively fast feedbacks that occur in the Arctic. A more comprehensive treatment of Arctic feedbacks is given in the companion paper on Arctic amplification (Miller et al., 2010).

2.1. Ice-albedo feedback

Changes in the seasonal and areal distribution of snow and ice exert strong influences on the planetary energy balance through their impact on Earth's albedo (Peixoto and Oort, 1992). Changes in albedo are most important in the Arctic summer, when solar radiation is at a maximum. Warming reduces ice and snow whereas cooling allows them to expand, so the changes in ice and snow act as positive feedbacks to amplify climate changes (e.g., Lemke et al., 2007).

2.2. Ice-insulation feedback

Sea ice also causes a positive insulation feedback, primarily in winter. By insulating the cold polar atmosphere in winter from the relatively warm ocean, little of the ocean's energy can be transferred to the atmosphere. If warming reduces sea ice, then the newly ice-free ocean heats the overlying atmosphere in winter months, amplifying the initial warming.

2.3. Vegetation feedbacks

A warming climate can cause tundra to give way to lower albedo shrub vegetation or even dark-green boreal forest (Chapin et al., 2005). The lower albedo of shrubs and boreal forest, especially in spring when high-albedo snowcover may still bury tundra, results in earlier warming and hence exerts a positive feedback on warming.

2.4. Permafrost feedbacks

Additional, but poorly understood feedbacks in the Arctic involve changes in the extent of permafrost, and how changes in cloud cover interact both with permafrost and with the release of carbon dioxide and methane from the land surface. Melting allows ancient plant debris to decompose, releasing greenhouse gases (CO_2 and/or CH_4) that mix globally, amplifying the initial warming by enhancing the planetary greenhouse effect.

2.5. Feedbacks during glacial-interglacial cycles

Additional slow positive feedbacks that operate on time scales of 10^4 years were important contributors to glacial-interglacial

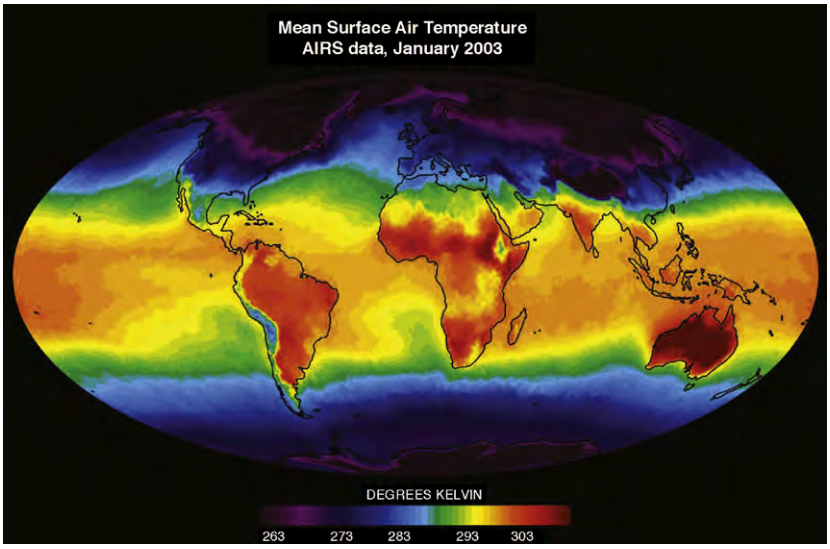

Fig. 3. Global mean observed near-surface air temperatures for the month of January, 2003 derived from the Atmospheric Infrared Sounder (AIRS) data. Contrast between equatorial and Arctic temperatures is greatest during the northern hemisphere winter. The transfer of heat from the tropics to the polar regions is a primary feature of the Earth's climate system (Color scale is in Kelvin degrees such that 0 °C = 273.15 K)

climate cycles. The growth of the Quaternary ice sheets increased the reflectivity of the Arctic, amplifying the initial cooling, and their great height across extensive regions produced additional cooling simply by increasing the average surface elevation. Colder ice-age oceans reduced atmospheric water vapor, a key greenhouse gas, and therefore a positive feedback on cooling, and reduced atmospheric water vapor dried the continents. As a result, atmospheric dust loads were higher, which contributed to additional cooling by blocking sunlight. Complex changes in the ocean-atmosphere circulation shifted CO_2 from the atmosphere to the ocean and reduced the atmospheric greenhouse effect, further amplifying cooling.

3. Proxies of Arctic Temperature and Precipitation

Temperature and precipitation are important climate variables. Climate change is typically driven by changes in key forcing factors, which are then amplified or retarded by regional feedbacks that affect temperature and precipitation.

Reconstructing temperature and precipitation in pre-industrial times requires reliable proxies that can be used to derive qualitative or, preferably, quantitative estimates of past climates. Most biological temperature proxies reflect dominantly summer, or growing/breeding season temperatures. Hence paleoclimate reconstructions tend to be dominated by summer. However, many geochemical proxies are more closely correlated with mean annual temperatures, or the balance between winter and summer contributions. In general, precipitation is more difficult to estimate than is temperature, so reconstructions of changes in precipitation in the past are less common, and typically less quantitative, than are reconstructions of past temperature changes.

Because feedbacks have strong regional variability, spatially variable responses to hemispherically symmetric forcing are common throughout the Arctic (e.g., Kaufman et al., 2004). Consequently, to capture the expected spatial variability, proxy climate reconstructions must be geographically distributed and span a wide range of geological time. In general, the use of several proxies to reconstruct past climates provides the most robust evidence for past changes in temperature and precipitation.

3.1. Vegetation/pollen

Estimates of past temperature from data that describe the distribution of vegetation (primarily fossil pollen assemblages, but also plant macrofossils including as fruits and seeds) may be relative (warmer or colder) or quantitative (°C of change). Most information pertains to the growing season, because plants are dormant in the winter and so are less influenced by winter climate. For example, evidence of boreal forest vegetation is interpreted to reflect warmer growing seasons than would evidence of tundra—and the general position of northern treeline today approximates the location of the July 10 °C isotherm.

Indicator species live within well-defined and relatively restricted modern climatic ranges. The appearance of these species in the fossil record indicates a specific climate range, or that the site exceeded a minimum summer temperature threshold or a winter minimum temperature of freezing tolerance (Fig. 4). This methodology was developed early in Scandinavia (Iversen, 1944). Matthews et al. (1990) used indicator species to constrain temperatures during the Last Interglaciation in northwest Canada, and Ritchie et al. (1983) used indicator species to highlight early Holocene warmth in northwest Canada. This technique has also been used extensively with fossil insect assemblages.

Numerical estimates of past temperatures from pollen assemblages generally follow one of two approaches. In the inverse-modeling approach, fossil data from one or more localities are used to provide temperature estimates for those localities. A "calibration set" of modern pollen assemblages is related mathematically to observed modern temperature, and the functions thus obtained are then applied to fossil data. This method was developed and applied in Scandinavia (e.g., Seppä et al., 2004). A variant of the inverse approach is analogue analysis, in which a large modern dataset with assigned climate data forms the basis for comparison with fossil spectra. Good matches are derived statistically, and the resulting set of analogues provides an estimate of the past mean temperature and accompanying uncertainty (Anderson et al., 1989, 1991). Inverse modeling relies upon observed modern relationships. Some plant species were more abundant in the past than they are today, and the fossil pollen spectra they produced may have no recognizable modern counterpart – so-called "no

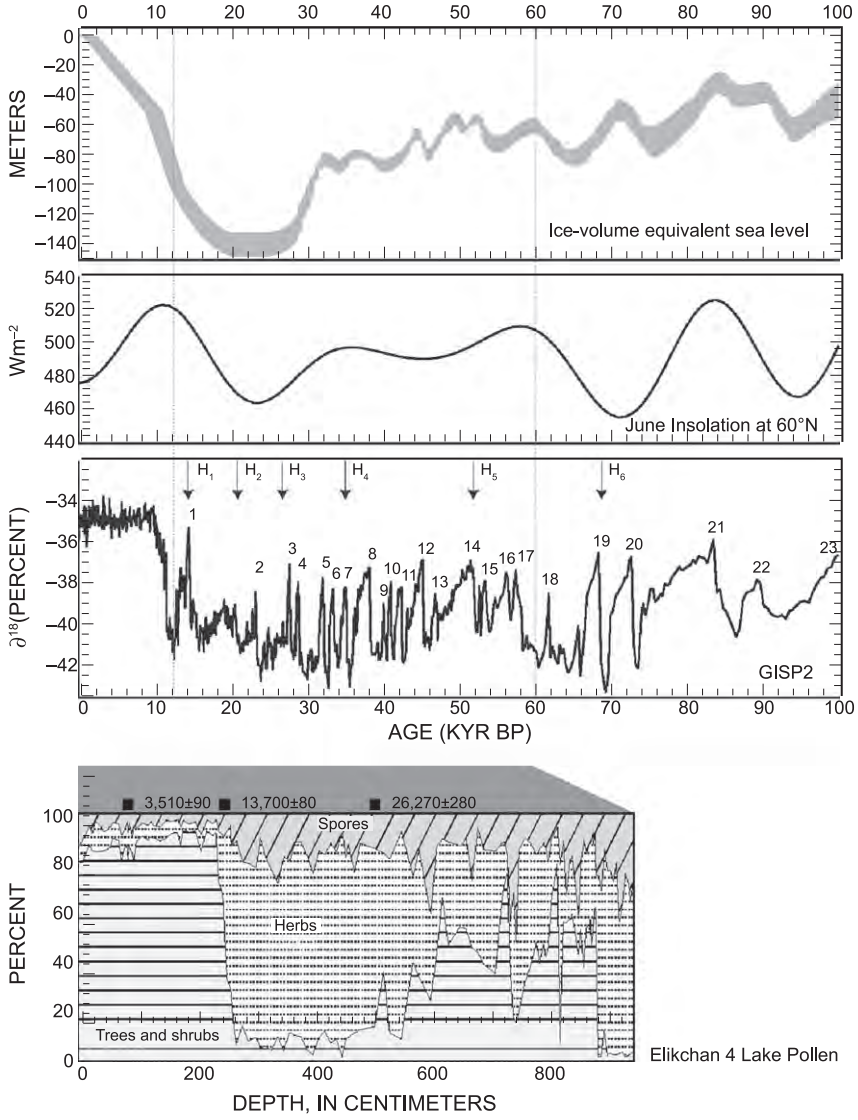

Fig. 4. Upper three panels: Correlation of global sea-level curve (Lambeck et al., 2002), Northern Hemisphere summer insolation (Berger and Loutre, 1991), and the Greenland Ice Sheet (GISP2) $\delta^{18}O$ record (Grootes et al., 1993), ages all given in calendar years. Bottom panel: temporal changes in the percentages of the main taxa of trees and shrubs, herbs and spores at Elikchan 4 Lake in the Magadan region of Chukotka, Russia. Lake core x-axis is depth, not time (Brigham-Grette et al., 2004). Habitat was reconstructed on the basis of modern climate range of collective species found in fossil pollen assemblages. The reconstruction can be used to estimate past temperatures or the seasonality of a particular site. The GISP2 record: Base of core roughly 60 ka (Lozhkin and Anderson, 1996). H1 above arrow, timing of Heinrich event event 1 (and so on); number 1 above curve, Dansgaard-Oscheger event (and so on). During approximately 27 ka to nearly 55 ka, vegetation, especially treeline, recovered for short intervals to nearly Holocene conditions at the same time that the isotopic record in Greenland suggests repeated warm warm-cold cycles of change. kyr BP, thousands of years before the present. [Copyright 2004 University of Utah, reproduced by permission of University of Utah.]

analogue" assemblages. Outside the envelope of modern observations, fossil pollen spectra, which are described in terms of pollen abundance, cannot be reliably related to past climate.

Because many fossil pollen assemblages have no modern analogues a forward modeling approach has been developed as an alternative method to estimate past temperatures (or other climate variables). The pollen data are not used to develop numerical values but are used to test an "hypothesis" about the status of past temperature. The hypothesis may be a conceptual model of the status of past climate, but typically it is represented by a climate-model simulation for a given time in the past. The climate simulation drives a vegetation model that assigns vegetation cover on the basis of bioclimatic rules (such as winter temperature minima or growing season temperatures). The resultant map is compared with a map of past vegetation developed from the fossil data. The philosophy of this approach is described by Prentice and Webb (1998). Such data and models have been compared for the Arctic by Kaplan et al. (2003) and Wohlfahrt et al. (2004). The advantage of this approach is that underlying the model simulation are hypothesized climatic mechanisms; those mechanisms allow not only the description, but also an explanation of past climate changes.

3.2. Dendroclimatology

Seasonal differences in temperature and precipitation produce annual rings that reflect distinct changes in the way trees grow and respond, year after year, to variations in the weather (Fritts, 1976). Alternating light and dark bands (couplets) of low-density early

wood (spring and summer) and higher-density late wood (summer to late summer) have been used to reproduce long time-series of regional climate change thought to directly influence the production of meristematic cells in the trees' vascular cambium, just below the bark. Cambial activity in many parts of the northern boreal forests can be short; late wood production very likely starts in late June and annual-ring width is complete by early August (e.g., Esper and Schweingruber, 2004). Fundamental to the use of tree rings is the fact that the average width of a tree ring couplet reflects some combination of environmental factors, largely temperature and precipitation, but it can also reflect local climatic variables such as wind stress, humidity and soil properties (see Bradley, 1999, for review). As a general guideline, growing season conditions favorable for the production of wide annual rings tend to be characterized by warmer than average summers with sufficient precipitation to maintain adequate soil moisture. Narrow tree rings occur during unusually cold or dry growing seasons.

The extraction of a climate signal from ring width and wood density (dendroclimatology) relies on the identification and calibration of regional climate factors and on the ability to distinguish local climate influences from regional noise (Fig. 5). How sites for tree sampling are selected is also important depending upon the climatological signal of interest. Trees in marginal growth sites, perhaps on drier substrates or near an ecological transition, are likely to be most sensitive to minor changes in temperature stress or moisture stress. On the other hand, trees in less-marginal sites likely reflect conditions of more widespread change. Arctic research is commonly focused on trees at the latitude and elevation limits of tree growth.

Pencil-sized increment cores or sanded trunk cross sections are routinely used for stereomicroscopic examination and measurement (Fig. 6). A number of tree species are utilized, most commonly varieties of the genera *Larix* (larch), *Pinus* (pine), and *Picea* (spruce). Raw ring-width time series are typically generated at a resolution of 0.01 mm along one or more radii of the tree, and these data are normalized for changes in ring width that reflect the natural increase in tree girth (a young tree produces wider rings). Ring widths for a number of trees are then averaged to produce a master curve for a particular site. The replication of many time series throughout a wide area at a particular site permits extraction of a climate-related signal and the elimination of anomalous ring biases caused by changes in competition or the ecology of any particular tree.

Dendroclimatology is statistically laborious, and a variety of approaches are used. Summaries can be found in Fritts (1976), Briffa and Cook (1990), Bradley (1999), his Chapter 10), and Luckman (2007).

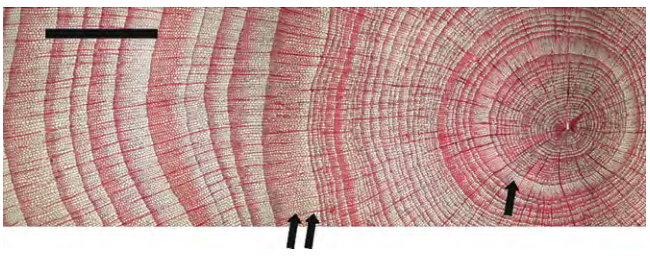

Fig. 5. Annual tree rings composed of seasonal early and late wood are clear in this a 64-year year-old *Larix siberica* from western Siberia (Esper and Schweingruber, 2004). Initial growth was restricted; narrow rings average 0.035 mm/year, punctuated by one thicker ring (one single arrow). Later (two arrows), tree-ring width abruptly at least doubled for more than three years. Ring widths increased to 0.2 mm/year. Scale bar is 1 mm. (Photograph courtesy of Jan Esper, Swiss Federal Research Institute).

3.3. Marine isotopic records

The oxygen isotope composition of the calcareous shells of planktic foraminifera accurately records the oxygen isotope composition of ambient seawater, modulated by the temperature at which the organisms built their shells and a modest vital effect (Epstein et al., 1953; Shackleton, 1967; Erez and Luz, 1982; Fig. 7). Most of the global ocean is well mixed with respect to its isotopic composition. Changes in deep ocean temperatures on Quaternary timescales are much smaller than for surface waters; consequently, the $\delta^{18}O$ of benthic foraminifera has become the global standard for climate evolution during the Quaternary (e.g., Lisiecki and Raymo, 2005). Marine isotope stages (MIS) are counted backward from the Holocene (MIS 1), with odd-numbered stages broadly reflecting interglacial conditions, and even-numbered stages reflecting glacial conditions. Some stages are further subdivided by adding letter suffixes (e.g., MIS 5e is the Last Interglaciation *sensu stricto*).

The Arctic Ocean is the least well mixed of the global oceans, and calcareous fossils are only sporadically preserved in its Quaternary sediment (see Matthiessen et al., 2009 for review). It has only a narrow deep connection to the Nordic Seas via Fram Strait, and the Nordic Seas are separated from the North Atlantic proper by a broad series of shallow ridges.

Arctic Ocean surface waters exhibit little temperature variability (everywhere between -1 and -2 °C). Hence, there is negligible temperature influence on the $\delta^{18}O$ of planktonic foraminifera (<0.2‰; Shackleton, 1974). Because meteoric waters, discharged into the ocean by precipitation and (indirectly) by river runoff, have much more negative $\delta^{18}O$ values than do ocean waters, differences in the $\delta^{18}O$ of planktonic foraminifera across the Arctic Ocean in the modern regime serve as a proxy for salinity, despite the complications of seasonal sea ice (Bauch et al., 1995; LeGrande and Schmidt, 2006). Accordingly, the spatial variability of surface-water salinity in the Arctic Ocean is recorded today by the $\delta^{18}O$ of planktonic foraminifera (Spielhagen and Erlenkeuser, 1994; Bauch et al., 1997).

The $\delta^{18}O$ of Quaternary planktonic foraminifera in sediment cores from the deep Arctic Ocean vary considerably on millennial time scales (e.g., Aksu, 1985; Scott et al., 1989; Stein et al., 1994; Nørgaard-Pedersen et al., 1998, 2003, 2007a,b; Polyak et al., 2004; Spielhagen et al., 2004, 2005), but the variability commonly exceeds the glacial-interglacial change in the $\delta^{18}O$ of seawater that results from isotopically light freshwater stored in continental ice sheets (about 1.0–1.2‰; Fairbanks, 1989; Adkins et al., 1997; Schrag et al. 2002). Large changes in the flux of isotopically light glacial meltwater into the Arctic Ocean can overprint the global $\delta^{18}O$ signal, as can changes in the flux of warm, saline Atlantic water through Fram Strait (Nørgaard-Pedersen et al., 2003). Because of these strong local influences in the $\delta^{18}O$ of Arctic Ocean surface waters it is difficult to reconstruct past temperatures or salinities from variations in calcite $\delta^{18}O$ in Arctic Ocean sediment cores. Similarly, it is difficult to use calcite $\delta^{18}O$ to correlate with the global MIS stratigraphy, hampering interpretation of Arctic Ocean sediment records.

3.4. Lacustrine isotopic records

Isotopic records preserved in lake sediment provide information on landscape change and hydrology. The $\delta^{18}O$ of precipitation reflects climate processes, including both temperature and source water trajectories. The $\delta^{18}O$ of aquatic biominerals, such as calcium carbonate, reflects lakewater $\delta^{18}O$, which in turn is controlled by the $\delta^{18}O$ of precipitation – unless evaporation from the lake is rapid compared with inflow of new water (Fig. 8). The $\delta^{18}O$ of open lakes (through-flowing drainages) is minimally affected by evaporation,

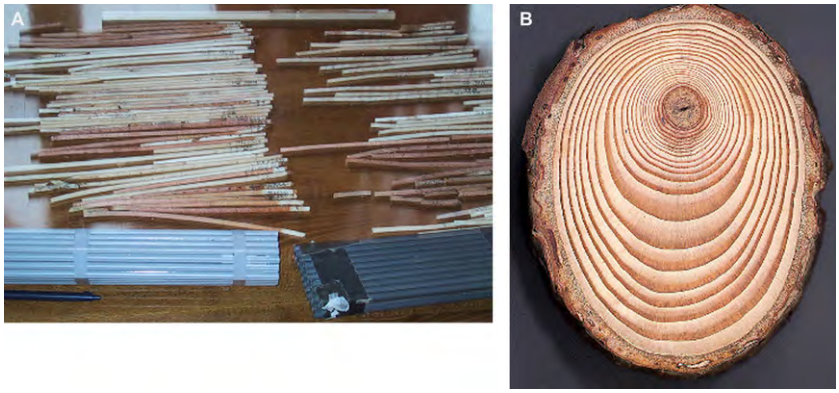

Fig. 6. Typical tree ring samples. (A) Increment cores taken from trees with a small small-bore hollow drill. They can be easily stored and transported in plastic soda straws for analysis in the laboratory. (B) Alternatively, cross sections or disks can be sanded for study. A cross section of *Larix decidua* root shows differing wood thickness within single rings, caused by exposure. (Photographs courtesy of Jan Esper and Holger Gärtner, Swiss Federal Research Institute, respectively).

as is $\delta^{18}O$ in some lakes supplied only by water flow through the ground (closed lakes). However, the $\delta^{18}O$ of closed lakes is at least in part controlled by lake hydrology. Unless independent evidence of lake hydrology is available, quantitative interpretation of $\delta^{18}O$ is difficult. Consequently, $\delta^{18}O$ is normally combined with additional climate proxies to constrain other variables and strengthen interpretations. For example, in rare cases, ice core records that are located near lakes can provide a $\delta^{18}O$ record that can aid interpretation of the relative contributions of temperature and moisture source to the lakewater $\delta^{18}O$ (Fisher et al., 2004; Anderson and leng, 2004; Anderson et al., 2006; Fig. 9). In addition to $\delta^{18}O$ in carbonate shells, $\delta^{18}O$ has been measured in diatom silica (Wolfe et al., 1996; Leng and Marshall, 2004; Leng and Barker, 2005; Schiff et al., 2008), and in organic cellulose (Sauer et al., 2001). The isotopic composition of bulk organic matter in lake sediments is complicated by the possibility of both within-lake and in-washed terrestrial sources. Recent advances in isolating biomarkers unique to aquatic and/or terrestrial sources in sufficient concentration for isotopic analyses may circumvent this problem (Huang et al., 2002).

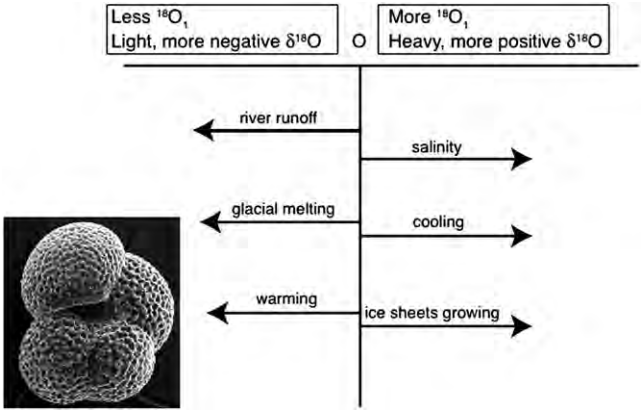

Fig. 7. Microscopic marine plankton known as (foraminiferaifers (see inset) grow a shell of calcium carbonate ($CaCO_3$) in or near isotopic equilibrium with ambient sea water. The oxygen isotope ratio measured in these shells can be used to determine the temperature of the surrounding waters. (The oxygen–isotope ratio is expressed in $\delta^{18}O$ parts per million (ppm) $= 10^3[(R_{sample}/R_{standard}) - 1]$, where $R_x = (^{18}O)/(^{16}O)$ is the ratio of isotopic composition of a sample compared to that of an established standard, such as ocean water. However, factors other than temperature can influence the ratio of ^{18}O to ^{16}O. Warmer seasonal temperatures, glacial meltwater, and river runoff with depleted values all will produce a more negative (lighter) $\delta^{18}O$ ratio. On the other hand, cooler temperatures or higher salinity waters will drive the ratio up, making it heavier, or more positive. The growth of large continental ice sheets selectively removes the lighter isotope (^{16}O), leaving the ocean enriched in the heavier isotope (^{18}O).

3.5. Ice cores

The most common way to deduce temperature from ice cores (Figs. 10 and 11) is through the isotopic content their water, $\delta^{18}O$ and δD. Pioneering studies (Dansgaard, 1964) showed that at high northern latitudes both $\delta^{18}O$ and δD are generally considered to represent the mean annual temperature at the core site, and the use of both measures together offers additional information about conditions at the source of the water vapor (e.g., Dansgaard et al., 1989). Spatial surveys (Johnsen et al., 1989) and models enabled with water isotopes (e.g., Hoffmann et al., 1998; Mathieu et al., 2002) show that there exists a strong spatial relationship between temperature and water isotope ratios. The relationship is

$$\delta = aT + b$$

where T is mean annual surface temperature, and δ is annual mean $\delta^{18}O$ or δD value in Arctic precipitation, and the slope, a, has values typically around 0.6 for Greenland $\delta^{18}O$.

Fig. 8. Lake El'gygytgyn in the Arctic Far East of Russia. Open and closed lake systems in the Arctic differ hydrologically according to the balance between inflow, outflow, and the ratio of precipitation to evaporation. These parameters are the dominant influence on lake stable stable-isotopic chemistry and on the depositional character of the sediments and organic matter. Lake El'gygytgyn is annually open and flows to the Bering Sea during July and August, but the outlet closes by early September as lake level drops and storms move beach gravels that choke the outlet. (Photograph by J. Brigham-Grette).

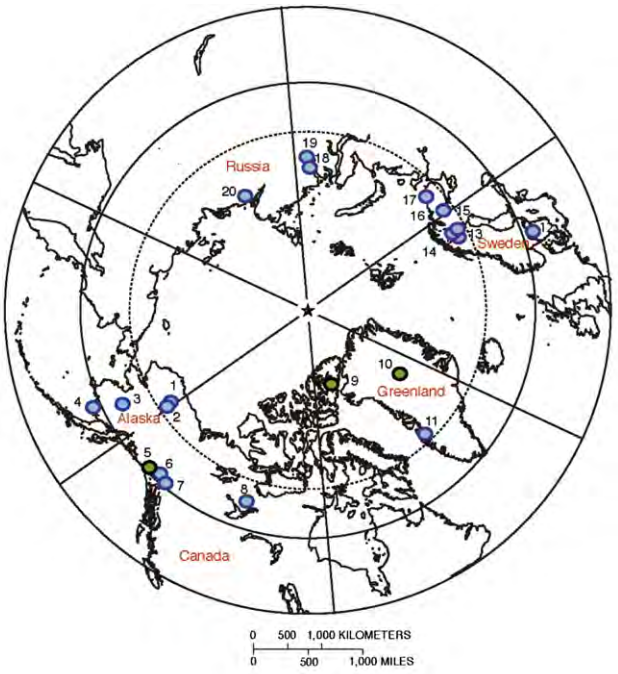

Core Locations:

1. Meli Lake (Anderson et al., 2001)
2. Tangled Up Lake (Anderson et al., 2001)
3. Farewll Lake (Hu et al., 2001)
4. Grandfather Lake (Hu and Shemesh., 2003)
5. Prospector Col Mt Logan (Fisher et al., 2004)
6. Jellybean Lake (Anderson et al., 2006)
7. Marcella Lake (Anderson et al., 2007)
8. Toronto Lake (Wolfe et al., 1996)
9. Agassiz Ice Cap (Fisher et al., 1995)
10. Summit Greenland (Grootes et al., 1993)
11. Lakes SS6 & Braya Sø (Anderson and Leng, 2004)
12. Lake Igelsjön (Hammarlund et al., 2003)
13. Lake Tibetus (Hammarlund et al., 2002)
14. Vuolep Allakasjaure (Rosqvist et al., 2004)
15. Lake 850 (Shemesh et al., 2001)
16. Chuna Lake (Jones et al., 2004)
17. Lakes Yarnyshnoe & Poteryanny Zub (Wolfe et al., 2000)
18. Middendorf Lake (Wolfe et al., 2000)
19. Derevanoi Lake (Wolfe et al., 2000)
20. Dolgoe Lake (Wolfe et al., 2000)

Fig. 9. Locations of Arctic and sub-Arctic lakes (blue) and ice cores (green) whose oxygen isotope records have been used to reconstruct Holocene paleoclimate. (Map adapted from the Atlas of Canada, ©2002. Her Majesty the Queen in Right of Canada, Natural Resources Canada./Sa Majesté la Reine du chef du Canada, Resources naturelles Canada.)

Temperature is not the only factor that can affect isotopic ratios in ice core water. Changes in the season when snow falls, in the source of the water vapor, and other factors are potentially important as well (Jouzel et al., 1997; Werner et al., 2000) (Fig. 12). For this reason, it is common, whenever possible, to calibrate the isotopic ratios using additional paleothermometers. For short intervals, instrumental records of temperature can be compared with isotopic ratios (e.g., Shuman et al., 1995). The few comparisons that have been done (summarized in Jouzel et al., 1997) tend to show δ/T gradients that are slightly lower than the spatial gradient. Accurate reconstructions of past temperature, but with low time resolution, are obtained from the use of borehole thermometry. The center of the Greenland Ice Sheet has not finished warming from the ice age, and the remaining cold temperatures reveal how cold the ice age was (Cuffey et al., 1995; Johnsen et al., 1995). Additional paleothermometers are available that use a thermal diffusion effect. Gas isotopes are separated slightly when an abrupt temperature change at the surface creates a temperature difference between the surface and the firn, below which bubbles are pinched off from the interconnected pore spaces in old snow. The size of the gas-isotope shift reveals the size of an abrupt temperature change, and the number of years between the indicators of an abrupt change in the ice and in the bubbles trapped in ice reveals the temperature before the abrupt change – if the snowfall rate before the abrupt change is known (Severinghaus et al., 1998; Severinghaus and Brook, 1999; Huber et al., 2006). These methods show that the value of the δ/T slope produced by many of the large changes recorded in Greenland ice cores was considerably less (typically by a factor of 2) than the spatial value, probably because of a relatively larger reduction in winter snowfall in colder times (Cuffey et al., 1995; Werner et al., 2000; Denton et al., 2005). The actual temperature changes were therefore larger than would be predicted by the standard calibration.

In summary, water isotopes in Arctic precipitation are a reliable proxy for mean annual air temperature, but for quantitative use, some means of calibrating them is required. They may be calibrated either against instrumental data by using an alternative estimate of temperature change, or through modeling, even for ice deposited during the Holocene (Schmidt et al., 2007).

3.6. Fossil assemblages and sea surface temperatures

Different planktonic species live preferentially at different temperatures in the modern ocean. These temperature-dependencies can be defined by modern observations, and then used to reconstruct past changes in sea-surface temperatures. An inherent assumption is that species maintain their preferences through time. With that assumption, the mathematical expression of these preferences plus the history of where the various species lived in the past can then be used to interpret past temperatures (Imbrie and Kipp, 1971; CLIMAP, 1981). This line of reasoning is primarily applied to near-surface species of foraminifera, diatoms, and

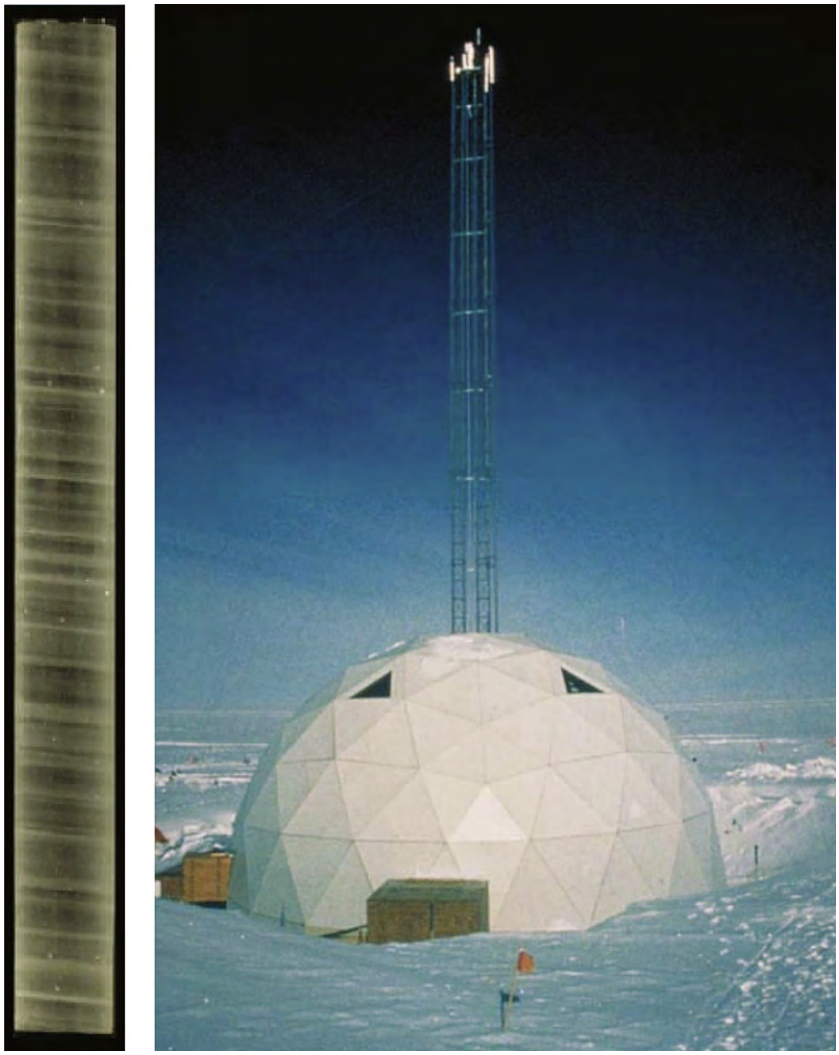

Fig. 10. (a) One-meter section of Greenland Ice Core Project-2 core from 1837 m depth showing annual layers. (Photograph courtesy of Eric Cravens, Assistant Curator, U.S. National Ice Core Laboratory). (b) Field site of Summit Station on top of the Greenland Ice Sheet (Photograph by Michael Morrison, GISP2 SMO, University of New Hampshire; NOAA Paleoslide Set)

dinoflagellates. Such methods are now commonly supported by sea-surface temperature estimates using emerging biomarker techniques outlined below.

3.7. Biogeochemistry

Within the past decade two new organic proxies have emerged that can be used to reconstruct past ocean surface temperatures. Both measurements are based on quantifying the proportions of biomarkers—molecules produced by restricted groups of organisms—preserved in sediments. In the case of the "$U^{k'}_{37}$ index" (Brassell et al., 1986; Prahl et al., 1988), a few closely related species of coccolithophorid algae are entirely responsible for producing the 37-carbon ketones (alkenones) used in the paleotemperature index, whereas crenarcheota (archea) produce the tetra-ether lipids that make up the TEX_{86} index (Wuchter et al., 2004). Although the specific function that the alkenones and glycerol dialkyl tetraethers serve for these organisms is unclear, the relationship of the biomarker $U^{k'}_{37}$ index to temperature has been confirmed experimentally in the laboratory (Prahl et al., 1988) and by extensive calibrations of modern surface sediments to overlying surface ocean temperatures (Muller et al., 1998; Wuchter et al., 2004; Conte et al., 2006). Biomarker compounds appear to be stable over the full Quaternary (Prahl et al., 1989; Grice et al., 1998; Teece et al., 1998; Herbert, 2003; Schouten et al., 2004). The TEX_{86} proxy has been applied to marine sediments 70–100 million years old.

Biomarker reconstructions have several advantages for reconstructing sea surface conditions in the Arctic. First, in contrast to $\delta^{18}O$ analyses of marine carbonates (outlined above), the confounding effects of salinity and ice volume do not compromise the utility of biomarkers as paleotemperature proxies. Both the $U^{k'}_{37}$ and TEX_{86} proxies can be measured reproducibly to high precision (analytical errors correspond to about 0.1 °C for $U^{k'}_{37}$ and 0.5 °C for TEX_{86}), and sediment extractions and gas or liquid chromatographic detections can be automated for high sampling rates. The abundances of biomarkers also provide insights into the composition of past ecosystems, so that links between the physical oceanography of the high latitudes and carbon cycling can be assessed. And lastly, organic biomarkers can usually be recovered from Arctic sediments that do not preserve carbonate or siliceous microfossils. It should be noted, however, that the organisms producing the alkenone and tetraethers may have been excluded from the Arctic during extreme cold periods; thus, continuous records cannot be guaranteed.

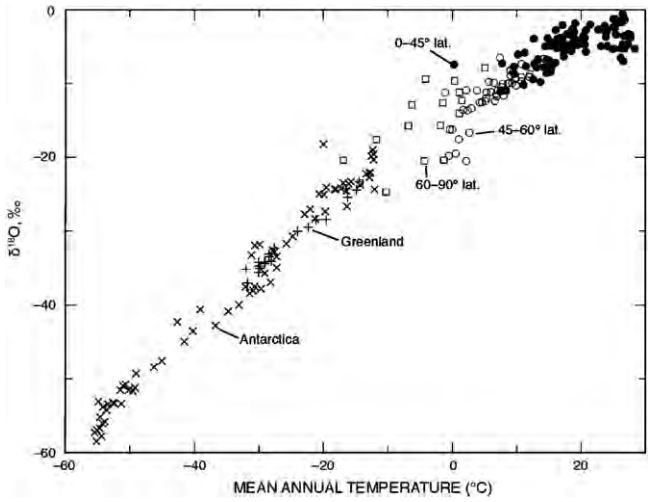

Fig. 11. Relation between isotopic composition of precipitation and temperature in the parts of the world where ice sheets exist. Sources of data as follows: International Atomic Energy Agency (IAEA) network (Fricke and O'Neil, 1999; calculated as the means of summer and winter data of their Table 1 for all sites with complete data). Open squares, poleward of 60° latitude (but with no inland ice-sheet sites); open circles, 45–60° latitude; filled circles, equatorward of 45° latitude. *x*, data from Greenland (Johnsen et al., 1989); +, data from Antarctica (Dahe et al., 1994). About 71% of Earth's surface area is equatorward of 45°, where dependence of $\delta^{18}O$ on temperature is weak to nonexistent. Only 16% of Earth's surface falls in the 45°–60° band, and only 13% is poleward of 60°. The linear array is clearly dominated by data from the ice sheets. (Source: Alley and Cuffey, 2001) [Reproduced by permission Mineralogical Society of America.]

The principal caveats in using biomarkers for paleotemperature reconstructions come from ecological and evolutionary considerations. Alkenones are produced by algae that are restricted to the photic zone, so paleotemperature estimates based on them apply to this layer, which approximates the sea-surface temperature. In the vast majority of the ocean, the alkenone signal recorded by sediments closely correlates with mean annual sea-surface temperature (Muller et al., 1998; Conte et al., 2006; Fig. 13). However, in the case of highly seasonal high-latitude oceans, where coccolithophorid blooms typically occur during the summer months, the temperatures inferred from the alkenone $U^{k'}_{37}$ index more closely approximates summer, rather than mean-annual sea-surface temperatures. A possible complication in past climate states is that the season of production may have been highly focused toward a short summer or to a more diffuse late spring–early fall productive season.

A survey of modern surface sediments in the North Atlantic and Nordic Seas (Rosell-Mele et al., 1995) shows that at colder water temperatures the original unsaturation ratio as defined by Brassell et al. (1986) most reliably estimates surface water temperatures because it includes the $U^{k'}_{37:4}$ alkenone type, which is common in the Nordic Seas although it is rare or absent in most of the world ocean including the Antarctic. The Brassell et al. (1986) unsaturation ratio provides reliable surface water temperature estimates as low as 6 °C, but errors increase at lower temperatures (Bendle and Rosell-Melé, 2004).

Although the marine crenarcheota that produce the tetraether membrane lipids used in the TEX_{86} index can range widely through the water column, the chemical basis for the TEX_{86} proxy is fixed by

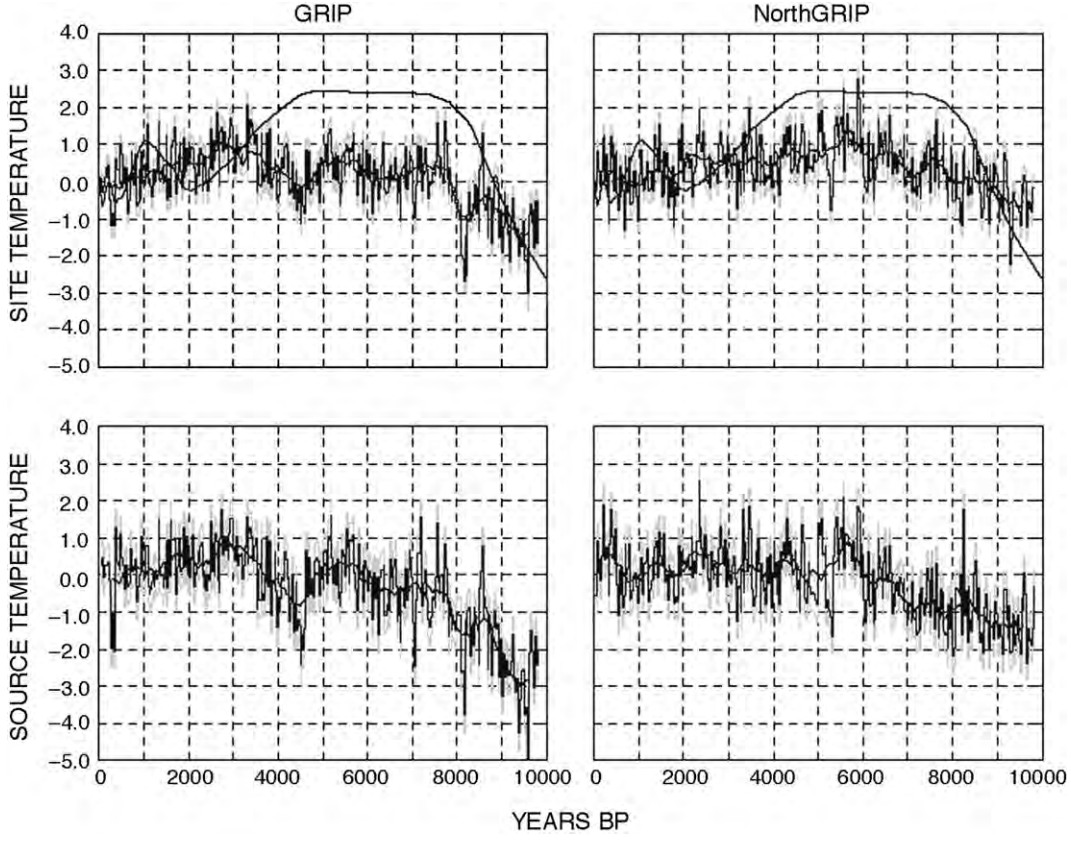

Fig. 12. Paleotemperature estimates of site and source waters from on Greenland: GRIP and NorthGrip (Masson-Delmotte et al., 2005). GRIP (left) and NorthGRIP (right) site (top) and source (bottom) temperatures derived from GRIP and NorthGRIP $\delta^{18}O$ and deuterium excess corrected for seawater $\delta^{18}O$ (until 6000 BP). Shaded lines in gray behind the black line provide an estimate of uncertainties due to the tuning of the isotopic model and the analytical precision. Solid line (in part above zigzag line), GRIP temperature derived from the borehole-temperature profile (Dahl-Jensen et al., 1998). [Copyright 2005 American Geophysical Union, reproduced by permission of American Geophysical Union.]

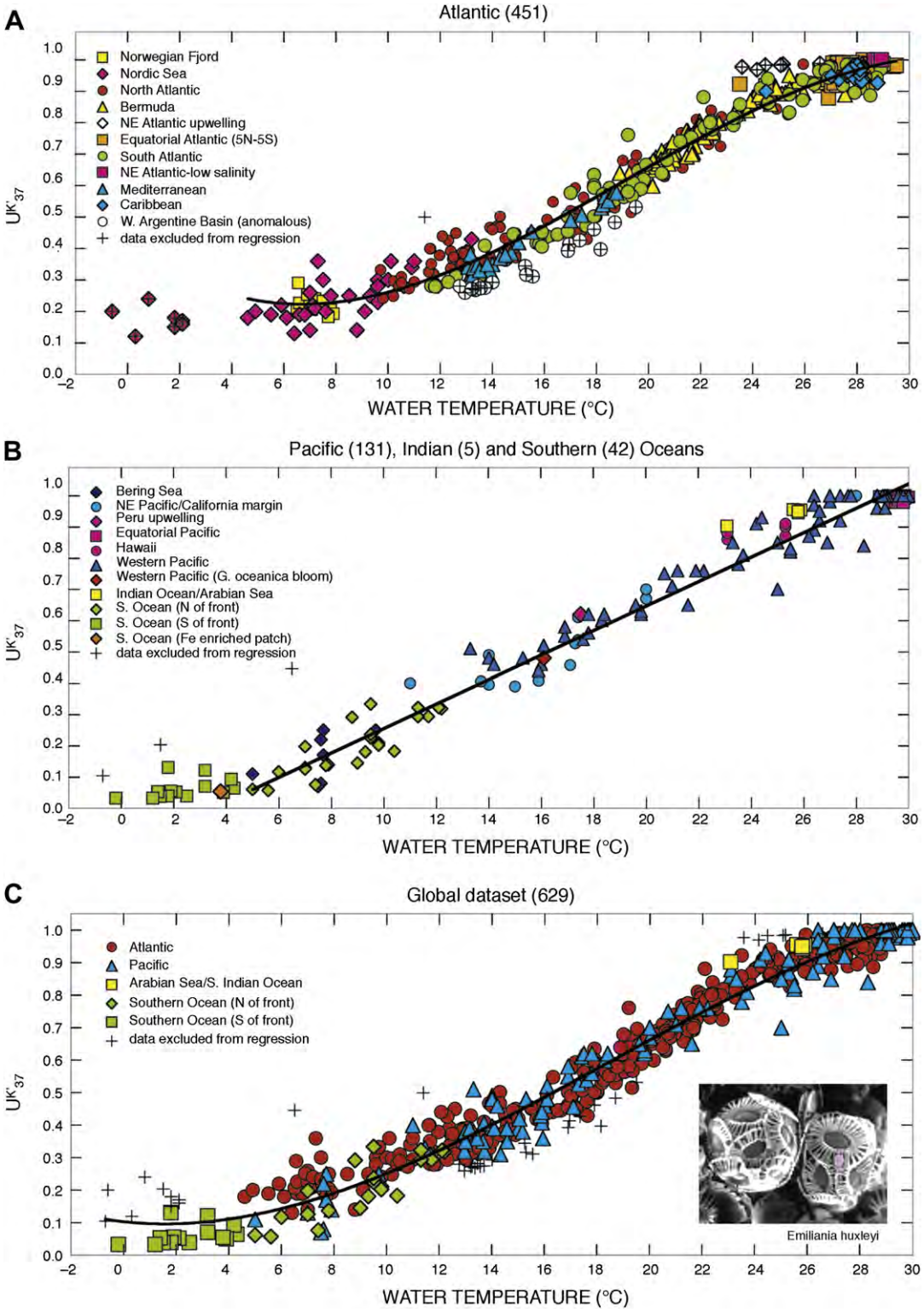

Fig. 13. Biomarker alkenone. $U^{K'}_{37}$ versus measured water temperature for ocean surface mixed layer (0–30 m) samples. (A) Atlantic region. Empirical 3rd-order polynomial regression for samples collected in >4 °C waters is $U^{K'}_{37} = -1.004 \times 10^{-4}\, T^3 + 5.744 \times 10^{-3}\, T^2 - 6.207 \times 10^{-2}\, T + 0.407$ ($r^2 = 0.98$, $n = 413$) (Outlier data from the southwest Atlantic margin and northeast Atlantic upwelling regime is excluded.) (B) Pacific, Indian, and Southern Ocean regions: the empirical linear regression of Pacific samples is $U^{K'}_{37} = 0.0391\, T - 0.1364$ ($r^2 = 0.97$, $n = 131$). Pacific regression does not include the Indian and Southern Ocean data. (C) Global data: the empirical 3rd order polynomial regression, excluding anomalous southwest Atlantic margin data, is $U^{K'}_{37} = -5.256 \times 10^{-5}\, T^3 + 2.884 \times 10^{-3}\, T^2 - 8.4933 \times 10^{-3}\, T + 9.898$ ($r^2 = 0.97$, n = 588). + = sample excluded from regressions (Conte et al., 2006). [Copyright 2006 American Geophysical Union, reproduced by permission of American Geophysical Union.]

processes in the photic zone, so that the sedimentary signal originates near the sea surface (Wuchter et al., 2005), just as for the $U^{k'}_{37}$ proxy. *In situ* analyses of particles suspended in the water column show that the tetraether lipids are most abundant in winter and spring months in many ocean provinces (Wuchter et al., 2005).

3.8. Biological proxies in lakes

Lakes and ponds are common in most Arctic regions and a wide range of biological climate proxies are preserved in their sediment (Smol and Cumming, 2000; Cohen, 2003; Pienitz et al., 2004; Schindler and Smol, 2006; Smol 2008). Diatom frustules (Douglas et al., 2004) and remains of non-biting flies (chironomid head capsules; Bennike et al., 2004) are among the biological indicators most commonly used to reconstruct past Arctic climates (Fig. 14). The calibration procedures and statistical treatments are similar to those described for other proxy indicators (e.g., Birks, 1998). The resulting mathematical relations are then used to reconstruct the environmental variables of interest on the basis of the distribution of indicator assemblages preserved in dated sediment cores (Smol, 2008). Where well-calibrated transfer functions are not available, such as for some parts of the Arctic, less-precise climate reconstructions are commonly based on the known ecological and life-history characteristics of the organisms.

3.9. Insect proxies

Insects are common and typically are preserved well in Arctic sediment, primarily in peat. Because many insect types live only within narrow ranges of temperature or other environmental conditions, the remains of particular insects in dated sediment accumulations provides useful information on past climates. Calibrating the observed insect data to climate involves extensive modern and recent collections, together with careful statistical analyses. For example, fossil beetles are typically related to temperature using what is known as the Mutual Climatic Range method (Elias et al., 1999; Bray et al., 2006). This method quantitatively assesses the relation between the modern geographical ranges of selected beetle species and modern meteorological data. A "climate envelope" is determined, within which a species can thrive. When used with paleodata, the method allows for the reconstruction of several parameters such as mean temperatures of the warmest and coldest months of the year.

3.10. Vegetation-derived precipitation estimates

Different plants live in wet and dry places, so indications of past vegetation may provide estimates of past wetness. Plants do not respond primarily to rainfall but instead to moisture availability, the difference between precipitation and evaporation, although some soils carry water downward so efficiently that dryness occurs even without much evaporation.

Where precipitation exceeds evaporation and growing conditions are moist, modern tundra vegetation is dominated by species such as *Sphagnum* (bog moss), *Eriophorum* (cotton-grass), and *Rubus chamaemorus* (cloudberry). In contrast, grasses dominate dry tundra and polar semi-desert. Such differences are evident today (Oswald et al., 2003) and can be also reconstructed from pollen and plant macrofossils preserved in sediments (e.g., Colinvaux, 1964; Ager and Brubaker, 1985; Lozhkin et al., 1993; Goetcheus and

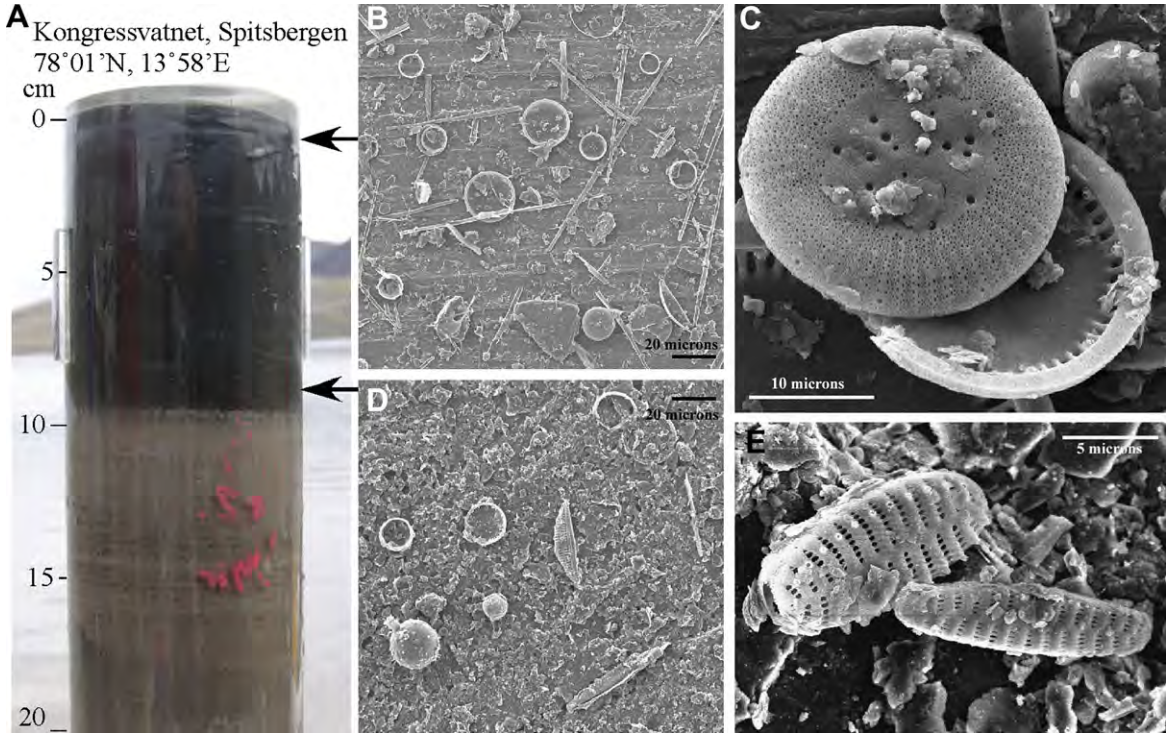

Fig. 14. Diatom assemblages are determined by a variety of environmental conditions in Arctic lake systems. Changes from one assemblage to another reflect changes in environmental controls such as light, nutrient availability, water chemistry, or temperature. Shown here is the upper 20 cm of a sediment core from Kongressvatnet, a deep polar lake on western Spitsbergen, Svalbard. (A) An abrupt transition from laminated silts to organic sediments at ~9 cm dated to 1880 A.D. records the retreat of glaciers from the lake's drainage catchment since end of the Little Ice Age. Recent assemblages (B) are characterized by abundant and diverse free-floating diatoms such as *Cyclotella* spp. (C). In contrast, diatom assemblages were less diverse and primarily bottom dwelling during the early 20th century with a greater abundance of the silica remains of Chysophytes (flagellate golden algae) (D). Across the Arctic, small diatoms of the Family Fragilariaceae (E) are common in sediments pre-dating the 20th Century, forming communities that, in many instances, indicate stable limnological conditions for several millennia.

Birks, 2001, Zazula et al., 2003). Some regions of Alaska and Siberia retain sand dunes that formed during the Last Glacial Maximum, and which reflect aridity and sparse vegetation cover; they are largely inactive today as moisture levels are sufficient to support dense vegetation cover in most areas.

In Arctic regions, deep snow cover very likely allows the persistence of shrubs that would be killed if exposed during the harsh winter cold and wind. For example, dwarf willow can survive if snow depths exceed 50 cm (Kaplan et al., 2003). Siberian stone pine (*Pinus pumila*) requires considerable snow to weigh down and bury its branches (Lozhkin et al., 2007). The presence of these species indicates certain minimum levels of winter snowfall.

Moisture levels can also be estimated quantitatively from pollen assemblages by means of formal techniques such as inverse and forward modeling, following techniques also used to estimate past temperatures. Moisture-related transfer functions have been developed, in Scandinavia for example (Seppä and Hammarlund, 2000). Kaplan et al. (2003) compared pollen-derived vegetation with vegetation derived from model simulations for the present and key times in the past. The pollen data indicated that model simulations for the Last Glacial Maximum tended to be "too moist"—the simulations generated shrub-dominated biomes whereas the pollen data indicated drier tundra dominated by grasses.

3.11. Lake-level derived precipitation estimates

Some lakes act as natural rain gauges. If precipitation increases relative to evaporation, lakes levels rise; such records provide information about moisture availability. Most of the water reaching a lake first soaked into the ground and flowed through spaces as groundwater, before it either seeped directly into the lake or else came back to the surface in a stream that flowed into the lake. Smaller amounts of water fall directly on the lake or flow over the land surface to the lake without first soaking in (e.g., MacDonald et al., 2000b). Lakes lose water to outflowing streams, groundwater, and by evaporation. If lake levels rise, the surface area will increase, increasing evaporative water loss, the area through which groundwater may leave and the hydraulic head that drives groundwater flow, as well as potentially opening new outlets. Because either an increase in precipitation or a reduction in evaporation will cause a lake level to rise, an independent estimate of either precipitation or evaporation is required before one can estimate the other on the basis of a history of lake levels (Barber and Finney, 2000). In some cases, where both long-term observational and paleolimnological data are available, the causative factors related to declining lake and pond water levels, including total desiccation of previously permanent water bodies, can be identified (Smol and Douglas, 2007a).

Former lake levels can be identified by deposits such as fossil shorelines (Fig. 15). Sometimes old shorelines are preserved under water and can be recognized in sonar surveys or other data, and these deposits can usually be dated. Furthermore, the sediments of the lake may retain a signature of lake-level fluctuations; coarse-grained material generally lies near the shore and finer grained materials offshore (Digerfeldt, 1988), and these too can be identified, sampled, and dated (Abbott et al., 2000).

For a given lake, modern values of the major inputs and outputs can be obtained empirically, and a model can then be constructed that simulates lake-level changes in response to changing precipitation and evaporation. Allowable pairs of precipitation and evaporation can then be estimated for any past lake level. Particularly in cases where precipitation is the primary control of water depth, it is possible to model lake level responses to past changes in precipitation (e.g., Vassiljev, 1998; Vassiljev et al., 1998). For interior Alaska, this technique suggested that precipitation at the Last Glacial Maximum was half the present value (Barber and Finney, 2000).

Fig. 15. Unnamed, hydrologically closed lake in the Yukon Flats Wildlife Refuge, Alaska. Concentric rings of vegetation developed progressively inward as water level fell, owing to a negative change in the lake's overall water balance. Historic Landsat imagery and air photographs indicate that these shorelines formed during within the last 40 years or so. (Photograph by Lesleigh Anderson.)

Biological groups living within lakes also leave fossil assemblages that can be interpreted in terms of lake level by comparing them with modern assemblages. In all cases, factors other than water depth (e.g., conductivity and salinity) may also influence the assemblages (MacDonald et al., 2000b), but these factors are themselves likely to be indirectly related to water depth. Aquatic plants, which are represented by pollen and macrofossils, tend to dominate from nearshore to moderate depths, and shifts in the abundance of pollen or seeds in one or more sediment profiles can indicate relative water-level changes (Hannon and Gaillard, 1997; Edwards et al., 2000). Diatom and chironomid (midge) assemblages may also be related quantitatively to lake depth by means of inverse modeling and the transfer functions used to reconstruct past lake levels (Korhola et al., 2000; Ilyashuk et al., 2005). For case studies, see, for example, Hannon and Gaillard (1997), Abbott et al. (2000), Edwards et al. (2000), Korhola et al. (2000) Pienitz et al. (2000), Anderson et al. (2005), and Ilyashuk et al. (2005).

3.12. Precipitation estimates from ice cores

Ice cores provide a direct way of recording the net precipitation rate at the core site. The initial thickness of an annual layer in an ice core (after mathematically accounting for the amount of air trapped in the ice) is the annual accumulation. Most ice cores are drilled in cold regions that produce little meltwater or runoff. Furthermore, sublimation, condensation and snowdrift generally are minimized so that the annual layer is a close approximation of the annual precipitation (Box et al., 2006). The thickness of layers deeper in the core must be corrected for the thinning produced as the ice sheet spreads under its own weight, but for most samples this correction can be made accurately with ice-flow models (e.g., Alley et al., 1993; Cuffey and Clow, 1997).

The annual-layer thickness also can be recorded using a component that varies regularly with a defined seasonal cycle. Suitable components include visible layering (e.g. Fig. 10a), which responds to changes in snow density or impurities (Alley et al., 1997), the seasonal cycle of water isotopes (Vinther et al., 2006),

and seasonal cycles in different chemical species (e.g. Rasmussen et al., 2006). Using more than one component gives extra security to the combined output of counted years and layer thicknesses.

Although the correction for strain (layer thinning) increases the uncertainty in estimates of absolute precipitation rate deeper in ice cores, estimates of changes in relative accumulation rate over subsections of the record along an ice core are more reliable (e.g., Kapsner et al., 1995). Because the accumulation rate combines with the temperature to control the rate at which snow is transformed to ice, and because the isotopic composition of the trapped air (Sowers et al., 1989) and the number of trapped bubbles in a sample (Spencer et al., 2006) record the results of that transformation, then accumulation rates can also be estimated from measurements of these parameters plus independent estimation of past temperature using techniques described above.

4. Early Cenozoic Warm Times

Records of the $\delta^{18}O$ of benthic foraminifera from the global ocean document a long-term cooling of the deep sea during the past 70 Ma (Fig. 16; Zachos et al., 2001) and the development of large Northern Hemisphere continental ice sheets 2.9–2.6 Ma ago (Duk-Rodkin et al., 2004). Because oceanic bottom waters originate in the polar oceans, Arctic climate history is broadly consistent with the global data reported by Zachos et al. (2001): general cooling and an increase in terrestrial ice volume through the Cenozoic was punctuated by short- and longer-lived reversals, by variations in cooling rate, and by additional features related to growth and shrinkage of ice once ice sheets were well established. A detailed Arctic Ocean record that is equivalent to the global results of Zachos et al. (2001) is not yet available. Because the Arctic Ocean is connected to the global ocean only by a single narrow deep channel and some intermittently exposed shallow shelves (e.g., Jakobsson and Macnab, 2006), the Arctic Ocean $\delta^{18}O$ record may differ from that of the other oceans as demonstrated by stable-isotopic data from Late Quaternary Arctic sediments (Polyak et al., 2004; Spielhagen et al., 2004; Adler et al., 2009). Emerging paleoclimate reconstructions from the Arctic Ocean derived from a recently recovered sediment record on the Lomonosov Ridge (Backman et al., 2006; Moran et al., 2006; Matthiessen et al., 2009) shed new light on the Cenozoic evolution of the Arctic Basin, but the data have yet to be fully integrated with evidence from high-latitude terrestrial records or with the other records from elsewhere in the Arctic Ocean.

Paleoclimate data clearly show warm Arctic conditions during the Cretaceous and early Cenozoic. For example, late Cretaceous Arctic Ocean temperatures of 15 °C (compared to ~-1.5 °C today) are indicated by TEX_{86}-based estimates (Jenkyns et al., 2004). The same indicator shows that peak Arctic Ocean temperatures near the North Pole rose from about 18 °C to more than 23 °C during the short-lived (multi-millennial) Paleocene-Eocene Thermal Maximum (PETM) about 55 Ma ago (Fig. 17; Moran et al., 2006; also see Sluijs et al., 2006, 2008). This rise was synchronous with warming on nearby lands from a previous temperature of about 17 °C to peak temperature during the PETM of about 25 °C (Weijers et al., 2007). By about 50 Ma ago, Arctic Ocean temperatures were about 10 °C and the relatively fresh surface waters were dominated by aquatic ferns (Brinkhuis et al., 2006). Restricted connections to the world ocean allowed the fern-dominated interval to persist for ~0.8 Ma. A return of more-vigorous interchange between the Arctic and North Atlantic oceans was accompanied by a warming in the central Arctic Ocean of about 3 °C (Brinkhuis et al., 2006). On Arctic lands during the Eocene (55–34 Ma), forests of *Metasequoia* dominated a landscape characterized by organic-rich floodplains and wetlands quite different from the modern tundra (McKenna, 1980; Francis, 1988; Williams et al., 2003).

Despite a widespread cooling and respective floral turnover at the Eocene-Oligocene transition ca 34 Ma ago (Wolfe, 1997; Zachos et al., 2008), terrestrial evidence shows that warm conditions persisted into the early Miocene (23–16 Ma ago), when the central Canadian Arctic Islands were covered in mixed conifer-hardwood forests similar to those of southern Maritime Canada and New England today (Whitlock and Dawson, 1990). *Metasequoia* was still present, although less abundant than in the Eocene. Deposits of the Beaufort Formation, thought to be of late Miocene or Pliocene age record an extensive riverside forest of pine, birch, and spruce that populated the Canadian Arctic Archipelago after a pronounced mid-Miocene cooling (White et al., 1997; Wolfe, 1997), but prior to the cutting the channels that now divide the islands.

During the well-documented warmth of the middle Pliocene (~3 Ma ago) forests occupied large regions near the Arctic Ocean that are currently polar deserts. Fossils of the marine bivalve *Arctica islandica*, that does not live where there is seasonal sea ice, found in marine deposits as young as 3.2 Ma old on Meighen Island at 80°N, likely record the peak Pliocene warmth of the ocean (Fyles et al., 1991). At a site on Ellesmere Island, paleoclimatic reconstructions based on ring-width and isotopic composition of wood suggest mean-annual temperatures 14 °C warmer than recently (Ballantyne

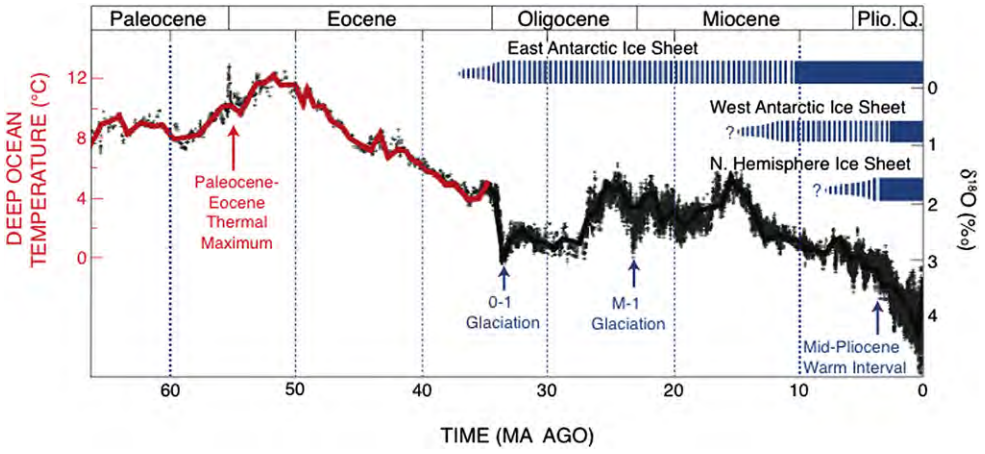

Fig. 16. Global compilation of more than 40 deep sea benthic $\delta^{18}O$ isotopic records taken from Zachos et al. (2001), updated with high-resolution Eocene through Miocene records from Billups et al. (2002), Bohaty and Zachos (2003), and Lear et al. (2004). Dashed blue bars, times when glaciers came and went or were smaller than now; solid blue bars, ice sheets of modern size or larger. (Figure and text modified from IPCC, 2007 Chapter 6, Paleoclimate, Jansen et al., 2007.)

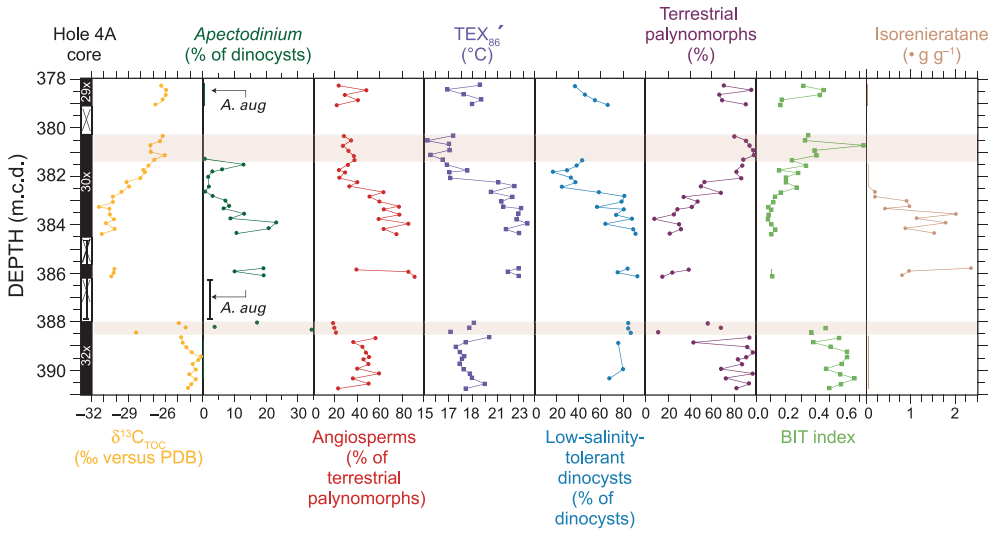

Fig. 17. Recovered sections and palynological and geochemical results across the Paleocene–Eocene Thermal Maximum about 55 Ma; IODP Hole 302-4A (87°52.00′N 136°10.64′E; 1288 m water depth, in the central Arctic Ocean basin). Mean annual surface-water temperatures (as indicated in the TEX_{86}' column) are estimated to have reached 23 °C, similar to water in the tropics today. (Error bars for Core 31X show the uncertainty of its stratigraphic position. Orange bars, indicate intervals affected by drilling disturbance.) Stable carbon isotopes are expressed relative to the PeeDee Belemnite standard. Dinocysts tolerant of low salinity comprise *Senegalinium* spp., *Cerodinium* spp., and *Polysphaeridium* spp., whereas *Membranosphaera* spp., *Spiniferites ramosus* complex, and *Areoligera-Glaphyrocysta* cpx. represent typical marine species. Arrows and *A. aug* (second column) indicate the first and last occurrences of dinocyst *Apectodinium augustum* – a diagnostic indicator of Paleocene-Eocene Thermal Maximum warm conditions (Sluijs et al., 2006). [Reprinted by permission from Macmillan Publishers Ltd.]

et al., 2006). Additional data from beetles and plants indicate mid-Pliocene conditions as much as 10 °C warmer than recently for mean summer conditions, and even larger wintertime warming to a maximum of 15 °C or more (Elias and Matthews, 2002). Although continental configurations were similar to modern, forests extended to the Arctic shoreline, nearly eliminating the Arctic tundra biome (Salzmann et al., 2008), and sea level reached ~25 m higher than present, implying much smaller Greenland and Antarctic ice sheets.

Much attention has been focused on learning the causes of the gradual transition from Cretaceous hothouse temperatures to the Quaternary ice age. Changes in greenhouse-gas concentrations appear to have played the dominant role, with changes in continental positions, sea level, and oceanic circulation also contributing.

Based on general circulation models, Barron et al. (1993) found that estimated changes in continental positions had little effect on the difference between Cretaceous and modern temperatures (also see Poulsen et al., 1999 and references therein). However, new climate models (Donnadieu et al., 2006), suggest that continental motions may have altered atmospheric and oceanic circulation to produce global average temperature changes of almost 4 °C from Early to Late Cretaceous. This result does not compare directly with modern conditions, but it does suggest that continental motions can notably affect climate. However, despite much effort, modeling does not indicate that the motion of continents by itself can explain either the long-term cooling trend from the Cretaceous to the Quaternary or the fluctuations within that cooling.

The direct paleoclimatic data provide one interesting perspective on the role of oceanic circulation in the warmth of the later Eocene. When the Arctic Ocean was brackish and water ferns (*Azolla* spp.) covered an ice-free ocean, meridional oceanic currents must have been weak relative to today for the fresh water to persist. Thus, heat transport by oceanic currents cannot explain the Arctic Ocean warmth of that time. The resumption of stronger currents and normal salinity was accompanied by a warming of about 3 °C (Brinkhuis et al., 2006); important, yes, but not the dominant difference in temperature between then and now.

Atmospheric CO_2 concentration has changed during the Cenozoic in response to many processes, but especially to those processes linked to plate tectonics and perhaps also to biological evolution. Many lines of proxy evidence (see Royer, 2006) show that atmospheric CO_2 was higher in the warm Cretaceous than it has been recently, and that it subsequently fell in parallel with the cooling (Fig. 18). Furthermore, climate models find that the changing CO_2 concentration is sufficient to explain much of the reconstructed cooling (e.g., Bice et al., 2006; Donnadieu et al., 2006).

A persistent difficulty is that models driven by changes in greenhouse gases (mostly CO_2) tend to underestimate Arctic warmth (e.g., Sloan and Barron, 1992). Many possible explanations have been offered for this situation: underestimation of CO_2 levels (Shellito et al., 2003; Bice et al., 2006); an enhanced greenhouse

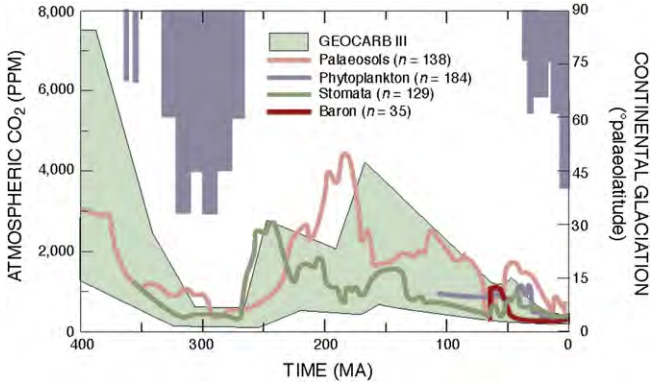

Fig. 18. Atmospheric CO_2 and continental glaciation 400 Ma to present. Vertical blue bars, timing and palaeolatitudinal extent of ice sheets (after Crowley, 1998). Plotted CO_2 records represent five-point running averages from each of four major proxies (see Royer, 2006 for details of compilation). Also plotted are the plausible ranges of CO_2 derived from the geochemical carbon cycle model GEOCARB III (Berner and Kothavala, 2001). All data adjusted to the Gradstein et al. (2004) time scale. Continental ice sheets grow extensively when CO_2 is low. (After Jansen et al., 2007, in IPCC, 2007 Fig. 6.1)

effect from polar stratospheric clouds during warm times (Sloan and Pollard, 1998; Kirk-Davidov et al., 2002); changed planetary obliquity (Sewall and Sloan, 2004); reduced biological productivity that provided fewer cloud-condensation nuclei and thus fewer reflective clouds (Kump and Pollard, 2008); and greater heat transport by tropical cyclones (Korty et al., 2008). Several of these mechanisms use feedbacks not normally represented in climate models that serve to amplify warming in the Arctic. Consideration of the literature cited above and of additional materials suggests some combination of stronger greenhouse-gas forcing (see Alley, 2003 for a review) and stronger long-term positive feedbacks than typically are included in models, rather than to a large change in Earth's orbit, although that cannot be excluded.

The Paleocene-Eocene Thermal Maximum (PETM) offers support for the hypothesis that greenhouse gases were the primary Cenozoic control on Arctic temperature changes because this rapid temperature increase occurred in the absence of any ice – and therefore the absence of any ice-albedo or snow-albedo feedbacks. This thermal maximum was achieved by a rapid (within a few centuries or less), widespread warming coincident with a large increase in atmospheric greenhouse-gas concentrations from a biological source (whether from sea-floor methane, living biomass, soils, or other sources remains debated; see Sluijs et al., 2008 for an extensively referenced summary of the event together with new data pertaining to the Arctic). Following the thermal maximum, the anomalous warmth decayed more slowly and the extra greenhouse gases dissipated over tens of thousands of years. In the Arctic the PETM occurred within a longer interval of restricted oceanic circulation into the Arctic Ocean (Sluijs et al., 2008), and it was too fast for any notable role from plate tectonics or evolving life. The reconstructed CO_2 change thus is strongly implicated in the warming (e.g., Zachos et al., 2008).

Taken very broadly, the Arctic changes parallel global changes during the Cenozoic, except that changes in the Arctic were larger than those globally averaged (e.g., Sluijs et al., 2008). In general, global and Arctic temperature trends parallel changing atmospheric CO_2 concentrations, which is the likely cause for most of the temperature change (e.g., Royer, 2006; Royer et al., 2007).

The well-documented warmth of the Arctic during the middle Pliocene remains somewhat enigmatic. Continental positions and ocean gateways were essentially the same as today, although sea level was ~25 m higher than present so that the Pacific connection to the Arctic Ocean may have allowed a greater exchange of waters that at present. It is also likely that the ocean transported more heat into the Arctic from the Atlantic during peak Pliocene warmth (Korty et al., 2008; Dowsett et al., 2009; Robinson, 2009), although the status of Arctic Ocean sea ice remains uncertain. Mid-Pliocene atmospheric CO_2 concentrations are estimated to have been $\sim 400 \pm 50$ ppmv (e.g. Kurschner et al., 1996; Raymo et al., 1996; Tripati et al., 2009; Pagani et al., 2010), which is statistically indistinguishable from the present atmospheric concentration of ~385 ppmv. The high-latitude warmth thus is likely to have originated primarily from changes in greenhouse-gas concentrations in the atmosphere, amplified by changes in oceanic or atmospheric circulation; other processes also may have contributed.

5. The Early Quaternary: ice-age warm times

Although scattered evidence for ice-rafted debris of possible glacial origin in high-latitude Northern Hemisphere oceans has been suggested to infer the development of glaciers and ice sheets at several stages starting as early as 47 Ma ago (e.g., Moran et al., 2006; Eldrett et al., 2007; Tripati et al., 2008), major growth of Arctic ice sheets and related reorganization of the climate system occurred between 3.0 and 2.5 Ma ago. As a result, the first large Northern Hemisphere continental ice sheets developed in the North American and Eurasian Arctic, marking the onset of the Quaternary Ice Age (Raymo, 1994). For the first 1.5–2.0 Ma, ice-age cycles appeared at 41 ka intervals, as the climate oscillated between glacial and interglacial states (Fig. 19). Among the prominent but apparently short-lived interglaciations during this period is one at about 2.4 Ma that is recorded especially well in the Kap København Formation, a 100-m-thick sequence of estuarine sediments that covered an extensive lowland area near the northern tip of Greenland (Funder et al., 2001).

The rich and well-preserved fossil fauna and flora in the Kap København Formation (Fig. 20) record warming from cold conditions into an interglacial followed by cooling during the subsequent 10–20 ka. During the peak warmth, forest trees reached the Arctic Ocean coast, 1000 km north of the northernmost trees today. Based on this warmth, Funder et al. (2001) suggested that the Greenland Ice Sheet must have been reduced to local ice caps in mountain areas (Fig. 20a). Although finely resolved time records are not available throughout the Arctic Ocean at that time, by analogy with present faunas along the Russian coast, the coastal zone would have been ice-free for 2–3 months in summer. Today this coast of Greenland experiences year-round sea ice, and models of diminishing sea ice in a warming world generally indicate long-term persistence of summertime sea ice off these shores (e.g., Holland et al., 2006). Thus, the reduced sea ice off northern Greenland during deposition of the Kap København Formation suggests a widespread interglacial during which Arctic sea ice was greatly diminished.

During the warm interval described above, precipitation was greater and temperatures were higher than at the peak of the current interglaciation, about 7 ka ago, and the temperature difference was larger during winter than during summer. Higher temperatures were not caused by notably greater solar insolation, owing to the relative repeatability of the Milankovitch variations over millions of years (e.g., Berger et al., 1992). Uncertainties in atmospheric CO_2 concentration, ocean heat transport, and perhaps other factors at the time of the Kap København Formation are sufficiently large to preclude strong conclusions about the causes of the unusual warmth.

Potentially correlative records of warm Early Quaternary interglacial conditions are found in deposits along coastal plains in northern and western Alaska. Interglacial marine transgressions that repeatedly flooded the Bering Strait modified the configuration of adjacent coastlines, altered regional continentality and reinvigorated the exchange of water masses between the North Pacific, Arctic, and North Atlantic oceans. Since the first submergence of the Bering Strait about 5.5–5.0 Ma ago (Marincovich and Gladenkov, 2001), this marine gateway allowed relatively warm Pacific water to reach as far north as the Beaufort Sea (Brigham-Grette and Carter, 1992). The Gubik Formation of northern Alaska records at least three warm high sea stands in the early Quaternary (Fig. 21). During the Colvillian transgression, about 2.7 Ma, the Alaskan Coastal Plain supported open boreal forest or spruce-birch woodland with scattered pine and rare fir and hemlock (Nelson and Carter, 1991). Warm marine conditions are confirmed by the general character of the ostracode fauna, which includes *Pterygocythereis vannieuwenhuisei* (Brouwers, 1987), an extinct species of a genus whose modern northern limit is the Norwegian Sea and which, in the northwestern Atlantic Ocean, is not found north of the southern cold-temperate zone (Brouwers, 1987). Despite the high sea level and relative warmth indicated by the Colvillian transgression, erratics (rocks not of local origin) in Colvillian deposits southwest of Barrow, Alaska, indicate that glaciers then terminated in the Arctic Ocean and produced icebergs large enough to reach northwest Alaska at that time.

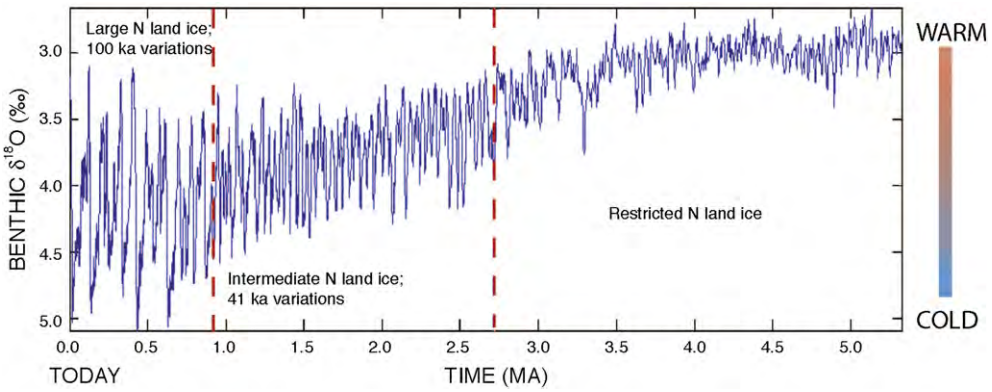

Fig. 19. The average isotopic composition ($\delta^{18}O$) of bottom-dwelling foraminifera from a globally distributed set of 57 sediment cores that record the last 5.3 Ma (modified from Lisiecki and Raymo, 2005). The $\delta^{18}O$ is controlled primarily by global ice volume and deep-ocean temperature, with less ice or warmer temperatures (or both) upward in the core. The influence of Milankovitch frequencies of Earth's orbital variation are present throughout, but glaciation increased about 2.7 Ma ago concurrently with establishment of a strong 41 ka variability linked to Earth's obliquity (changes in tilt of Earth's spin axis), and the additional increase in glaciation about 1.2–0.7 Ma parallels a shift to stronger 100 ka variability. Dashed lines are used because the changes seem to have been gradual. The general trend toward higher $\delta^{18}O$ that runs through this series reflects the long-term drift toward a colder Earth that began in the early Cenozoic (see Fig. 16). http://lorraine-lisiecki.com/stack.html

The subsequent Bigbendian transgression (about 2.5 Ma ago), characterized by rich molluscan faunas including the gastropod *Littorina squalida* and the bivalve *Clinocardium californiense* (Carter et al., 1986), indicates renewed warmth along northern Alaska. The modern northern limit of both of these mollusk species is well to the south (Norton Sound, Alaska). The presence of sea otter bones suggests that the limit of seasonal ice on the Beaufort Sea was restricted during the Bigbendian interval to positions north of the Colville River and thus well north of typical 20th-century positions (Carter et al., 1986); modern sea otters cannot tolerate severe seasonal sea-ice conditions (Schneider and Faro, 1975).

The Fishcreekian transgression (about 2.4–2.1 Ma ago) has been correlated with the Kap København Formation on Greenland (Brigham-Grette and Carter, 1992). However, age control is imprecise, and Brigham (1985) and Goodfriend et al. (1996) suggested that the Fishcreekian could be as young as 1.4 Ma. This deposit contains several mollusk species that currently are found only south of the winter sea ice margin. Moreover, sea otter remains and the intertidal gastropod *Littorina squalida* at Fish Creek suggest that perennial sea ice was absent or severely restricted during the Fishcreekian transgression (Carter et al., 1986). Correlative deposits rich in mollusk species that currently live only well to the south are reported from the coastal plain at Nome, Alaska (Kaufman and Brigham-Grette, 1993).

The available data clearly indicate episodes of relatively warm conditions that correlate with high sea levels and reduced sea ice in the early Quaternary. The high sea levels suggest the melting of land ice. Thus the correlation of warmth with diminished ice on land and at sea is analogous to features of contemporary change, as indicated by recent instrumental observations, model results, and data from other time intervals.

6. The Mid-Pleistocene Transition (MPT): 41 ka and 100 ka worlds

Throughout the Quaternary the cyclical waxing and waning of continental ice sheets has dominated global climate variability in response to variations in solar insolation caused by features of Earth's orbit. After the onset of glaciation in North America about 2.7 Ma ago (Raymo, 1994), ice grew and shrank as Earth's obliquity (tilt) varied in its 41 ka cycle. But between 1.2 and 0.7 Ma, the variations in ice volume became larger and slower, and an approximately 100-ka period has dominated during the last 700 ka or so (Fig. 19). Although Earth's eccentricity varies with an

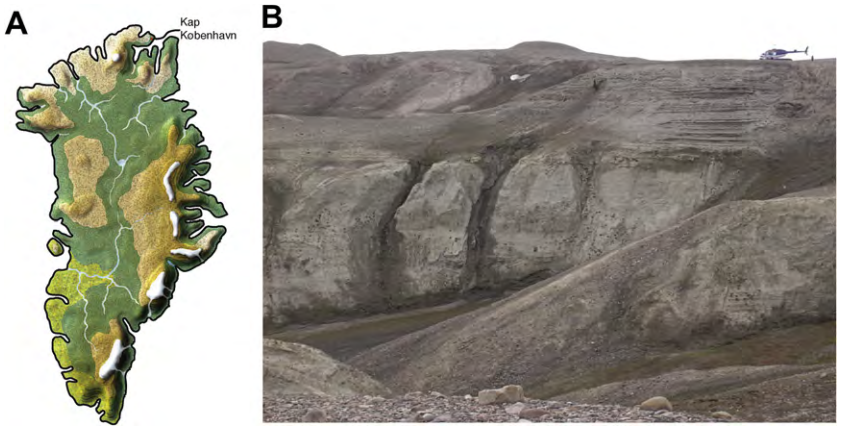

Fig. 20. (A) Greenland without ice for the last time? Dark green, boreal forest; light green, deciduous forest; brown, tundra and alpine heaths; white, ice caps. The north-south temperature gradient is constructed from a comparison between North Greenland and northwest European temperatures, using standard lapse rate; distribution of precipitation assumed to retain the Holocene pattern. Topographical base, from model by Letreguilly et al. (1991) of Greenland's sub-ice topography after isostatic recovery. (B) Upper part of the Kap København Formation, North Greenland. The sand was deposited in an estuary about 2.4 Ma; it contains abundant well-preserved leaves, seeds, twigs, and insect remains. (Figure and Photograph of by S.V. Funder.).

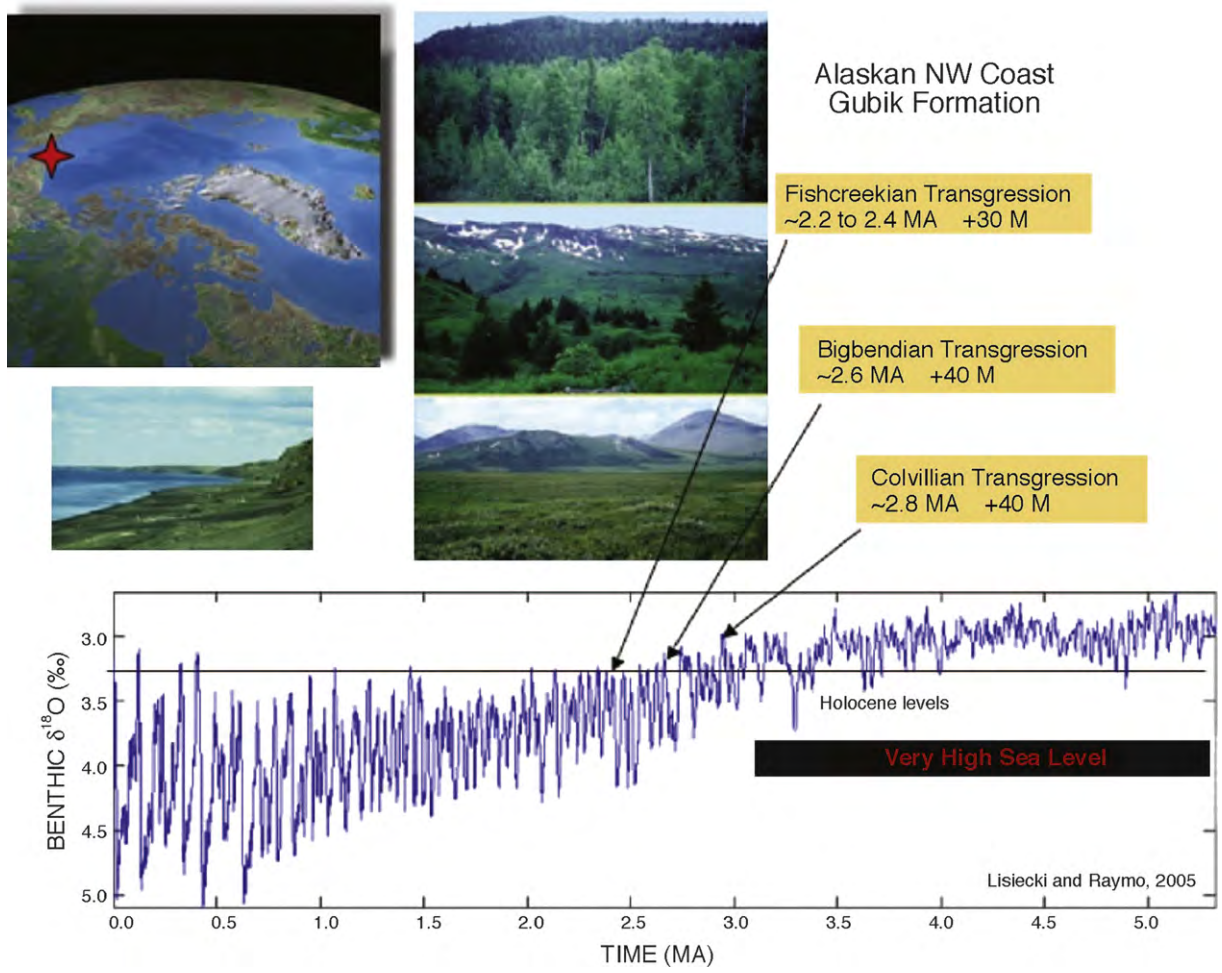

Fig. 21. The largely marine Gubik Formation, North Slope of Alaska, contains three superposed lower units that record relative sea level as high +30 to +40 m. Pollen in these deposits suggests that borderland vegetation at each of these times was less forested; boreal forests or spruce-birch woodlands at 2.7 Ma gave way to larch and spruce forests at about 2.6 Ma and to open tundra by about 2.4 Ma (see photographs by Robert Nelson, Colby College, who analyzed the pollen; oldest at top). Isotopic reference time series of Lisiecki and Raymo (2005) suggests best as assignments for these sea level events (Brigham-Grette and Carter, 1992). [Reprinted by permission Arctic Institute of North America.]

approximately 100 ka period, this variation does not cause as much change in solar insolation in the key regions of ice growth as do precession and obliquity cycles, so eccentricity in unlikely to be the cause of this change; the reason for the dominant 100 ka period in ice volume remains obscure.

The MPT is of particular interest because it does not seem to have been caused by any major change in Earth's orbital behavior, and so the transition likely reflects a fundamental threshold within the climate system. Models for the 100 ka variability commonly assign a major role to the ice sheets themselves and especially to the Laurentide Ice Sheet, which dominated the total global change in ice volume (e.g., Marchant and Denton, 1996). Roe and Allen (1999) assessed six different explanations of this behavior and found that all fit the data rather well; no one model has superiority over another.

A key observation that must be satisfied in any explanation for this change is that the ice sheets of the last 700 ka were larger in volume but smaller in area than were earlier ice sheets (Boellstorff, 1978; Balco et al., 2005a,b; Clark et al., 2006). Clark and Pollard (1998) used this observation to argue that the early Laurentide Ice Sheets must have had a substantially lower surface elevation than in the late Pleistocene, possibly by as much as 1 km. They argued that at the onset of the Quaternary, ice sheets advanced over easily deformed water-saturated weathered terrain. The low basal shear strength allowed fast ice flow, producing aerial extensive, but relatively thin ice sheets. Successive glacial cycles gradually eroded the regolith, eventually exposing irregular bedrock in the central region. With increased resistance to basal sliding, the ice sheets eventually became thicker with a steeper surface profile, but not quite as extensive aerially as the early Quaternary ice sheets, despite their greater ice volume.

Other hypotheses emphasize the gradual global cooling that began in the early Cenozoic (Raymo et al., 1997, 2006; Ruddiman, 2003). If, for example, the 100-ka cycle requires that the Laurentide Ice Sheet grow sufficiently large and thick to trap enough of Earth's internal heat that thaws the ice-sheet bed, then long-term cooling may have reached the threshold at which the ice sheet became thick enough. Marshall and Clark (2002) modeled the growth and decay of the Laurentide Ice Sheet and found that during growth the ice was frozen to its bed, decreasing flow velocities. After many tens of thousands of years, the modeled ice had thickened sufficiently to trap enough geothermal heat to thaw the bed, which allowed faster flow. Faster flow of the ice sheet lowered the surface gradient, which allowed warming and melting. Behavior such as that described could cause the main variations of ice volume to be slower than the orbitally driven variations in insolation. Alternative hypotheses require interactions in the Southern Ocean between the ocean and sea ice and between the ocean and

the atmosphere (Gildor et al., 2002). For example, Toggweiler (2008) suggested that because of the close connection between the southern westerly winds and meridional overturning circulation in the Southern Ocean, shifts in wind fields could control the exchange of CO_2 between the ocean and the atmosphere. Carbon models support the notion that weathering and the burial of carbonate can be perturbed in ways that alter deep ocean carbon storage and result in 100 ka CO_2 cycles. Others have suggested that 100 ka cycles and CO_2 might be controlled by variability in obliquity cycles (i.e., two or three 41 ka cycles Huybers, 2006) or by variable precession cycles (altering the 19 ka and 23 ka cycles; Raymo, 1997). Ruddiman (2006) recently furthered these ideas but suggested that since 900 ka ago, CO_2-amplified ice growth continued at the 41 ka intervals but that polar cooling dampened ice ablation. His CO_2-feedback hypothesis suggests a mechanism that combines the control of 100 ka cycles with precession cycles (19 ka and 23 ka) and with tilt cycles (41 ka).

Other hypotheses also exist for these changes. A complete explanation of the onset of extensive glaciation on North America and Eurasia as well as Greenland about 2.8 Ma ago, or of the transition from 41 ka to 100 ka ice-age cycles, remains the object of ongoing investigations.

7. A link between ice volume, air temperature and greenhouse gases

The globally averaged temperature decrease during the 100-ka ice-age cycles was about 5–6 °C (Jansen et al., 2007). Larger decreases are calculated for the Arctic and close to the ice sheets, with a decrease of ~22 °C atop the Greenland Ice Sheet at the last glacial maximum (Cuffey et al., 1995). The total change in solar radiation reaching the planet during these cycles was near zero, but orbital features served primarily to change insolation seasonally and geographically.

Many factors probably contributed to this large temperature change despite the small global change in total insolation (Jansen et al., 2007). Cooling produced growth of reflective ice that increased the planetary albedo, while the great height of the ice sheets on its own reduced Arctic temperatures as well. Complex changes, especially in the ocean, reduced atmospheric carbon dioxide concentrations, and both oceanic and terrestrial changes reduced atmospheric water vapor, methane and nitrous oxide, all of which are greenhouse gases; changes in water vapor and carbon dioxide were most important. Increasing aridity in some areas and glacial outwash in others produced additional dust that reduced the flux of insolation reaching the planet's surface (e.g., Mahowald et al., 2006). Cooling caused regions formerly forested to give way to grasslands, tundra or dune fields, further increasing the planetary albedo. While Earth's orbital features paced the ice-age cycles, strong positive feedbacks are required to provide quantitatively accurate explanations of the observed glacial and interglacial changes.

The relation between climate and carbon dioxide has been strongly correlated for at least the past 800 ka (Siegenthaler et al., 2005, Fig. 22, Lüthi et al., 2008), and the growth and shrinkage of ice, cooling and warming of the globe, and other changes have repeated along similar, although not identical paths. Differences between some successive cycles that are of interest are discussed next.

8. Marine Isotopic Stage 11 – a long interglaciation

Following the mid-Pleistocene transition, the growth and decay of ice sheets followed a 100 ka cycle: brief, warm interglaciations lasted 10 to about 40 ka, after which ice progressively increased in volume to a maximum, before ice volumes decreased rapidly and the planet transitioned into the next interglaciation (e.g., Kellogg, 1977; Ruddiman et al., 1986; Jansen et al., 1988; Heinrich and Baumann, 1994; Bauch and Erlenkeuser, 2003). As discussed above, this 100 ka cycle is unlikely to be linked to the changes in the eccentricity of Earth's orbit about the Sun because the 100 ka eccentricity cycle produces so little change in solar isolation reaching the Earth.

The eccentricity exhibits an additional cycle of ~400 ka; Earth's orbit goes from almost round to more eccentric to almost round in about 100 ka, but the maximum eccentricity reached in these 100-ka cycles increases and decreases within a 400-ka cycle (Berger and Loutre, 1991; Loutre, 2003). When the orbit is almost round, there is little effect from Earth's precession. But, about 400 ka ago, during marine isotope stage (MIS) 11, the 400-ka cycle caused a nearly round orbit to persist. The MIS 11 interglaciation lasted longer than previous or subsequent interglaciations (see Droxler et al., 2003 and references therein; Kandiano and Bauch, 2007; Jouzel et al., 2007), perhaps because the summer insolation at high northern latitudes did not become low enough at the end of the first 10 ka precession hemicycle to allow ice growth in the Arctic. When Earth's orbit is nearly round, there is little change in insolation during a precession cycle (Fig. 23).

Mid- and low-latitude paleoclimate records show that MIS 11 lasted ~30 ka, rather than the typical 10 ka duration, but sediments containing MIS 11 are rare in the Arctic (cf. Kaufman and Brigham-Grette, 1993) and their temperature signals are inconclusive (see Stanton-Frazee et al., 1999; Bauch et al., 2000; Droxler and Farrell, 2000; Helmke and Bauch, 2003). Sea level during MIS 11 was higher than at any time since (cf. Olson and Hearty, 2009), and data from Greenland are consistent with notable shrinkage or loss of the ice sheet accompanying the long warmth, although the dating is poorly constrained (Willerslev et al., 2007).

9. Marine Isotopic Stage 5e: The Last Interglaciation

The warmest millennia of at least the past 250,000 years occurred during MIS 5, and especially during the warmest part of that interglaciation, MIS 5e (McManus et al., 1994; Fronval and Jansen, 1997; Bauch et al., 1999; Kukla, 2000). At that time global ice volumes were smaller than they are today, and Earth's orbital parameters aligned to produce a strong positive anomaly in solar radiation during summer throughout the Northern Hemisphere (Berger and Loutre, 1991). Between 130 and 127 ka, the average solar radiation during the key summer months (May, June, and July) was about 11% greater than solar radiation at present throughout the Northern Hemisphere, and a slightly greater anomaly, 13%, existed over the Arctic. Greater solar energy in summer, melting of the large Northern Hemisphere ice sheets, and intensification of the North Atlantic Drift (Chapman et al., 2000; Bauch and Kandiano, 2007) combined to reduce Arctic Ocean sea ice, allow expansion of boreal forest to the Arctic Ocean shore throughout large regions, reduce permafrost, and melt almost all glaciers in the Northern Hemisphere (CAPE Last Interglacial Project Members, 2006).

High solar radiation in summer during MIS 5e, amplified by key boundary-condition feedbacks (especially sea ice, seasonal snow cover, and atmospheric water vapor), collectively produced summer temperature anomalies 4–5 °C above present over most Arctic lands (CAPE Last Interglacial Project Members, 2006), substantially above the average Northern Hemisphere summer temperature anomaly (1 ± 1 °C above present; CLIMAP Project Members, 1984; Bauch and Erlenkeuser, 2003). MIS 5e demonstrates the strength of positive feedbacks on Arctic warming (CAPE Last Interglacial Project Members, 2006; Otto-Bliesner et al., 2006).

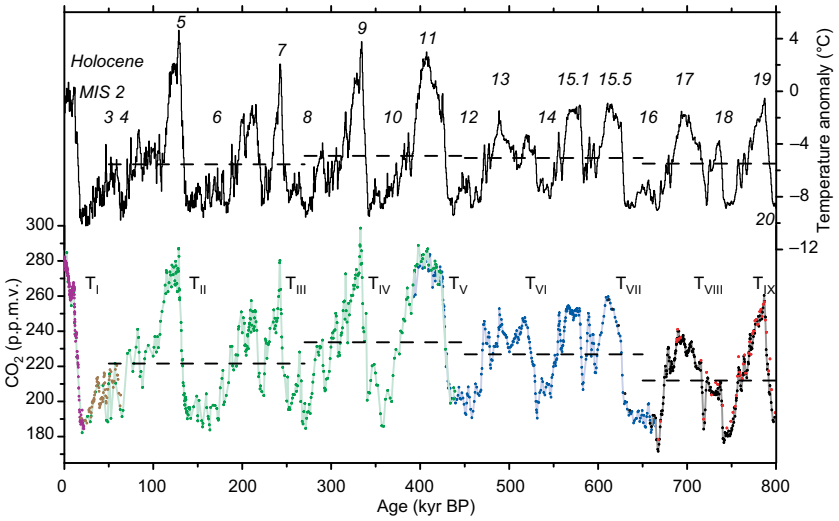

Fig. 22. Compilation of CO_2 records and EPICA Dome C temperature anomaly over the past 800 ka from Lüthi et al. (2008). The Dome C temperature anomaly record with respect to the mean temperature of the last millennium (based on original deuterium data interpolated to a 500-year resolution), plotted on the EDC3 timescale, is given as a black step curve. Data for CO_2 are from Dome C (solid circles in purple, blue, black: this work, measured at Bern; red open circles: this work, measured at Grenoble), Taylor Dome (brown) and Vostok (green). All CO_2 values are on the EDC3_gas_a age scale. Horizontal lines are the mean values of temperature and CO_2 for the time periods 799–650, 650–450, 450–270 and 270–50 ka BP. Glacial terminations are indicated using Roman numerals in subscript (for example TI); Marine Isotope Stages (MIS) are given in italic Arabic numerals. [Copyright 2008, reprinted with permission from Nature Publishing Group]

9.1. Terrestrial MIS 5e records

Summers throughout the Arctic were warmer during MIS 5e than at present, but the magnitude of warming differed spatially (Fig. 24). Positive summer temperature anomalies were largest around the Atlantic sector, where summer warming was typically 4–6 °C. This anomaly extended into Siberia, but it decreased from Siberia westward to the European sector (0–2 °C), and eastward toward Beringia (2–4 °C). The Arctic coast of Alaska had sea-surface temperatures 3 °C above recent values and considerably less summer sea ice than recently, but much of interior Alaska had smaller anomalies (0–2 °C) that probably extended into western Canada. In contrast, northeastern Canada and parts of Greenland had summer temperature anomalies of about 5 °C, and perhaps more. A stratified lacustrine sequence from the eastern Canadian Arctic the captures the penultimate interglacial, as well as MIS 5e and the Holocene suggests that for at least this portion of the Arctic, only full interglacials were warm enough for lakes to be ice-free in summers long enough for the preservation of biotic-bearing sediment; the record also suggested that 20th Century warming represents a no-analogue situation for the lake (Axford et al., 2009).

Precipitation and winter temperatures are more difficult to reconstruct for MIS 5e than are summer temperatures. In northeastern Europe, the latter part of MIS 5e was characterized by a marked increase in winter temperatures. A large positive winter temperature anomaly also occurred in Russia and western Siberia, although the timing is not as well constrained (Troitsky, 1964; Gudina et al., 1983; Funder et al., 2002). Qualitative precipitation estimates for most other sectors indicate wetter conditions than in the Holocene.

9.2. Marine MIS 5e records

Low sedimentation rates in the central Arctic Ocean and the rare preservation of carbonate fossils limit the number of sites at which MIS 5e can be reliably identified in sediment cores. Peak concentrations of a foraminifer species that usually dwells in subpolar waters were found in MIS 5e zones and interpreted to indicate relatively warm interglacial conditions and much reduced sea-ice cover in the interior Arctic Ocean (Nørgaard-Pedersen et al., 2007a, b; Adler et al., 2009). Interpretation of these and other proxies is complicated by the strong vertical stratification in the Arctic Ocean; today, warm Atlantic water (>1 °C) is in most areas isolated from the atmosphere by a relatively thin layer of cold (<-1 °C) low-salinity surface layer, limiting the transfer of heat to the atmosphere. It is not always possible to determine whether subpolar foraminifera found in Arctic Ocean sediment cores lived in warm waters that remained isolated from the atmosphere below the cold surface layer, or whether the warm Atlantic water had displaced the cold surface layer and was interacting with the atmosphere and affecting its energy balance.

Landforms and fossils from the western Arctic and Bering Strait indicate vastly reduced sea ice during MIS 5 (Fig. 25). The winter sea-ice limit is estimated to have been as much as 800 km farther north than its average 20th-century position, and summer sea ice was likely to have been much reduced relative to present (Brigham-Grette and Hopkins, 1995). These reconstructions are consistent with the northward migration of treeline by hundreds of kilometers throughout much of Alaska and the expansion of treeline to the Arctic Ocean coast in the Far East of Russia (Lozhkin and Anderson, 1995).

10. Marine Isotopic Stage 3 Warm Intervals

The Arctic temperature and precipitation history through MIS 3 (about 70–30 ka ago) is difficult to reconstruct because of the paucity of continuous records and the difficulty in providing a secure time frame. The $\delta^{18}O$ record of temperature change over the Greenland Ice Sheet and other ice-core data show that the North Atlantic region experienced repeated episodes of rapid, high-magnitude climate change, when temperatures rapidly increased by as much as 15 °C (reviewed by Alley, 2007 and references therein), and that each warm period lasted several hundred to a few thousand years. These brief climate excursions are found not only in the Greenland Ice Sheet but are also recorded in cave sediments in China and Yemen (Wang et al., 2001; Burns et al., 2003; Dykoski et al., 2005), in high-resolution marine records off California (Behl and Kennett, 1996), and sediment cores from the Cariaco Basin

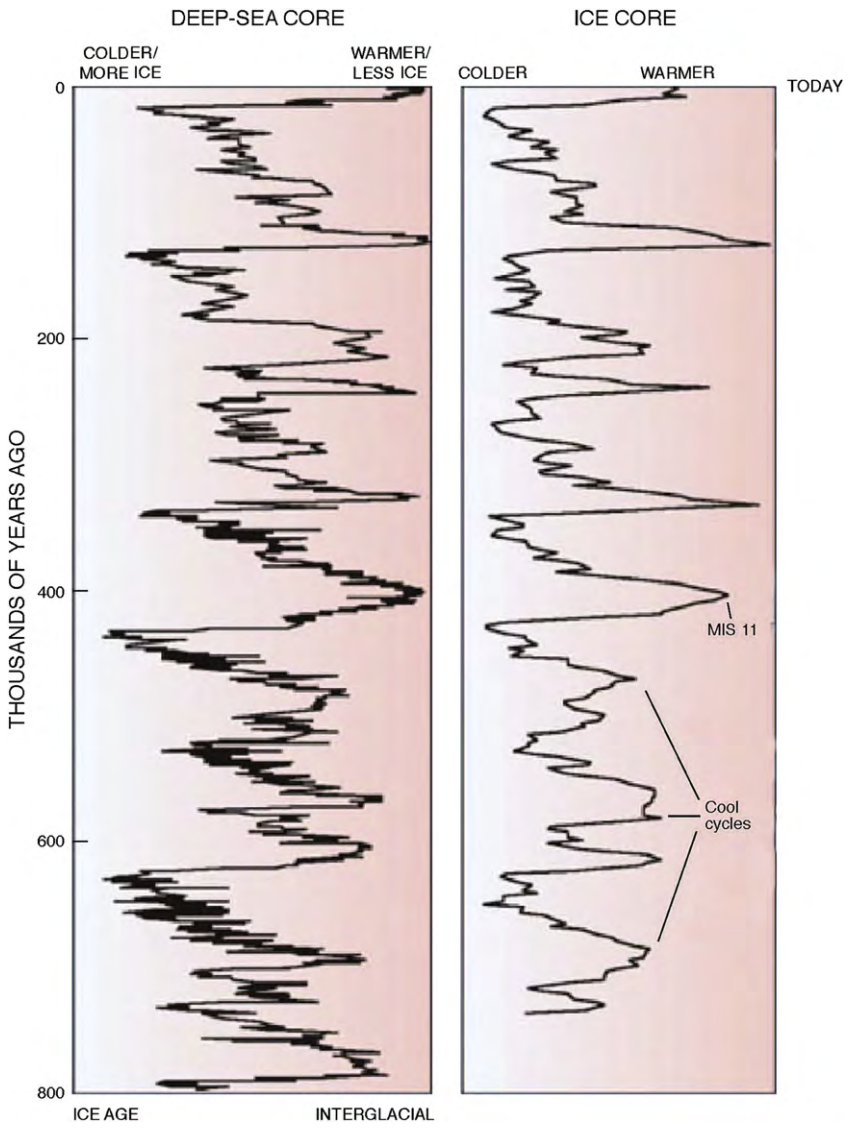

Fig. 23. Glacial cycles of the past 800 ka derived from marine-sediment and ice cores (McManus, 2004). The history of deep-ocean temperatures and global ice volume inferred from $\delta^{18}O$ measured in bottom-dwelling foraminifera shells preserved in Atlantic Ocean sediments. Air temperatures over Antarctica inferred from the ratio of deuterium to hydrogen in ice from central Antarctica (EPICA, 2004). Marine isotope stage 11 (MIS 11) is an interglacial whose orbital parameters were similar to those of the Holocene, yet it lasted about twice as long as most interglacials. Note the smaller magnitude and less-pronounced interglacial warmth of the glacial cycles that preceded MIS 11. Interglaciations older than MIS 11 were less warm than subsequent integlaciations. [Reprinted by permission from Macmillan Publishers Ltd.]

(Hughen et al., 1996.), the Arabian Sea (Schulz et al., 1998) and the Sea of Okhotsk (Nürnberg and Tiedemann, 2004), among many other sites. Proxies in Greenland ice cores reflect climate change in distant as well as local regions. For example, most of the methane trapped in ice-core bubbles was produced in tropical wetlands; none was produced on Greenland (Severinghaus et al., 1998). These ice-core records demonstrate clearly that climate changes were broadly synchronous across wide areas, and that the timing of these changes agrees within the stated uncertainties. Rapid climate changes within MIS 3 were thus hemispheric to global in nature (see review by Alley, 2007) and are considered a sign of large-scale coupling between the crysophere, ocean, and atmosphere (Bard, 2002). The cause of these events is still debated. However, Broecker and Hemming (2001) and Bard (2002) among others suggested that they were likely the result of major and abrupt reorganizations of the ocean's thermohaline circulation, probably related to ice sheet instabilities that introduced large quantities of fresh water and icebergs into the North Atlantic (Alley, 2007). Such large and abrupt oscillations were linked to changes in North Atlantic surface conditions and probably to large-scale oceanic circulation. Such abrupt changes, persisted into the Holocene (MIS 1), although still linked to an ice-age cause. The youngest was only about 8.2 ka ago when a large lake dammed by the receding Laurentide Ice Sheet flooded catastrophically when the ice-dam failed (Barber et al., 1999; Alley and Ágústsdóttir, 2005).

During MIS 3 ice sheets were somewhat reduced compared with ice volumes during MIS 2 and MIS 4, and sea level was slightly higher, but the coastline was still well offshore in most places, and the increased continentality very likely contributed to relatively high summer temperatures that presumably were offset by colder winters. For example, on the New Siberian Islands in the East Siberian Sea, Andreev et al. (2001) documented the existence of graminoid-rich tundra covering wide areas of the emergent shelf during MIS 3, with summer temperatures possibly 2 °C higher than during the 20th century. At Elikchan 4 Lake in the upper Kolyma drainage, the sediment record contains at least three MIS 3

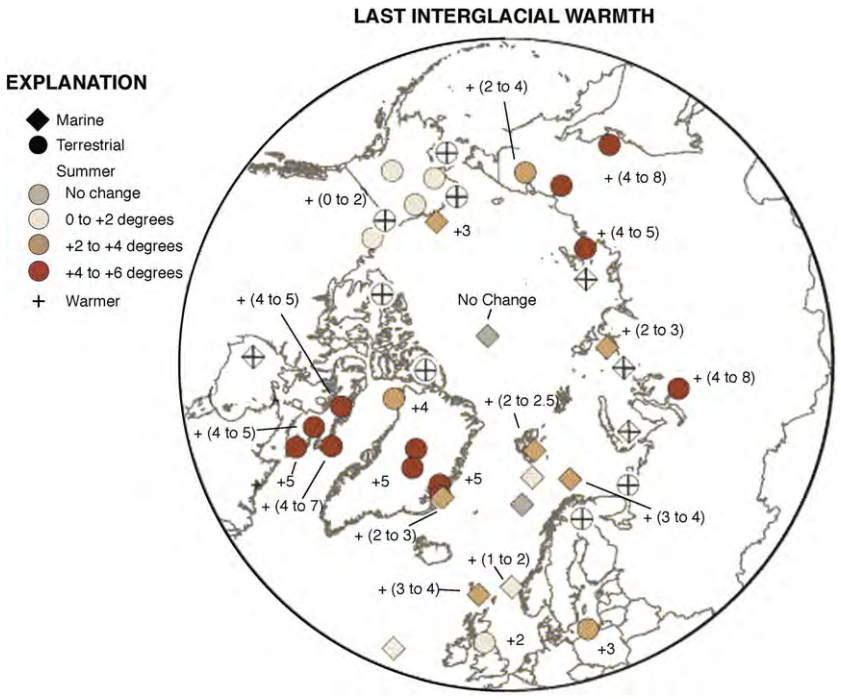

Fig. 24. Polar projection showing regional maximum LIG Last Interglacial summer temperature anomalies relative to present summer temperatures; derived from paleotemperature proxies (see Tables 1 and 2, in CAPE Last Interglacial Project Members, 2006). Circles, terrestrial; squares, marine sites. [Copyright 2006, reprinted with permission from Elsevier.] Note that the that central Arctic Ocean point indicating 'no change' was based on a single data point that has recently been shown to be much younger than the LIG. The companion paper on the history of the Arctic Ocean (Polyak et al., 2010) indicates substantial LIG warming and sea ice reduction throughout the Arctic Ocean.

intervals when summer temperatures and treeline reached late Holocene conditions (Anderson and Lozhkin, 2001). MIS 3 insect faunas in the lower Kolyma are thought to have thrived in summers that were 1–4.5 °C higher than recently (Alfimov et al., 2003). Variable paleoenvironmental conditions were typical of the MIS 3 (Karaginskii) period throughout Arctic Russia, although uncertainties in radiocarbon dating near its upper limit preclude regional correlations.

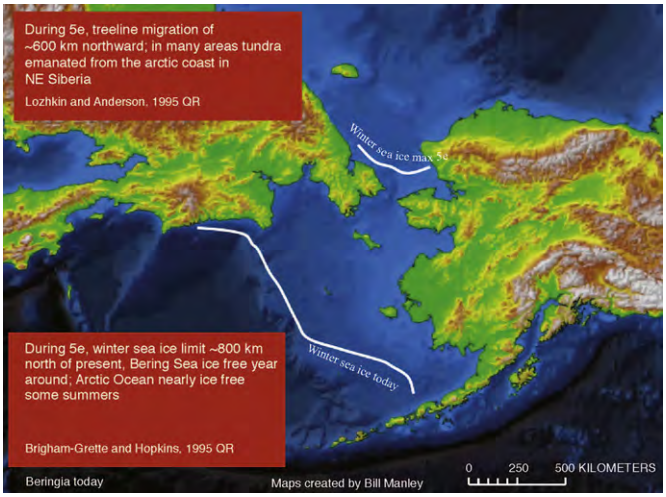

Fig. 25. Winter sea–ice limit during MIS 5e and at present. Fossiliferous paleoshorelines and marine sediments were used by Brigham-Grette and Hopkins (1995) to evaluate the seasonality of coastal sea ice on both sides of the Bering Strait during the Last Interglaciation. Winter sea limit is estimated to have been north of the narrowest section of the strait, 800 km north of modern limits. Pollen data derived from Last Interglacial lake sediments suggest that tundra was nearly eliminated from the Russian coast at this time (Lozhkin and Anderson, 1995). In Chukokta during the warm interglaciation, additional open water favored some taxa tolerant of deeper winter snows. (Base map by William Manley, http://instaar.colorado.edu/QGISL).

The warmest widespread MIS 3 interval in Beringia occurred 44–35 ka ago (Anderson and Lozhkin, 2001); it is well represented in proxies from interior sites although there is little or no vegetation response in areas closest to Bering Strait. Summer warmth appears to have been strongest in eastern Beringia where temperatures were only 1–2 °C lower than at present between 45 and 33 ka ago (Elias, 2007). The warmest interval in interior Alaska (Fox Thermal Event), about 40–35 ka ago, was marked by spruce forest tundra, although in the Yukon, forests were most dense a little earlier, about 43–39 ka ago (Anderson and Lozhkin, 2001).

Although MIS 3 climates of western Beringia achieved modern or near modern conditions during several intervals, climatic conditions in eastern Beringia appear to have been harsher than modern conditions for all of MIS 3. Consistent with this pattern, the transition from MIS 3 to MIS 2 is marked by a shift from warm-moist to cold-dry conditions in western Beringia, but is absent or subtle in all but a few records in Alaska (Anderson and Lozhkin, 2001).

11. Marine Isotopic Stage 2, The Last Glacial Maximum (30–15 ka)

The Last Glacial Maximum (LGM) was particularly cold in the Arctic but also cold globally. During peak cooling of the LGM, planetary temperatures were 5–6 °C lower than at present (Farrera et al., 1999; Braconnot et al., 2007; Jansen et al., 2007), whereas mean annual temperatures in central Greenland were depressed more than 20 °C (Cuffey et al., 1995; Dahl-Jensen et al., 1998), with a similar summer temperature reduction estimated for Beringia (Elias et al., 1996). Much of the Arctic lands lay beneath continental ice sheets, and the Arctic Ocean was mantled by a continuous cover of sea ice and entrapped icebergs (Darby et al., 2006; Bradley and England, 2008; Geirsdóttir et al., 2008). The lack of ocean-

atmosphere transfer of heat during winter months would result in exceptionally cold winters, not only over the Arctic Ocean proper, but also across adjacent lands. These factors together limit the direct records of LGM climate across most of the Arctic. The available evidence for terrestrial ecosystems suggests that low- and high-shrub tundra were extremely restricted during the LGM, and largely replaced by polar desert or graminoid and forb tundra and an intergradation of steppe and tundra in the north Eurasian interior (Bigelow et al., 2003), ecosystem changes consistent with cold, dry climates with little snow cover.

Global ice volumes peaked about 21 ka ago. Rising solar insolation across the Northern Hemisphere in summer due to orbital features and rising greenhouse gases caused Northern Hemisphere ice sheets to begin to recede from near their maxima shortly after 20 ka ago, with the rate of recession increasing noticeably after about 16 ka ago (see, e.g., Alley et al., 2002; Dyke et al., 2003; Clark et al., 2004). Most coastlines became ice-free before 12 ka ago, and ice continued to melt rapidly as summer insolation reached a peak (about 9% above modern insolation) about 11 ka ago. An extensive literature addresses the patterns of deglaciation, and for the North Atlantic in particular, the climatic fluctuations that occurred within the deglacial period.

12. Marine Isotopic Stage 1, The Holocene

The transition from MIS 2 to MIS 1, which marks the start of the Holocene, is commonly placed at the abrupt termination of the Younger Dryas cold event, about 11.7 ka ago (Rasmussen et al., 2006). By 6 ka ago, sea level and ice volumes were close to those observed more recently, and greenhouse gases in the atmosphere differed little from pre-industrial conditions (e.g., Jansen et al., 2007). A wide variety of evidence from terrestrial and marine archives indicates that peak MIS 1 Arctic summertime warmth was achieved during the early Holocene, when most regions of the Arctic experienced sustained summer temperatures that exceeded observed 20th century values. This period of peak warmth, which is geographically variable in its timing (Kaufman et al., 2004), is generally referred to as the Holocene Thermal Maximum (HTM). The ultimate driver of the warming was orbital forcing, which produced increased summer solar radiation across the Northern Hemisphere. At 70 °N June insolation about 4 ka was about 15 Wm^{-2} larger than present, and June insolation 11 ka ago was about 45 Wm^{-2} larger than present, for a total change of about 9% (Fig. 26; Berger and Loutre, 1991). January insolation did not change because there is no insolation that far north in January.

High-resolution (decades to centuries) archives containing multiple climate proxies are available for most of the Holocene throughout the Arctic. Consequently, the Holocene record allows evaluation of the range of natural climate variability and of the magnitude of climate change in response to relatively small changes in forcings.

12.1. Holocene Thermal Maximum

Most Arctic paleoenvironmental records for the HTM record primarily summer temperatures. Many different proxies have been exploited to derive these reconstructions, including biological proxies such as pollen, diatoms, chironomids, dinoflagellate cysts, and other microfossils; elemental and isotopic geochemical indices from lacustrine and marine sediments, and ice cores; borehole temperatures; age distributions of radiocarbon-dated tree stumps north of (or above) current treeline, and the distributions of thermophilous marine mollusks and whales (Fig. 27).

A recent synthesis of 140 Arctic paleoclimatic and paleoenvironmental records extending from Beringia westward to Iceland (Kaufman et al., 2004) outlines the nature of the HTM in the western Arctic (Fig. 28a). Of the sites included in the synthesis 85% contain evidence of the HTM, with an average duration of 2.1 ka in Beringia to 3.5 ka in Greenland. The interval from 10 to 4 ka ago contains the greatest number of sites recording HTM conditions and the greatest spatial extent of those conditions in the western Arctic (Fig. 28c). The HTM thermal maximum began first in

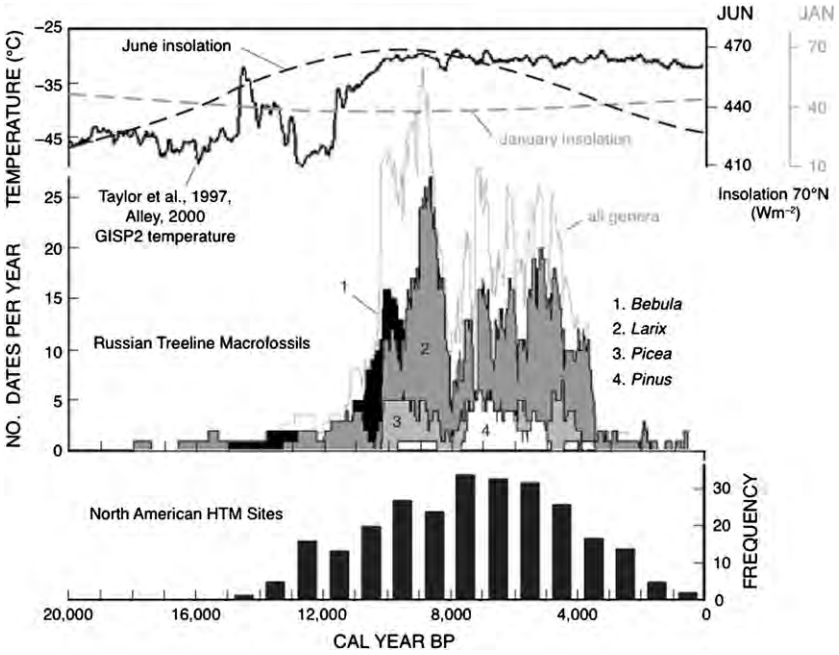

Fig. 26. The Arctic Holocene Thermal Maximum. Items compared, top to bottom: seasonal insolation patterns at 70°N (Berger and Loutre, 1991), and reconstructed Greenland air temperature from the GISP2 drilling project (Taylor et al., 1997; Alley, 2000); age distribution of radiocarbon-dated fossil remains of various tree genera from north of present treeline (MacDonald et al., 2008); and the frequency of Western Arctic sites that experienced Holocene Thermal Maximum conditions (Kaufman et al., 2004).

Beringia, where warmer-than-present summers became established 14–13 ka ago. Intermediate ages for HTM initiation (10–8 ka ago) are apparent in the Canadian Arctic Archipelago and in central Greenland. The HTM on Iceland occurred a bit later, 8–6 ka ago, whereas the onset on Svalbard was earlier, by 10.8 ka ago (Svendsen and Mangerud, 1997). The latest general HTM onset (7–4 ka ago) was in the continental portions of central and eastern Canada (Fig. 28b). Similarly, the earliest termination of the HTM occurred in Beringia. Most regions registered summer cooling by 5 ka ago. The average summer temperature anomaly during the HTM across the western Arctic was 1.65 °C, although they ranged from 0.5 to 3.0 °C, with the largest changes in the North Atlantic sector and the smallest over North Pacific sector.

Much of the pattern of the onset of the HTM can be explained in part by regional proximity to the continental ice sheets, which depressed temperatures nearby until the ice melted back, and to changes in freshwater delivery to the North Atlantic. Milankovitch cycling has also been suggested to explain the spatial variability of the Holocene Thermal Maximum (Maximova and Romanovsky, 1988).

Records for sea-ice conditions in the Arctic Ocean and adjacent channels have been developed by radiocarbon-dating indicators including the remains of open-water proxies such as whales and walrus, warm-water marine mollusks, changes in the microfauna preserved in marine sediments, and more recently in biomarkers diagnostic of sea-ice or sea-ice-free organisms (see Polyak et al., 2010, for a complete treatment of the history of Arctic Ocean sea ice). These reconstructions parallel the terrestrial record for the most part. They demonstrate that an increased mass of warm Atlantic water moved into the Arctic Ocean at about the beginning of the Holocene. Dates on the first appearance of the obligate Atlantic water taxon *Mytilus edulis* on northern Svalbard are ca 10.6 ka (Salvigsen et al., 1992; Salvigsen, 2002), with peak penetration of Atlantic water reflected the occurrence of *Modiolis modiolis* by ca 9.3 ka and a strong Atlantic water presence in the Arctic Ocean until 8 ka (Salvigsen, 2002). Most thermophilous mollusks disappear from Svalbard by about 5 ka, about the same time that the first evidence of Neoglaciation appears around the northern North Atlantic. Dates on the flooding of Bering Strait range from ~12 ka ago (Keigwin et al., 2006) to slightly before 13 ka ago (England and Furze, 2008), although precise dating remains dependent on knowledge of the marine reservoir age at that time. The influx of Pacific water to the Arctic Ocean peaked about 9–5 ka, then diminishing through the late Holocene. The extra ocean heat from both Atlantic and Pacific sources, coupled with increased summer insolation, decreased the area of perennial sea-ice cover

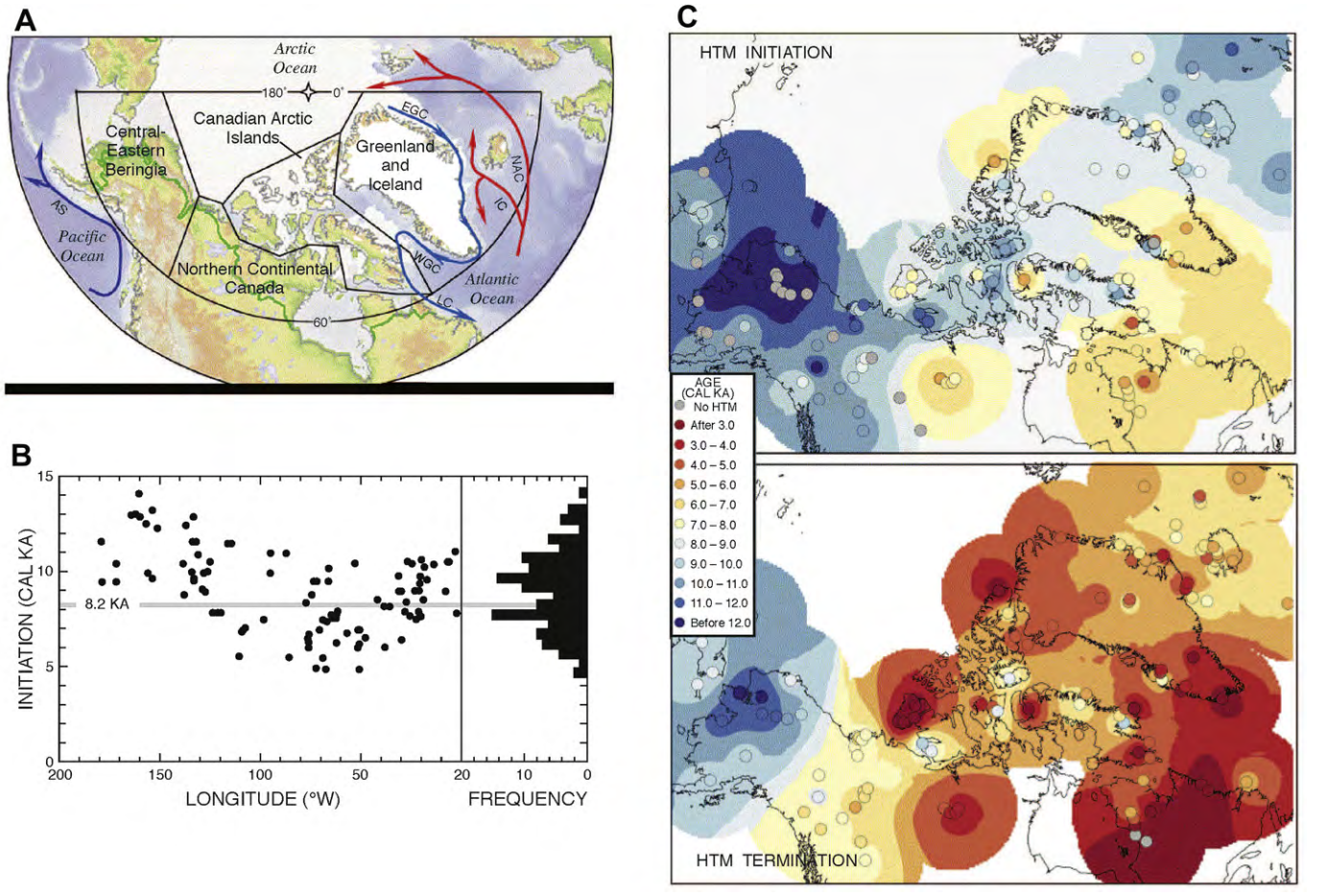

Fig. 27. Arctic temperature reconstructions. Upper panel: Holocene summer melting on the Agassiz Ice Cap, northern Ellesmere Island, Canada. "Melt" indicates the fraction of each core section that contains evidence of melting (from Koerner and Fisher, 1990). Middle panel: Estimated summer temperature anomalies in central Sweden. Black bars, elevation of ^{14}C- dated sub-fossil pine wood samples (*Pinus sylvestris* L.) in the Scandes Mountains, central Sweden, relative to temperatures at the modern pine limit in the region. Dashed line, upper limit of pine growth is indicated by the dashed line. Changes in temperature estimated by assuming a lapse rate of 6 °C km^{-1} (from Dahl and Nesje, 1996, based on samples collected by L. Kullman and by G. and J. Lundqvist). Lower panel: Paleotemperature reconstruction from oxygen isotopes in calcite sampled along the growth axis of a stalagmite from a cave at *Mo i Rana*, northern Norway. Growth ceased around A.D. 1750 (from Lauritzen 1996; Lauritzen and Lundberg 1999). Horizontal lines indicate the average 20th Century values for each variable. Figure from Bradley (2000). [Copyright 2000, reproduced with permission from Elsevier.]

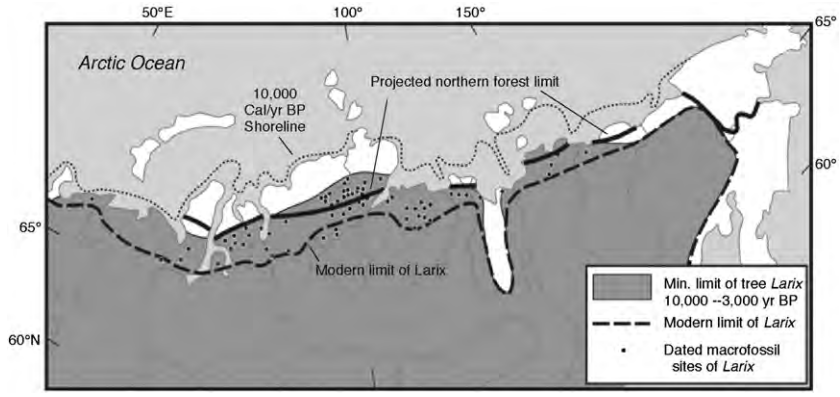

Fig. 28. The timing of initiation and termination of the Holocene Thermal Maximum in the western Arctic (Kaufman et al., 2004). (A) Regions reviewed in Kaufman et al., 2004. (B) Initiation of the Holocene Thermal Maximum in the western Arctic. Longitudinal distribution (left) and frequency distribution (right). (C) Spatial-temporal pattern of the Holocene Thermal Maximum in the western Arctic. Upper panel, initiation; lower panel, termination. Dot colors bracket ages of the Holocene Thermal Maximum; ages contoured using the same color scheme. Gray dots, equivocal evidence for the Holocene Thermal Maximum. [Copyright 2004, reprinted with permission from Elsevier.]

during the early Holocene. Decreased sea-ice cover in the western Arctic during the early Holocene also may be indicated by changes in concentrations of sea-salt sodium in the Penny Ice Cap (eastern Canadian Arctic; Fisher et al., 1998) and the Greenland Ice Sheet (Mayewski et al., 1997). In most regions, perennial sea ice increased in the late Holocene, although it has been suggested that sea ice declined in the Chukchi Sea (de Vernal et al., 2005), possibly in response to changing rates of Atlantic water inflow in Fram Strait.

As summer temperatures increased through the early Holocene, North American treeline expanded northward into regions formerly mantled by tundra, although the northward extent appears to have been limited to perhaps a few tens of kilometers beyond its recent position (Seppä et al., 2003; Gajewski and MacDonald, 2004). In contrast, some treeline species expanded well beyond their current limits in the Eurasian Arctic. Dated macrofossils indicate that individuals of the tree genera *Betula* (birch) and *Larix* (larch) lived far north of the modern treeline across most of northern Eurasia between 11 and 10 ka ago (Kremenetski et al., 1998; MacDonald et al., 2000a,b, 2008), and *Larix* extended beyond its modern limits as early 13–12 ka ago in eastern Siberia (Binney et al., 2009). In the Taimyr Peninsula of Siberia and nearby regions the most northerly limit reached by trees during the Holocene was more than 200 km north of the current treeline (Fig. 29). Spruce (*Picea*) advanced slightly later than the other two genera. Interestingly, pine (*Pinus*), which now forms the conifer treeline in Fennoscandinavia and the Kola Peninsula of Russia, does not appear to have established appreciable forest cover at or beyond the present treeline in the Kola Peninsula until around 7 ka ago (MacDonald et al., 2000a). However, quantitative reconstructions of temperature suggest that summer temperatures were above modern by 9 ka ago (Seppä and Birks, 2001, 2002; Hammarlund et al., 2002; Solovieva et al., 2005), and the development of extensive pine cover at and north of the present treeline appears to have been delayed relative to this warming. Treeline began to retreat southward across northern Eurasia 3-4 ka ago (Binney et al., 2009).

The timing of the HTM in the Eurasian Arctic overlaps the widest expression of the HTM in the western Arctic (Fig. 28), but it differs in two respects. The timing of onset and termination in Eurasia shows much less variability than in North America, and the magnitude of the treeline expansion and retreat is far greater in the Eurasian Arctic. Fossil pollen and other indicators of vegetation or temperature from the northern Eurasian margin also support the contention of a prolonged warming and northern extension of treeline during the early and middle Holocene (Fig. 28; Hyvärinen, 1976; Seppä, 1996; Clayden et al., 1997; Velichko et al., 1997; Kaakinen and Eronen, 2000; Pisaric et al., 2001; Seppä and Birks, 2001, 2002; Gervais et al., 2002; Hammarlund et al., 2002; Solovieva et al., 2005).

Changes in landforms suggest that permafrost in Siberia degraded during the HTM. A synthesis of Russian data by Astakhov (1995) indicates that melting permafrost was apparent north of the Arctic Circle only in the European North, not in Siberia. In the Siberian North, permafrost partially thawed only locally, and thawing was almost entirely confined to areas under thermokarst lakes that actively formed there during the HTM. Areas south of the Arctic Circle appear to have experienced deep thawing (100–200 m depth) through the HTM, followed by renewed permafrost expansion after 3 ka. The deep thawing and subsequent renewal of surface permafrost in these regions produced an extensive thawed layer sandwiched between shallow (20–80 m deep) more recently frozen ground and deeper Pleistocene permafrost throughout much of northwestern Siberia.

Quantitative estimates of HTM summer temperature anomalies along the northern margins of Eurasia and adjacent islands range from 1 to 3 °C. The geographic position of northern treeline across Eurasia is largely controlled by summer temperature and the length of the growing season (MacDonald et al., 2008), and in some areas the magnitude of treeline displacement there suggests a summer warming equivalent of 2.5–7.0 °C (see for example Birks, 1991; Wohlfarth et al., 1995; MacDonald et al., 2000a; Seppä and Birks, 2001, 2002; Hammarlund et al., 2002; Solovieva et al., 2005). Sea-surface temperature anomalies during the HTM were as much as 4–5 °C for the eastern North Atlantic sector and adjacent Arctic Ocean (Salvigsen et al., 1992; Koç et al., 1993). HTM Summer temperature anomalies in the western Arctic ranged from 0.5 to 3 °C, with the largest anomalies in the North Atlantic sector (Kerwin et al., 1999; Kaufman et al., 2004; Flowers et al., 2008).

12.2. Neoglaciation

Many climate proxies are available to characterize the overall pattern of Late Holocene climate change. Following the HTM, most proxy summer temperature records from the Arctic indicate an overall cooling trend through the late Holocene. Cooling is first recognized between 6 and 3 ka ago, depending on the threshold for change of each particular proxy. Records that exhibit a shift by 6–5 ka ago typically also reflect intensified summer cooling about 3 ka (Fig. 27).

Most mountain glaciers and ice caps around the Arctic expanded in the second half of the Holocene. The term “Neoglaciation” is

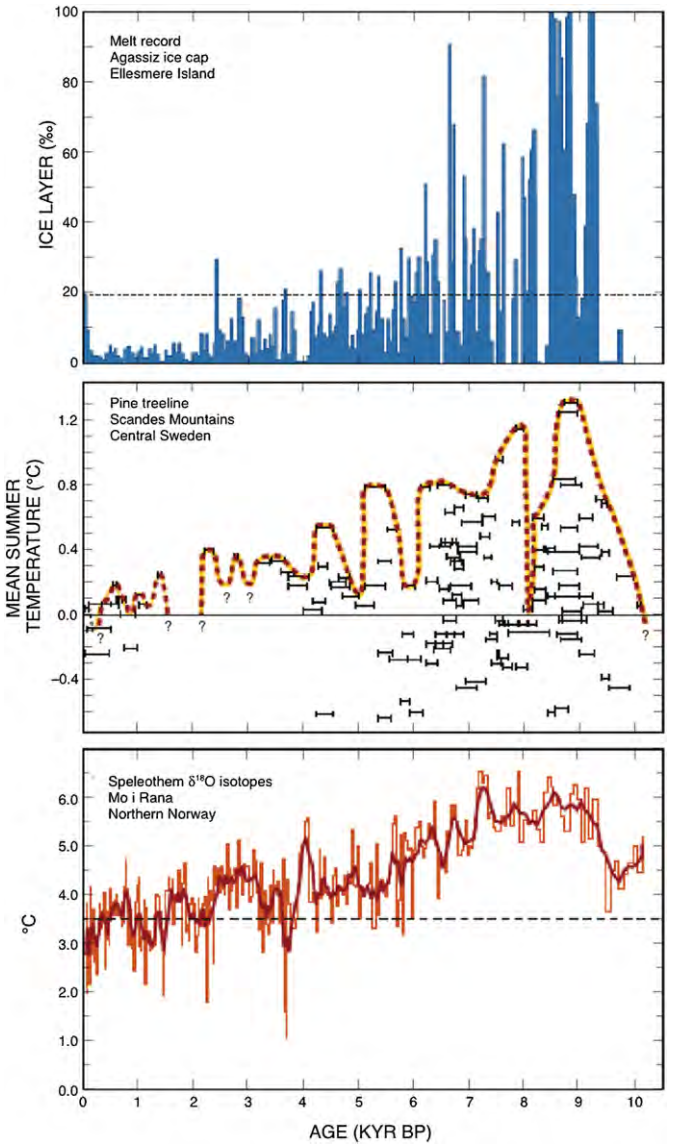

Fig. 29. The northward extension of larch (*Larix*) treeline across the Eurasian Arctic. Treeline today compared with treeline during the Holocene Thermal Maximum and with anticipated northern forest limits (ACIA, 2005b) due to climate warming (MacDonald et al., 2008).

widely applied to this episode of glacier growth (or in some cases re-formation), following the maximum glacial retreat during the HTM (Porter and Denton, 1967). During the Holocene, glacier mass balance has been dominantly controlled by summer temperature (Koerner, 2005), and the expansion of glaciers throughout the Arctic is interpreted to reflect a decrease in summer temperatures.

The former extent of glaciers is inferred from dated moraines and proglacial sediments deposited in lakes and marine settings. For example, ice-rafted debris (Andrews et al., 1997) and the glacial geologic record (Funder, 1989) indicate that outlet glaciers of the Greenland Ice Sheet readvanced between 6 and 4 ka ago. Multi-proxy records from 10 glaciers or glaciated areas in Norway show evidence for increased activity by 5 ka ago (Nesje et al., 2001, 2008). Major advances of outlet glaciers from northern Icelandic ice caps began by 5 ka (Stötter et al., 1999; Geirsdóttir et al., 2009b). In the European Arctic, glaciers expanded on Franz Josef Land (Lubinski et al., 1999) and Svalbard (Svendsen and Mangerud, 1997) by 5 ka ago, although sustained growth primarily began around 3 ka ago. An early Neoglacial advance of mountain glaciers is registered in Alaska, most prominently in the Brooks Range (Ellis and Calkin, 1984; Calkin, 1988). In southwest Alaska, mountain glaciers in the Ahklun Mountains did not reform until about 3 ka ago (Levy et al., 2003). Neoglacial advances began in Arctic Canada by 5 ka ago, with additional expansion about 2.5 ka ago (Miller et al., 2005)

Neoglacial summer cooling is supported by several other lines of evidence: a reduction in melt layers in the Agassiz Ice Cap (Koerner and Fisher, 1990) and in Greenland (Alley and Anandakrishnan, 1995); the decrease in $\delta^{18}O$ values in Devon Island (Fisher, 1979) and Greenland (Vinther et al., 2008) ice cores, and indications from borehole thermometry (Cuffey et al., 1995); the retreat of large marine mammals and warm-water-dependent mollusks from the Canadian Arctic (Dyke and Savelle, 2001); the southward migration of the northern treeline across central Canada (MacDonald et al., 1993), Eurasia (MacDonald et al., 2000b), and Scandinavia (Barnekow and Sandgren, 2001); the expansion of sea-ice cover along the shores of the Arctic Ocean on Ellesmere Island (England et al., 2008), in Baffin Bay (Levac et al., 2001), and in the Bering Sea (Cockford and Frederick, 2007); and the shift in vegetation communities inferred from plant macrofossils and pollen around the Arctic, including Wrangel Island (Lozhkin et al., 2001; Bigelow et al., 2003). The assemblage of microfossils and the stable isotope ratios of foraminifera indicate a shift toward colder, lower salinity sea-surface conditions about 5 ka along the East Greenland Shelf (Jennings et al., 2002) and the western Nordic seas (Koç and Jansen, 1994), suggesting increased influx of sea ice from the Arctic Ocean. Where quantitative estimates of temperature change are available, they generally indicate that summer temperature decreased by 1–2 °C during this initial phase of cooling.

The general pattern of an early- to middle-Holocene thermal maximum followed by Neoglacial cooling forms a multi-millennial trend that, in most places, culminated in the 19th century. Superposed on the long-term cooling trend were many centennial-scale warmer and colder summer intervals, which are expressed to a varying extent and are interpreted with various levels of confidence in different proxy records. The most intensively studied centennial-scale climate oscillations are those of the past 2 ka (Kaufman et al., 2009).

12.3. Medieval Warm Period (MWP)

The Medieval Warm Period (MWP; also referred to as the Medieval Climate Anomaly or MCA) was initially recognized on the basis of several lines of evidence in Western Europe, but the term is commonly applied to other regions to refer to any of the relatively warm intervals of various magnitudes and at various times between about 950 and 1200 AD (Lamb, 1977) (Fig. 30). In the Arctic, evidence for climate variability, such as relative warmth, during this interval is based on changes in glacier length, marine sediments, speleothems, ice cores, borehole temperatures, tree rings, and archaeology. The most consistent records of the MWP come from the North Atlantic sector of the Arctic. Western Greenland (Crowley and Lowery, 2000), the Greenland Ice Sheet summit (Dahl-Jensen et al., 1998), Swedish Lapland (Grudd et al., 2002), northern Siberia (Naurzbaev et al., 2002), Arctic Canada (Anderson et al., 2008), and Iceland (Geirsdóttir et al., 2009a) were all relatively warm around 1000 AD. During Medieval time, Inuit populations moved out of Alaska into the eastern Canadian Arctic and hunted whale from skin boats in regions perennially ice-covered in the 20th century (McGhee, 2004).

The evidence for Medieval warmth throughout the rest of the Arctic is less clear (Kaufman, 2009). However, some indications of Medieval warmth include the general retreat of glaciers in southeastern Alaska (Reyes et al., 2006; Wiles et al., 2008) and the wider

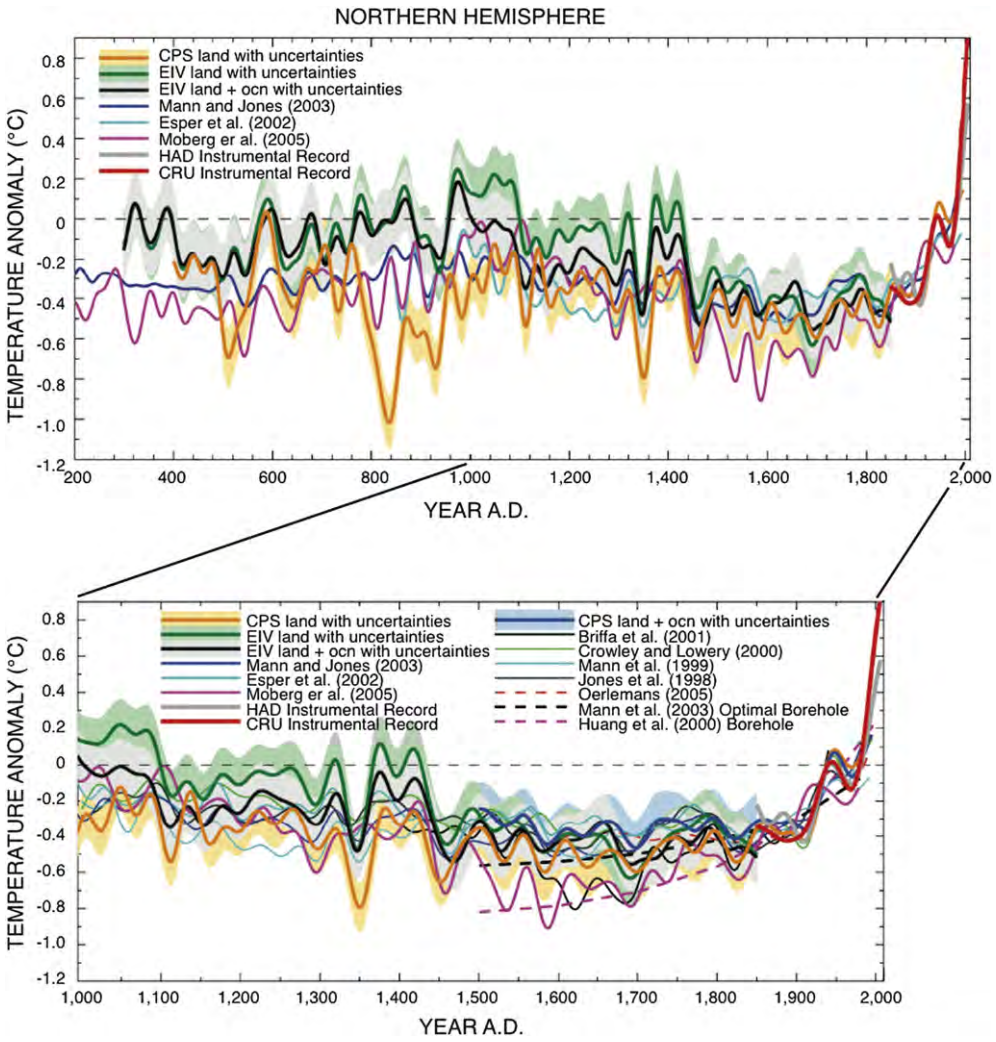

Fig. 30. Updated composite proxy-data reconstruction of Northern Hemisphere temperatures for most of the last 2000 years, compared with other published reconstructions. Estimated confidence limits, 95%. All series have been smoothed with a 40-year low-pass filter. The Medieval Warm Period (MWP) (aka Medieval Climate Anomaly) occurs about 950–1200 AD. The array of reconstructions demonstrate that the warming documented by instrumental data during the past few decades exceeds that of any warm interval of the past 2000 years, including that estimated for the MWP. All reconstructions are based on climate proxies, with the exception of the two reconstructions of the instrumental record (HAD and CRU). (Figure from Mann et al., 2008). CPS, composite plus scale methodology; CRU, East Anglia Climate Research unit, a source of instrumental data; EIV, error-in-variables; HAD, Hadley Climate Center. [Reprinted with permission National Academy of Sciences.]

tree rings in some high-latitude tree-ring records from Asia and North America (D'Arrigo et al., 2006). However, D'Arrigo et al. (2006) emphasized the uncertainties involved in estimating Medieval warmth relative to that of the 20th century, owing in part to the sparse geographic distribution of proxy data as well as to the less coherent variability of tree growth temperature estimates. Hughes and Diaz (1994) argued that the Arctic as a whole was not anomalously warm throughout Medieval time (also see Bradley et al., 2003b, and National Research Council, 2006). Medieval warmth is generally ascribed to reduction in sulfate aerosols from explosive volcanism (Crowley, 2000; Goosse et al., 2005; also see Jansen et al., 2007). Warming around the North Atlantic and adjacent regions may have been linked to changes in oceanic circulation as well (Broecker, 2001).

12.4. Climate of the past millennium and the Little Ice Age

Given the importance of understanding climate in the most recent past and the richness of the available evidence, intensive scientific effort has resulted in numerous temperature reconstructions for the past millennium (Jones et al., 1998; Mann et al., 1998; Briffa et al., 2001; Esper et al., 2002; Crowley et al., 2003; Mann and Jones, 2003; Moberg et al., 2005; National Research Council, 2006; Jansen et al., 2007), and especially the last 500 years (Bradley and Jones, 1992; Overpeck et al., 1997). Most of these reconstructions are based on annually resolved proxy records, primarily tree rings, and they attempt to extract a record of air-temperature change over large regions or entire hemispheres. Data from Greenland ice cores and a few annually laminated lake sediment records are also included in these compilations. Recently, multi-decadally averaged temperature records have been explored for comparison (e.g., Kaufman, 2009 and references therein). In general, the temperature records are broadly similar: they show modest summer warmth during Medieval times, a variable, but colder climate from about 1250–1850 AD, followed by warming as shown by both paleoclimate proxies and the instrumental record. Less is known about changes in precipitation, which is spatially and temporally more variable than temperature.

The trend toward colder summers after about 1250 AD coincides with the onset of the Little Ice Age (LIA), which persisted until about

1850 AD, although the timing and magnitude of specific cold intervals were different in different places. Proxy climate records, both glacial and non-glacial from around the Arctic and for the Northern Hemisphere as a whole, show that the coldest interval of the Holocene was sustained sometime between about 1500 and 1900 AD (Bradley et al., 2003a) and during this interval glacier lengths reached their Neoglacial maxima. Recent evidence from the Canadian Arctic indicates that, following substantial recession in Medieval times, glaciers and ice caps began to expand again between 1250 and 1300 AD. Expansion was further amplified about 1450 AD after which ice caps only receded to their pre-LIA margins in recent decades (Anderson et al., 2008).

Glacier mass balances throughout most of the Northern Hemisphere during the Holocene are closely correlated with summer temperature (Koerner, 2005), and the widespread evidence of glacier re-advances across the Arctic during the LIA is consistent with estimates of summer cooling based on tree rings. The climate history of the LIA has been extensively studied in natural and historical archives, and it is well documented in Europe and North America (Grove, 1988). Historical evidence from the Arctic is relatively sparse, but it generally agrees with historical records from northwest Europe (Grove, 1988). Icelandic written records indicate that the duration and extent of sea ice in the Nordic Seas were higher during the LIA than during Medieval times or the past century (Ogilvie and Jónsson, 2001).

The average temperature of the Northern Hemisphere during the LIA was less than 1 °C lower than in the late 20th century (Bradley and Jones, 1992; Hughes and Diaz, 1994; Crowley and Lowery, 2000), but regional temperature anomalies varied. LIA cooling appears to have been stronger in the Atlantic sector of the Arctic than in the Pacific (Kaufman et al., 2004), perhaps because changes in ocean circulation promoted the development of sea ice in the North Atlantic, which further amplified LIA cooling there (Broecker, 2001; Miller et al., 2005).

The LIA also shows evidence of multi-decadal climatic variability, such as widespread warming during the middle through late 18th century (e.g., Cronin et al., 2003). Although the initiation of the LIA and the structure of climate fluctuations during this multi-centennial interval vary around the Arctic, most records show warming beginning in the late 19th century (Overpeck et al., 1997; Smol et al., 2005; Smol and Douglas, 2007b). The end of the LIA was apparently more uniform both spatially and temporally than its initiation (Overpeck et al., 1997).

The climate change that led to the LIA is manifested in proxy records other than those that reflect temperature. For example, it was associated with a positive shift in transport of dust and other chemicals to the summit of Greenland (O'Brien et al., 1995), perhaps related to deepening of the Icelandic low-pressure system (Meeker and Mayewski, 2002). According to modeling studies, the negative phase [see http://www.ldeo.columbia.edu/res/pi/NAO] of the North Atlantic Oscillation could have been amplified during the LIA (Shindell et al., 2001) whereas, in the North Pacific, either the Aleutian Low was significantly weakened or atmospheric circulation patterns were altered to produce a stronger zonal flow, during the LIA (Fisher et al., 2004; Anderson et al., 2005).

Seasonal cooling into the LIA was in part a consequence of the Holocene-long decrease in Northern Hemisphere summer insolation due to the orbital changes described earlier, intensified by increased explosive volcanism. This transition was probably aided by decreased solar luminosity, as recorded by sunspot numbers as far back as 1600 AD (Renssen et al., 2005; Ammann et al., 2007; Jansen et al., 2007), and amplified by strong positive feedbacks, especially expanded Arctic Ocean sea ice and terrestrial snow cover, possibly enhanced by a weakening of the meridional circulation in the northern North Atlantic.

13. Placing 20th century Arctic warming in a millennial perspective

Much scientific effort has been devoted to learning how 20th and 21st century warmth compares with warmth during earlier times (e.g., National Research Council, 2006; Jansen et al., 2007). Owing to the orbital changes affecting midsummer insolation (a drop in June insolation of about 1 Wm^{-2} at 75 °N. and 2 Wm^{-2} at 90 °N during the last millennium; Berger and Loutre, 1991), additional forcing was needed in the 20th century to give the same summertime temperatures as achieved in the Medieval Warm Period.

Thin, cold ice caps in the eastern Canadian Arctic preserve intact vegetation beneath them that was killed by the expanding ice. As these ice caps melt, they expose this dead vegetation, which can be dated by radiocarbon with a precision of a few decades. A recent compilation of more than 50 radiocarbon dates on dead vegetation emerging from beneath thin ice caps on northern Baffin Island shows that some ice caps formed more than 1600 years ago and persisted through Medieval times before melting early in the 21st century (Anderson et al., 2008).

Records of the melting from ice caps offer another view by which 20th century warmth can be placed in a millennial perspective. The most detailed record comes from the Agassiz Ice Cap in the Canadian High Arctic, for which the percentage of summer melting of each season's snowfall is reconstructed for the past 10 ka (Fisher and Koerner, 2003). The percent of melt follows the general trend of decreasing summer insolation from orbital changes, but some brief departures are substantial. Of particular note is the significant increase in melt percentage during the past century; current percentages are greater than any other melt intensity since at least 1700 years ago, and melting is greater than in any sustained interval since 5–4 ka ago.

As reviewed by Smol and Douglas (2007b), changes in lake sediments and their biota record climatic and other changes in the lakes. Extensive changes especially in the post-1850 interval are most easily interpreted in terms of warming above the Medieval warmth on Ellesmere Island and probably in other regions, although explanations have been debated and explored (also see Douglas et al., 1994; Douglas, 2007; Smol et al., 2005; Smol and Douglas, 2007a,b). D'Arrigo et al. (2006) show tree-ring evidence from a few North American and Eurasian sites that imply that summers were cooler in the Medieval Warm Period than in the late 20th century, although the statistical confidence is weak. Tree-ring and treeline studies in western Siberia (Esper and Schweingruber, 2004) and Alaska (Jacoby and RD'Arrigo, 1995) suggest that warming since 1970 has been optimal for tree growth and follows a circumpolar trend. Hantemirov and Shiyatov (2002) have records from the Yamal Peninsula, Russia, well north of the Arctic Circle, that show how summer temperatures of recent decades are the most favorable for tree growth within the past 4 ka.

The National Research Council (2006; p. 3) evaluated the available published data on globally and hemispherically averaged temperatures for the last millennium, and found that "Presently available proxy evidence indicates that temperatures at many, but not all, individual locations were higher during the past 25 years than during any period of comparable length since A.D. 900". Greater uncertainties for hemispheric or global reconstructions were identified in assessing older comparisons.

Although high-resolution records of the past millennium in the Arctic are rare, 14 new Arctic lake-sediment records were recently published in a dedicated issue of the Journal of Paleolimnology (2009, v.41-1). Six of these records extend back at least 1 ka at decadal resolution. These six records were combined with an additional 17 published records from lakes, ice, and trees to

reconstruct summer temperature for the Arctic for the past 2 ka that could be compared with climate-model simulations (Kaufman et al., 2009). The combination of data and models indicate that the first-order cooling trend dominating most of the past 2 ka is linked to decreasing summer insolation from orbital factors, and that this trend was reversed during the 20th Century, despite continued reduction of summer insolation across the Arctic. The warmest 50-year interval in the 2 ka composite record occurred between 1950 and 2000 AD.

14. Conclusions

The histories of temperature and precipitation across Arctic lands during the Cenozoic exhibits certain broad trends despite the limitations caused by scattered, and incomplete records. Arctic climate proxies for the most part reflect summer temperature anomalies, although ice core proxies more commonly reflect mean annual temperatures. Precipitation changes in the past are more difficult to reconstruct than are paleotemperatures, in part due to the greater spatial variability of precipitation, but also due to the weak correlation between most proxies and precipitation amount. Nevertheless, some broad patterns clearly emerge.

On all time scales through the Cenozoic, temperature changes have been greater in the Arctic than for the Northern Hemisphere as a whole, for both summer and annual mean changes. This greater sensitivity reflects the powerful positive feedbacks acting across the Arctic that amplify changes due to external forcings. The strongest feedback on short timescales (decadal to millennial) is the expansion and contraction of sea ice, with additional positive feedbacks from changing seasonal snowcover, changing distribution of forest and tundra ecosystem boundaries, growth and decay of permafrost, and changes in the strength of the ocean's meridional overturning circulation. On longer timescales (multi-millennial), changes in the location and rate of deep convection in the North Atlantic, and the growth and decay of continental ice sheets are particularly important feedbacks, through changes energy transfer, CO_2 budgets, albedo, and ice height, and to a lesser extent, a negative feedback resulting from isostatic compensation to the increased ice load that lowers the ice surface. Accompanying changes in sea-surface temperatures control the amount of water vapor released to the atmosphere, influencing the greenhouse effect.

The primary forcing through the Cenozoic has been a generally steady decrease in greenhouse gas forcing (with some notable perturbations) that produced a first order temperature decline through most of the Cenozoic. Although this first-order temperature decline continued through the Quaternary, high frequency temperature variations across the Arctic were superimposed on the gradual cooling trend, tied to the initiation of continental ice sheets. Throughout the Quaternary, changes in the seasonal and geographic distribution of solar insolation caused by irregularities in Earth's orbital parameters, primarily axial tilt (obliquity) and precession of the equinoxes, have paced the expansion and retreat of Northern Hemisphere ice sheets, with global climate consequences. Arctic Quaternary climates have also responded to variations in greenhouse gas forcings on glacial-interglacial timescales. Within the Holocene the general decreases in summer temperatures have been driven by precession, with modulations to the cooling trend resulting from changes in the frequency of sulfur-rich explosive volcanic eruptions, and to small changes in solar luminosity. The strong warming trend of the past century across the Arctic, and of the past 50 years in particular, stands in stark contrast to the first-order Holocene cooling trend, and is very likely a result of increased greenhouse gases that are a direct consequence of anthropogenic activities.

The great temperature reduction across the Arctic during glaciations increased the pole-to-equator thermal gradient, increasing planetary wind speeds, and the Arctic cold was amplified globally by reduced atmospheric water vapor and CO_2, the two most important greenhouse gases. Reduced atmospheric water vapor resulted in globally drier and dustier conditions on average, and ice sheet instabilities had dramatic impacts on the oceanic meridional overturning circulation, both with global consequences.

For past 4 Ma the continents have been in essentially their modern positions, although some important oceanic gateways have been altered. Within this interval there are four time periods where there are sufficient paleotemperature reconstructions to obtain a first-order comparison between Arctic and Northern Hemisphere or global temperature anomalies. These time periods are the Mid-Pliocene warm period, the Last Interglaciation, the Last Glacial Maximum and the early Holocene thermal maximum. In all four cases, Arctic temperature anomalies substantially exceeded Northern Hemisphere average anomalies. In a companion paper, Miller et al. (2010) attempt to quantify the magnitude of Arctic amplification of temperature changes during these intervals.

Acknowledgments

We express our appreciation to the Earth Surface Processes Team of the U.S. Geological Survey in Denver for assistance in ms preparation. The following authors each acknowledge at least partial support from the United States National Science Foundation as follows: GHM, grants ARC 0714074 and ATM-0318479; RBA, grants 0531211 and 0424589; JWCW, grants 0806387, 0537593 and 0519512; LP, grants ARC-0612473 and ARC-0806999; LDH, grant OPP-0652838; DSK, grant ARC-0455043; MCS, grants ARC-0531040, ARC-0531302. MSVD, JPS, and APW collectively acknowledge financial support through grants from the Canadian Natural Sciences and Engineering Research Council, and logistical support from the Polar Continental Shelf Project.

References

Abbott, M.B., Finney, B.P., Edwards, M.E., Kelts, K.R., 2000. Lake-level reconstructions and paleohydrology of Birch Lake, central Alaska, based on seismic reflection profiles and core transects. Quaternary Research 53, 154–166.

ACIA, 2005a. Arctic Climate Impact Assessment. Cambridge University Press, Cambridge, U.K., 1042 pp.

Arctic Climate Impact Assessment (ACIA), 2005b. Arctic Climate Impact Assessment. Cambridge University Press, Cambridge, U.K., 1024 pp.

Adkins, J.F., Boyle, E.A., Keigwin, L.D., Cortijio, E., 1997. Variability of the North Atlantic thermohaline circulation during the last interglacial period. Nature 390, 154–156.

Adler, R.E., Polyak, L., Ortiz, J.D., Kaufman, D.S., Channell, J.E.T., Xuan, C., Grottoli, A. G., Sellen, E., Crawford, K.A., 2009. Sediment record from the western Arctic Ocean with an improved Late Quaternary age resolution: HOTRAX core HLY0503-8JPC, Mendeleev Ridge. Global Planetary Change 68, 18–29.

Ager, T.A., Brubaker, L.B., 1985. Quaternary palynology and vegetation history of Alaska. In: Bryant Jr., V.M., Holloway, R.G. (Eds.), Pollen Records of Late-Quaternary North American Sediments. American Association of Stratigraphic Palynologists, Dallas, pp. 353–384.

Aksu, A.E., 1985. Planktonic foraminiferal and oxygen isotope stratigraphy of CESAR cores 102 and 103 – preliminary results. In: Jackson, H.R., Mudie, P.J., Blasco, S. M. (Eds.), Initial Geological Report on CESAR – The Canadian Expedition to Study the Alpha Ridge, Arctic Ocean. Geological Survey of Canada Paper 84-22, pp. 115–124.

Alfimov, A.V., Berman, D.I., Sher, A.V., 2003. Tundra–steppe insect assemblages and the reconstruction of the Late Pleistocene climate in the lower reaches of the Kolyma River. Zoologicheskiy Zhurnal 82, 281–300 (in Russian).

Alley, R.B., 2000. The Younger Dryas cold interval as viewed from central Greenland. Quaternary Science Reviews 19, 213–226.

Alley, R.B., 2003. Paleoclimatic insights into future climate challenges. Philosophical Transactions of the Royal Society of London, Series A 361 (1810), 1831–1849.

Alley, R.B., 2007. Wally was right: predictive ability of the North Atlantic "conveyor belt" hypothesis for abrupt climate change. Annual Review of Earth and Planetary Sciences 35, 241–272.

Alley, R.B., Ágústsdóttir, A.M., 2005. The 8 k event: cause and consequences of a major Holocene abrupt climate change. Quaternary Science Reviews 24, 1123–1149.
Alley, R.B., Anandakrishnan, S., 1995. Variations in melt-layer frequency in the GISP2 ice core: implications for Holocene summer temperatures in central Greenland. Annals of Glaciology 21, 64–70.
Alley, R.B., Cuffey, K.M., 2001. Oxygen- and hydrogen-isotopic ratios of water in precipitation: beyond paleothermometry. In: Valley, J.W., Cole, D. (Eds.), Stable Isotope Geochemistry. Mineralogical Society of America Reviews in Mineralogy and Geochemistry 43, 527–553.
Alley, R.B., Meese, D.A., Shuman, C.A., Gow, A.J., Taylor, K.C., Grootes, P.M., White, J. W.C., Ram, M., Waddington, E.D., Mayewski, P.A., Zielinski, G.A., 1993. Abrupt increase in snow accumulation at the end of the Younger Dryas event. Nature 362, 527–529.
Alley, R.B., Shuman, C.A., Meese, D.A., Gow, A.J., Taylor, K.C., Cuffey, K.M., Fitzpatrick, J.J., Grootes, P.M., Zielinski, G.A., Ram, M., Spinelli, G., Elder, B., 1997. Visual-stratigraphic dating of the GISP2 ice core – basis, reproducibility, and application. Journal of Geophysical Research 102, 26,367–26,381.
Alley, R.B., Brook, E.J., Anandakrishnan, S., 2002. A northern lead in the orbital band: north–south phasing of ice-age events. Quaternary Science Reviews 21 (1–3), 431–441.
Alley, R.B., Andrews, J.T., Brigham-Grette, J., Clarke, G.K.C., Cuffey, K.M., Fitzpatrick, J. J., Funder, S., Marshall, S.J., Miller, G.H., Mitrovica, J.X., Muhs, D.R., Otto-Bleisner, B., Polyak, L., White, J.W.C., 2010. History of the Greenland Ice Sheet: Paleoclimatic Insights. Quaternary Science Reviews 29, 1728–1756.
Ammann, C.M., Joos, F., Schimel, D.S., Otto-Bliesner, B.L., Tomas, R.A., 2007. Solar influence on climate during the past millennium – results from transient simulations with the NCAR Climate System Model. Proceedings of the National Academy of Sciences 104 (10), 3713–3718.
Anderson, N.J., Leng, M.J., 2004. Increased aridity during the early Holocene in West Greenland inferred from stable isotopes in laminated-lake sediments. Quaternary Science Reviews 23, 841–849.
Anderson, P.M., Lozhkin, A.V., 2001. The stage 3 interstadial complex (Karginskii/middle Wisconsinan interval) of Beringia: variations in paleoenvironments and implications for paleoclimatic interpretations. Quaternary Science Reviews 20, 93–125.
Anderson, P.M., Bartlein, P.J., Brubaker, L.B., Gajewski, K., Ritchie, J.C., 1989. Modern analogues of late Quaternary pollen spectra from the western interior of North America. Journal of Biogeography 16, 573–596.
Anderson, P.M., Bartlein, P.J., Brubaker, L.B., Gajewski, K., Ritchie, J.C., 1991. Vegetation–pollen–climate relationships for the arcto-boreal region of North America and Greenland. Journal of Biogeography 18, 565–582.
Anderson, L., Abbott, M.B., Finney, B.P., 2001. Holocene climate inferred from oxygen isotope ratios in lake sediments, central Brooks Range, Alaska. Quaternary Research 55, 313–321.
Anderson, L., Abbott, M.B., Finney, B.P., Edwards, M.E., 2005. Palaeohydrology of the Southwest Yukon Territory, Canada, based on multiproxy analyses of lake sediment cores from a depth transect. The Holocene 15, 1172–1183.
Anderson, L., Abbott, M.B., Finney, B.P., Burns, S.J., 2006. Erratum to "Regional atmospheric circulation change in the North Pacific during the Holocene inferred from lacustrine carbonate oxygen isotopes, Yukon Territory, Canada [Quaternary Research 64 (2005) 21–35]". Quaternary Research 65, 350–351.
Anderson, L., Abbott, M.B., Finney, B.P., Burns, S.J., 2007. Late Holocene moisture balance variability in the southwest Yukon Territory, Canada. Quaternary Science Reviews 26, 130–141.
Anderson, R.K., Miller, G.H., Briner, J.P., Lifton, N.A., DeVogel, S.B., 2008. A millennial perspective on Arctic warming from ^{14}C in quartz and plants emerging from beneath ice caps. Geophysical Research Letters 35, L01502. doi:10.1029/2007GL032057.
Andreev, A.A., Peteet, D.M., Tarasov, P.E., Romanenko, F.A., Filimonova, L.V., Sulerzhitsky, L.D., 2001. Late Pleistocene interstadial environment on Faddeyevskiy Island, East-Siberian Sea, Russia. Arctic, Antarctic, and Alpine Research 33, 28–35.
Andrews, J.T., Smith, L.M., Preston, R., Cooper, T., Jennings, A.E., 1997. Spatial and temporal patterns of iceberg rafting (IRD) along the East Greenland margin, ca 68 N, over the last 14 cal ka. Journal of Quaternary Science 12, 1–13.
Astakhov, V.I., 1995. The mode of degradation of Pleistocene permafrost in West Siberia. Quaternary International 28, 119–121.
Axford, Y., Briner, J.P., Cooke, C.A., Francis, D.R., Michelutti, N., Miller, G.H., Smol, J.P., Thomas, E.K., Wilson, C.R., Wolfe, A.P., 2009. Recent changes in a remote Arctic lake are unique within the past 200,000 years. Proceedings of the National Academy of Science. doi:10.1073/pnas.0907094106.
Backman, J., Moran, K., McInroy, D.B., Mayer, L.A., 2006. Expedition 302 scientists. Proceedings of IODP 302. doi:10.2204/iodp.proc.302.2006 Edinburgh (Integrated Ocean Drilling Program Management International, Inc.).
Balco, G., Rovey, C.W., Stone, O.H., 2005a. The First Glacial Maximum in North America. Science 307, 222.
Balco, G., Stone, O.H., Jennings, C., 2005b. Dating Plio-Pleistocene glacial sediments using the cosmic-ray-produced radionuclides ^{10}Be and ^{26}Al. American Journal of Science 305, 1–41.
Ballantyne, A.P., Rybczynski, N.L., Baker, P.A., Harington, C.R., White, D., 2006. Pliocene Arctic temperature constraints from the growth rings and isotopic composition of fossil larch. Palaeogeography, Palaeoclimatology, Palaeoecology 242, 188–200.
Barber, V.A., Finney, B.P., 2000. Lake Quaternary paleoclimatic reconstructions for interior Alaska based on paleolake-level data and hydrologic models. Journal of Paleolimnology 24, 29–41.
Barber, D.C., Dyke, A., Hillaire-Marcel, C., Jennings, A.E., Andrews, J.T., Kerwin, M.W., Bilodeau, G., McNeely, R., Southon, J., Morehead, M.D., Gagnon, J.-M., 1999. Forcing of the cold event of 8200 years ago by catastrophic drainage of Laurentide lakes. Nature 400, 344–348.
Bard, E., December 2002. Climate shocks – abrupt changes over millennial time scales. Physics Today, 32–38.
Barnekow, L., Sandgren, P., 2001. Palaeoclimate and tree-line changes during the Holocene based on pollen and plant macrofossil records from six lakes at different altitudes in northern Sweden. Review of Palaeobotany and Palynology 117, 109–118.
Barron, E.J., Fawcett, P.J., Pollard, D., Thompson, S., 1993. Model simulations of Cretaceous climates – the role of geography and carbon-dioxide. Philosophical Transactions of the Royal Society of London Series B-Biological Sciences 341 (1297), 307–315.
Bauch, D., Schlosser, P., Fairbanks, R.G., 1995. Freshwater balance and the sources of deep and bottom waters in the Arctic Ocean inferred from the distribution of $H_2^{18}O$. Progress in Oceanography 35, 53–80.
Bauch, D., Carstens, J., Wefer, G., 1997. Oxygen isotope composition of living *Neogloboquadrina pachyderma* (sin.) in the Arctic Ocean. Earth and Planetary Science Letters 146, 47–58.
Bauch, H.A., Erlenkeuser, H., 2003. Interpreting glacial-1nterglacial changes in ice volume and climate from subarctic deep-water foraminiferal $\delta^{18}O$. In: Droxler, A.W., Poore, R.Z., Burckle, L.H. (Eds.), Earth's Climate and Orbital Eccentricity: The Marine Isotope Stage 11 Question. American Geophysical Union Geophysical Monograph Series 137, 87–102.
Bauch, H.A., Kandiano, E.S., 2007. Evidence for early warming and cooling in North Atlantic surface waters during the last interglacial. Paleoceanography 22, PA1201. doi:10.1029/2005PA001252.
Bauch, H.A., Erlenkeuser, H., Fahl, K., Spielhagen, R.F., Weinelt, M.S., Andruleit, H., Henrich, R., 1999. Evidence for a steeper Eemian than Holocene sea surface temperature gradient between Arctic and sub-Arctic regions. Palaeogeography, Palaeoclimatology, Palaeoecology 145, 95–117.
Bauch, H.A., Erlenkeuser, H., Helmke, J.P., Struck, U., 2000. A paleoclimatic evaluation of marine oxygen isotope stage 11 in the high-northern Atlantic (Nordic seas). Global and Planetary Change 24, 27–39.
Behl, R.J., Kennett, J.P., 1996. Brief interstadial events in the Santa Barbara Basin, NE Pacific, during the past 60 kyr. Nature 379, 243–246.
Bendle, J.A., Rosell-Melé, A., 2004. Distributions of U^k_{37} and U^k_{37} in the surface waters and sediments of the Nordic Seas: implications for paleoceanography. Geochemistry, Geophysics, Geosystems 5, 3589–3600. doi:10.1029/2004GC000741. Q11013.
Bennike, O., Brodersen, K.P., Jeppesen, E., Walker, I.R., 2004. Aquatic invertebrates and high latitude paleolimnology. In: Pienitz, R., Douglas, M.S.V., Smol, J.P. (Eds.), Long-Term Environmental Change in Arctic and Antarctic Lakes. Springer, Dordrecht, pp. 159–186.
Berger, A., Loutre, M.F., 1991. Insolation values for the climate of the last 10 million years. Quaternary Science Reviews 10, 297–317.
Berger, A., Loutre, M.F., Laskar, J., 1992. Stability of the astronomical frequencies over the Earth's history for paleoclimate studies. Science 255 (5044), 560–566.
Berner, R.A., Kothavala, Z., 2001. GEOCARB III: a revised model of atmospheric CO_2 over Phanerozoic time. American Journal of Science 301 (2), 182–204.
Bice, K.L., Birgel, D., Meyers, P.A., Dahl, K.A., Hinrichs, K.U., Norris, R.D., 2006. A multiple proxy and model study of Cretaceous upper ocean temperatures and atmospheric CO_2 concentrations. Paleoceanography 21 (2), PA2002.
Bigelow, N., Brubaker, L.B., Edwards, M.E., Harrison, S.P., Prentice, I.C., Anderson, P. M., Andreev, A.A., Bartlein, P.J., Christensen, T.R., Cramer, W., Kaplan, J.O., Lozhkin, A.V., Matveyeva, N.V., Murrary, D.F., McGuire, A.D., Razzhivin, V.Y., Ritchie, J.C., Smith, B., Walker, D.A., Gajewski, K., Wolf, V., Holmqvist, B.H., Igarashi, Y., Kremenetskii, K., Paus, A., Pisaric, M.F.J., Volkova, V.S., 2003. Climate change and Arctic ecosystems – 1. Vegetation changes north of 55°N between the last glacial maximum, mid-Holocene, and present. Journal of Geophysical Research 108 (D19), 8170. doi:10.1029/2002JD002558.
Billups, K., Channell, J.E.T., Zachos, J., 2002. Late Oligocene to early Miocene geochronology and paleoceanography from the subantarctic South Atlantic. Paleoceanography 17 (1), 1004. doi:10.1029/2000PA000568.
Binney, H.A., Willis, K.J., Edwards, M.E., Bhagwat, S.A., Anderson, P., Andreev, A.A., Blaauw, M., Damblon, F., Haesaerts, P., Kienast, F., Kremenetski, K.V., Krivonogov, S.K., Lozhkin, A.V., Macdonald, G.M., Novenko, E.Y., Oksanen, P., Sapelko, T.V., Valiranta, M., Vazhenina, L., 2009. The distribution of Late Quaternary woody taxa in Eurasia: evidence from a new macrofossil database. Quaternary Science Reviews 28, 2445–2464.
Birks, H.H., 1991. Holocene vegetational history and climatic change in west Spitzbergen – plant macrofossils from Skardtjorna, an arctic lake. The Holocene 1, 209–218.
Birks, H.J.B., 1998. Numerical tools in palaeolimnology – progress, potentialities, and problems. Journal of Paleolimnology 20, 307–332.
Boellstorff, J., 1978. North American Pleistocene stages reconsidered in light of probably Pliocene–Pleistocene continental glaciation. Science 202 (2004365), 305–307.
Bohaty, S.M., Zachos, J.C., 2003. Significant Southern Ocean warming event in the late middle Eocene. Geology 31, 1017–1020. doi:10.1130/G19800.1.

Box, J.E., Bromwich, D.H., Veenhuis, B.A., Bai, L.-S., Stroeve, J.C., Rogers, J.C., Steffen, K., Haran, T., Wang, S.-H., 2006. Greenland ice-sheet surface mass balance variability (1988–2004) from calibrated Polar MM5 output. Journal of Climate 19 (12), 2783–2800.

Braconnot, P., Otto-Bliesner, B., Harrison, S., Joussaume, F.S., Peterchmitt, J.-Y., Abe-Ouchi, A., Crucifix, M., Driesschaert, E., Fichefet, T., Hewitt, C.D., Kageyama, M., Kitoh, A., Laine, A., Loutre, M.-F., Marti, O., Merkel, U., Ramstein, G., Valdes, P., Weber, S.L., Yu, Y., Zhao, Y., 2007. Results of PMIP2 coupled simulations of the Mid-Holocene and Last Glacial Maximum – part 1: experiments and large-scale features. Climates of the Past 3, 261–277.

Bradley, R.S., 1999. Paleoclimatology: Reconstructing Climates of the Quaternary, second ed. Academic Press, New York, 613 pp.

Bradley, R.S., 2000. Past global changes and their significance for the future. Quaternary Science Reviews 19, 391–402.

Bradley, R.S., England, J.H., 2008. The Younger Dryas and the Sea of Ancient Ice. Quaternary Research 70, 1–10.

Bradley, R.S., Jones, P.D. (Eds.), 1992. Climate Since AD 1500. Routlege, London, 677 pp.

Bradley, R.S., Briffa, K.R., Cole, J., Osborn, T.J., 2003a. The climate of the last millennium. In: Alverson, K.D., Bradley, R.S., Pedersen, T.F. (Eds.), Paleoclimate, Global Change and the Future. Springer, Berlin, pp. 105–141.

Bradley, R.S., Hughes, M.K., Diaz, H.F., 2003b. Climate in Medieval time. Science 302, 404–405. doi:10.1126/science.1090372.

Brassell, S.C., Eglinton, G., Marlowe, I.T., Pflaumann, U., Sarnthein, M., 1986. Molecular stratigraphy – a new tool for climatic assessment. Nature 320, 129–133.

Bray, P.J., Blockey, S.P.E., Coope, G.R., Dadswell, L.F., Elias, S.A., Lowe, J.J., Pollard, A.M., 2006. Refining mutual climatic range (MCR) quantitative estimates of paleotemperature using ubiquity analysis. Quaternary Science Reviews 25 (15–16), 1865–1876.

Briffa, K., Cook, E., 1990. Methods of response function analysis. In: Cook, E.R., Kairiukstis, L.A. (Eds.), Methods of Dendrochronology. Kluwer, Dordrecht, The Netherlands, pp. 165–178.

Briffa, K.R., Osborn, T.J., Schweingruber, F.H., Harris, I.C., Jones, P.D., Shiyatov, S. G., Vaganov, E.A., 2001. Low-frequency temperature variations from a northern tree ring density network. Journal of Geophysical Research 106, 2929–2941.

Brigham, J.K., 1985. Marine stratigraphy and amino acid geochronology of the Gubik Formation, western Arctic Coastal Plain, Alaska. Doctoral dissertation, University of Colorado, Boulder. U.S. Geological Survey Open-File Report 85-381, 21 pp.

Brigham-Grette, J., Carter, L.D., 1992. Pliocene marine transgressions of northern Alaska – circumarctic correlations and paleoclimate. Arctic 43 (4), 74–89.

Brigham-Grette, J., Hopkins, D.M., 1995. Emergent-marine record and paleoclimate of the last interglaciation along the northwest Alaskan coast. Quaternary Research 43, 154–173.

Brigham-Grette, J., Lozhkin, A.V., Anderson, P.M., Glushkova, O.Y., 2004. Paleoenvironmental conditions in western Beringia before and during the Last Glacial Maximum. In: Madsen, D.B. (Ed.), Entering America: Northeast Asia and Beringia Before the Last Glacial Maximum. University of Utah Press, pp. 29–61 (Chapter 2).

Brinkhuis, H., Schouten, S., Collinson, M.E., Sluijs, A., Damsfte, J.S.S., Dickens, G.R., Huber, M., Cronin, T.M., Onodera, J., Takahashi, K., Bujak, J.P., Stein, R., van der Burgh, J., Eldrett, J.S., Harding, I.C., Lotter, A.F., Sangiorgi, F., Cittert, H.V.V., de Leeuw, J.W., Matthiessen, J., Backman, J., Moran, K., Expedition 302 Scientists, 2006. Episodic fresh surface waters in the Eocene Arctic Ocean. Nature 441 (7093), 606–609.

Broecker, W.S., 2001. Was the Medieval warm period global? Science 291 (5508), 1497–1499. doi:10.1126/science.291.5508.1497.

Broecker, W.S., Hemming, S., 2001. Climate swings come into focus. Nature 294 (5550), 2308–2309.

Brouwers, E.M., 1987. On Prerygocythereis vunnieuwenhuisei Brouwers sp.nov. In: Bate, R.H., Home, D.J., Neale, J.W., Siveter, D.J. (Eds.), A Stereo-atlas of Ostracode Shells Part 1. British Micropaleontological Society, London, vol. 14, pp. 17–20.

Burns, S.J., Fleitmann, D., Matter, D., Kramers, J., Al-Subbary, A.A., 2003. Indian Ocean climate and an absolute chronology over Dansgaard/Oeschger Events 9 to 13. Science 301, 1365–1377.

Calkin, P.E., 1988. Holocene glaciation of Alaska (and adjoining Yukon Territory, Canada). Quaternary Science Reviews 7, 159–184.

CircumArctic PaleoEnvironments (CAPE) – Last Interglacial Project Members (Anderson, P., Bennike, O., Bigelow, N., Brigham-Grette, J., Duvall, M., Edwards, M., Frechette, B., Funder, S., Johnsen, S., Knies, J., Koerner, R., Lozhkin, A., Marshall, S., Matthiessen, J., Macdonald, G., Miller, G., Montoya, M., Muhs, D., Otto-Bliesner, B., Overpeck, J., Reeh, N., Sejrup, H.P., Spielhagen, R., Turner C., Velichko, A., 2006. Last Interglacial Arctic warmth confirms polar amplification of climate change. Quaternary Science Reviews 25, 1383–1400.

Carter, L.D., Brigham-Grette, J., Marincovich Jr., L., Pease, V.L., Hillhouse, U.S., 1986. Late Cenozoic Arctic Ocean sea ice and terrestrial paleoclimate. Geology 14, 675–678.

Chapin III, F.S., Sturm, M., Serreze, M.C., Mcfadden, J.P., Key, J.R., Lloyd, A.H., Rupp, T. S., Lynch, A.H., Schimel, J.P., Beringer, J., Chapman, W.L., Epstein, H.E., Euskirchen, E.S., Hinzman, L.D., Jia, G., Ping, C.L., Tape, K.D., Thompson, C.D.C., Walker, D.A., Welker, J.M., 2005. Role of land-surface changes in Arctic summer warming. Science 310, 657–660.

Chapman, M.R., Shackleton, N.J., Duplessy, J.-C., 2000. Sea surface temperature variability during the last glacial-interglacial cycle –Assessing the magnitude and pattern of climate change in the North Atlantic. Palaeogeography, Palaeoclimatology, Palaeoecology 157, 1–25.

Clark, P.U., Pollard, D., 1998. Origin of the Middle Pleistocene transition by ice sheet erosion of regolith. Paleoceanography 13, 1–9.

Clark, P.U., McCabe, A.M., Mix, A.C., Weaver, A.J., 2004. Rapid rise of sea level 19,000 years ago and its global implications. Science 304, 1141–1144.

Clark, P.U., Archer, D., Pollard, D., Blum, J.D., Rial, J.A., Brovkin, V., Mix, A.C., Pisias, N. G., Roy, M., 2006. The middle Pleistocene transition: characteristics, mechanisms, and implications for long-term changes in atmospheric pCO_2. Quaternary Science Reviews 25, 3150–3184.

Clayden, S.L., Cwynar, L.C., MacDonald, G.M., Velichko, A.A., 1997. Holocene pollen and stomates from a forest-tundra site on the Taimyr Peninsula, Siberia. Arctic and Alpine Research 29, 327–333.

Climate Long-Range Investigation Mapping and Prediction (CLIMAP) Project Members, 1981. Seasonal reconstructions of the Earth's surface at the last glacial maximum. In: Map and Chart Series MC-36. Geological Society of America. 1–18.

Climate Long-Range Investigation Mapping and Prediction (CLIMAP) Project Members, 1984. The last interglacial ocean. Quaternary Research 21, 123–224.

Cockford, S.J., Frederick, S.G., 2007. Sea ice expansion in the Bering Sea during the Neoglacial – evidence from archeozoology. The Holocene 17, 699–706.

Cohen, A.S., 2003. Paleolimnology – the History and Evolution of Lake Systems. Oxford University Press, Oxford, U.K., 528 pp.

Colinvaux, P.A., 1964. The environment of the Bering Land Bridge. Ecological Monographs 34, 297–329.

Conte, M.H., Sicre, M., Rühlemann, C., Weber, J.C., Schulte, S., Schulz-Bull, D., Blanz, T., 2006. Global temperature calibration of the alkenone unsaturation index ($U^{K}_{37'}$) in surface waters and comparison with surface sediments. Geochemistry, Geophysics, Geosystems 7, Q02005. doi:10.1029/2005GC001054.

Cronin, T.M., Dwyer, G.S., Kamiyac, T., Schwedea, S., Willarda, D.A., 2003. Medieval Warm Period, Little Ice Age and 20th century temperature variability from Chesapeake Bay. Global and Planetary Change 36, 17–29.

Crowley, T.J., 1998. Significance of tectonic boundary conditions for paleoclimate simulations. In: Crowley, T.J., Burke, K.C. (Eds.), Tectonic Boundary Conditions for Climate Reconstructions. Oxford University Press, New York, pp. 3–17.

Crowley, T.J., 2000. Causes of climate change over the past 1000 years. Science 289, 270–277.

Crowley, T.J., Lowery, T., 2000. How warm was the Medieval warm period? Ambio 29, 51–54.

Crowley, T.J., Baum, S.K., Kim, K.Y., Hegerl, G.C., Hyde, W.T., 2003. Modeling ocean heat content changes during the last millennium. Geophysical Research Letters 30, 1932. doi:10.1029/2003GL017801.

Cuffey, K.M., Clow, G.D., 1997. Temperature, accumulation, and ice sheet elevation in central Greenland through the last deglacial transition. Journal of Geophysical Research 102 (C12), 26,383–26,396.

Cuffey, K.M., Clow, G.D., Alley, R.B., Stuiver, M., Waddington, E.D., Saltus, R.W., 1995. Large arctic temperature change at the Wisconsin–Holocene glacial transition. Science 270 (5235), 455–458.

D'Arrigo, R., Wilson, R., Jacoby, G., 2006. On the long-term context for late twentieth century warming. Journal of Geophysical Research 111, D03103. doi:10.1029/2005JD006352.

Dahe, Q., Petit, J.R., Jouzel, J., Stievenard, M., 1994. Distribution of stable isotopes in surface snow along the route of the 1990 International Trans-Antarctic Expedition. Journal of Glaciology 40, 107–118.

Dahl, S.O., Nesje, A., 1996. A new approach to calculating Holocene winter precipitation by combining glacier equilibrium-line altitudes and pine-tree limits: a case study from Hardangerjokulen, central southern Norway. The Holocene 6 (4), 381–398. doi:10.1177/095968369600600401.

Dahl-Jensen, D., Mosegaard, K., Gundestrup, N., Clow, G.D., Johnsen, S.J., Hansen, A. W., Balling, N., 1998. Past temperatures directly from the Greenland Ice Sheet. Science 282, 268–271.

Dansgaard, W., 1964. Stable isotopes in precipitation. Tellus 16, 436–468.

Dansgaard, W., White, J.W.C., Johnsen, S.J., 1989. The abrupt termination of the Younger Dryas climate event. Nature 339, 532–534.

Darby, D.A., Polyak, L., Bauch, H., 2006. Past glacial and interglacial conditions in the Arctic Ocean and marginal seas – a review. In: Wassman, P. (Ed.), Structure and Function of Contemporary Food Webs on Arctic Shelves – a Pan-Arctic Comparison. Progress in Oceanography 71, 129–144.

Delworth, T.L., Knutson, T.R., 2000. Simulation of early 20th century global warming. Science 287, 2246.

de Vernal, A., Hillaire-Marcel, C., Darby, D.A., 2005. Variability of sea ice cover in the Chukchi Sea (western Arctic Ocean) during the Holocene. Paleoceanography 20, PA4018. doi:10.1029/2005PA001157.

Denton, G.H., Alley, R.B., Comer, G.C., Broecker, W.S., 2005. The role of seasonality in abrupt climate change. Quaternary Science Reviews 24, 1159–1182.

Digerfeldt, G., 1988. Reconstruction and regional correlation of Holocene lake-level fluctuations in Lake Bysjön, South Sweden. Boreas 17, 237–263.

Donnadieu, Y., Pierrehumbert, R., Jacob, R., Fluteau, F., 2006. Modelling the primary control of paleogeography on Cretaceous climate. Earth and Planetary Science Letters 248, 426–437.

Douglas, M.S.V., 2007. Environmental change at high latitudes. In: Starratt, S.W. (Ed.), Geological and Environmental Applications of the Diatom – Pond Scum to Carbon Sink. The Paleontological Society Papers, vol. 13, pp. 169–179.

Douglas, M.S.V., Smol, J.P., Blake Jr., W., 1994. Marked post-18th century environmental change in high Arctic ecosystems. Science 266, 416–419.
Douglas, M.S.V., Smol, J.P., Pienitz, R., Hamilton, P., 2004. Algal indicators of environmental change in arctic and antarctic lakes and ponds. In: Pienitz, R., Douglas, M.S.V., Smol, J.P. (Eds.), Long-Term Environmental Change in Arctic and Antarctic Lakes. Springer, Dordrecht, pp. 117–157.
Dowsett, H.J., Chandler, M.A., Robinson, M.M., 2009. Surface temperatures of the Mid-Pliocene North Atlantic Ocean: implications for future climate. Philosophical Transactions of the Royal Society of London A 367, 69–84.
Droxler, A.W., Farrell, J.W., 2000. Marine isotope stage 11 (MIS11): new insights for a warm future. Global and Planetary Change 24 (1), 1–5.
Droxler, A.W., Alley, R.B., Howard, W.R., Poore, R.Z., Burckle, L.H., 2003. Unique and exceptionally long interglacial marine isotope stage 11 – window into Earth future climate. In: Droxler, A.W., Poore, R.Z., Burckle, L.H. (Eds.), Earth's Climate and Orbital Eccentricity – The Marine Isotope Stage 11 Question. Geophysical Monograph 137. American Geophysical Union, pp. 1–14.
Duk-Rodkin, A., Barendregt, R.W., Froese, D.G., Weber, F., Enkin, R.J., Smith, I.R., Zazula, G.D., Waters, P., Klassen, R., 2004. Timing and Extent of Plio-Pleistocene glaciations in North-Western Canada and East-Central Alaska. In: Ehlers, J., Gibbard, P.L. (Eds.), Quaternary Glaciations-Extent and Chronology, Part II, North America. Elsevier, New York, pp. 313–345.
Dyke, A.S., Savelle, J.M., 2001. Holocene history of the Bering Sea bowhead whale (Balaena mysticetus) in its Beaufort Sea summer grounds off southwestern Victoria Island, western Canadian Arctic. Quaternary Research 55, 371–379.
Dyke, A.S., Moore, A., Robertson, L., 2003. Deglaciation of North America. Geological Survey of Canada. Open File 1574. (published on CD-ROM).
Dykoski, C.A., Edwards, R.L., Cheng, H., Yuan, D., Cai, Y., Zhang, M., Lin, Y., Qing, J., An, Z., Revenaugh, J., 2005. A high-resolution, absolute-dated Holocene and deglacial Asian monsoon record from Dongge Cave, China. Earth and Planetary Science Letters 233, 71–86.
Edwards, M.E., Bigelow, N.H., Finney, B.P., Eisner, W.R., 2000. Records of aquatic pollen and sediment properties as indicators of late-Quaternary Alaskan lake levels. Journal of Paleolimnology 24, 55–68.
Eldrett, J.S., Harding, I.C., Wilson, P.A., Butler, E., Roberts, A.P., 2007. Continental ice in Greenland during the Eocene and Oligocene. Nature 446, 176–179.
Elias, S.A., 2007. Beetle records – Late Pleistocene North America. In: Elias, S.A. (Ed.), Encyclopedia of Quaternary Science. Elsevier, Amsterdam, pp. 222–236.
Elias, S.A., Anderson, K., Andrews, J.T., 1996. Late Wisconsin climate in the northeastern United States and southeastern Canada, reconstructed from fossil beetle assemblages. Journal of Quaternary Science 11, 417–421.
Elias, S.A., Andrews, J.T., Anderson, K.H., 1999. New insights on the climatic constraints on the beetle fauna of coastal Alaska derived from the mutual climatic range method of paleoclimate reconstruction. Arctic, Antarctic, and Alpine Research 31, 94–98.
Elias, S.A., Matthews Jr., J.V., 2002. Arctic North American seasonal temperatures in the Pliocene and Early Pleistocene, based on mutual climatic range analysis of fossil beetle assemblages. Canadian Journal of Earth Sciences 39, 911–920.
Ellis, J.M., Calkin, P.E., 1984. Chronology of Holocene glaciation, central Brooks Range, Alaska. Geological Society of America Bulletin 95, 897–912.
England, J.H., Furze, M.F.A., 2008. New evidence from the western Canadian Arctic Archipelago for the resubmergence of Bering Strait. Quaternary Research 70, 60–67.
England, J.H., Lakeman, T.R., Lemmen, D.S., Bednarski, J.M., Stewart, T.G., Evans, D.J. A., 2008. A millennial-scale record of Arctic Ocean sea ice variability and the demise of the Ellesmere Island ice shelves. Geophysical Research Letters 35, L19502. doi:10.1029/2008GL034470.
EPICA Community Members, 2004. Eight glacial cycles from an Antarctic ice core. Nature 429, 623–628.
Epstein, S., Buchsbaum, H., Lowenstam, H., Urey, H.C., 1953. Revised carbonate-water isotopic temperature scale. Geological Society of America Bulletin 64, 1315–1325.
Erez, J., Luz, B., 1982. Temperature control of oxygen-isotope fractionation of cultured planktonic foraminifera. Nature 297, 220–222.
Esper, J., Cook, E.R., Schweingruber, F.H., 2002. Low-frequency signals in long tree-ring chronologies for reconstructing past temperature variability. Science 295, 2250–2253.
Esper, J., Schweingruber, F.H., 2004. Large-scale treeline changes recorded in Siberia. Geophysical Research Letters 31, L06202. doi:10.1029/2003GL019178.
Fairbanks, R.G., 1989. A 17,000-year glacio-eustatic sea level record – influence of glacial melting rates on the Younger Dryas event and deep-ocean circulation. Nature 343, 612–616.
Farrera, I., Harrison, S.P., Prentice, I.C., Ramstein, G., Guiot, J., Bartlein, P.J., Bonnelle, R., Bush, M., Cramer, W., von Grafenstein, U., Holmgren, K., Hooghiemstra, H., Hope, G., Jolly, D., Lauritzen, S.-E., Ono, Y., Pinot, S., Stute, M., Yu, G., 1999. Tropical climates at the Last Glacial Maximum: a new synthesis of terrestrial palaeoclimate data. I. Vegetation, lake-levels and geochemistry. Climate Dynamics 15, 823–856.
Fisher, D.A., 1979. Comparison of 100,000 years of oxygen isotope and insoluble impurity profiles from the Devon Island and Camp Century ice cores. Quaternary Research 11, 299–304.
Fisher, D.A., Koerner, R.M., 2003. Holocene ice core climate history, a multi-variable approach. In: Mackay, A., Battarbee, R., Birks, J., Oldfield, F. (Eds.), Global Change in the Holocene. Arnold, London, pp. 281–293.
Fisher, D., Koerner, R.M., Reeh, N., 1995. Holocene climatic records from Agassiz Ice Cap, Ellesmere Island, NWT, Canada. The Holocene 5, 19–24.
Fisher, D.A., Koerner, R.M., Bourgeois, J.C., Zielinski, G., Wake, C., Hammer, C.U., Clausen, H.B., Gundestrup, N., Johnsen, S., Goto-Azuma, K., Hondoh, T., Blake, E., Gerasimoff, M., 1998. Penny Ice Cap cores, Baffin Island, Canada, and the Wisconsinan Foxe Dome connection – two states of Hudson Bay ice cover. Science 279, 692–695.
Fisher, D.A., Wake, C., Kreutz, K., Yalcin, K., Steig, E., Mayewski, P., Anderson, L., Aheng, J., Rupper, S., Zdanowicz, C., Demuth, M., Waskiewicz, M., Dahl-Jensen, D., Goto-Azuma, K., Bourgeois, J.B., Koerner, R.M., Sekerka, J., Osterberg, E., Abbott, M.B., Finney, B.P., Burns, S.J., 2004. Stable isotope records from Mount Logan, eclipse ice cores and nearby Jellybean Lake. Water cycle of the North Pacific over 2000 years and over five vertical kilometers – sudden shift and tropical connections. Geographie Physique et Quaternaire 58, 9033–9048.
Flowers, G.E., Björnsson, H., Geirsdóttir, Á., Miller, G.H., Black, J.L., Clarke, G.K.C., 2008. Holocene climate conditions and glacier variation in central Iceland from physical modelling and empirical evidence. Quaternary Science Reviews 27, 797–813.
Francis, J.E., 1988. A 50-million-year-old fossil forest from Strathcona Fiord, Ellesmere Island, Arctic Canada – evidence for a warm polar climate. Arctic 41 (4), 314–318.
Fricke, H.C., O'Neil, J.R., 1999. The correlation between $^{18}O/^{16}O$ ratios of meteoric water and surface temperature: its use in investigating terrestrial climate change over geologic time. Earth and Planetary Science Letters 170, 181–196.
Fritts, H.C., 1976. Tree Rings and Climate. London Academic Press, London, U.K., 576 pp.
Fronval, T., Jansen, E., 1997. Eemian and early Weichselian (140–60 ka) paleoceanography and paleoclimate in the Nordic seas with comparisons to Holocene conditions. Paleoceanography 12, 443–462.
Funder, S., 1989. Quaternary geology of East Greenland. In: Fulton, R.J. (Ed.), Quaternary Geology of Canada and Greenland, Geological Society of America Decade of North American Geology K1, pp. 756–763.
Funder, S., Bennike, O., Böcher, J., Israelson, C., Petersen, K.S., Simonarson, L.A., 2001. Late Pliocene Greenland – the Kap København formation in North Greenland. Bulletin of the Geological Society of Denmark 48, 177–184.
Funder, S., Demidov, I., Yelovicheva, Y., 2002. Hydrography and mollusc faunas of the Baltic and the White Sea-North Sea seaway in the Eemian. Palaeogeography, Palaeoclimatology, Palaeoecology 184, 275–304.
Fyles, J.G., Marincovich Jr., L., Mathews Jr., J.V., Barendregt, R., 1991. Unique mollusc find in the Beaufort Formation (Pliocene) Meighen Island, Arctic Canada. In: Current Research, Part B. Geological Survey of Canada, pp. 461–468. Paper 91-1B.
Gajewski, K., MacDonald, G.M., 2004. Palynology of North American Arctic Lakes. In: Pienitz, R., Douglas, M.S.V., Smol, J.P. (Eds.), Long Term Environmental Change in Arctic and Antarctic Lakes. Springer, Netherlands, pp. 89–116.
Geirsdóttir, A., Miller, G.H., Wattrus, N.J., Björnsson, H., Thors, K., 2008. Stabilization of glaciers terminating in closed water bodies: evidence and broader implications. Geophysical Research Letters 35, L17502. doi:10.1029/2008GL034432.
Geirsdóttir, A., Miller, G.H., Thordarson, T., Olafsdottir, K., 2009a. A 2000 year record of climate variations reconstructed from Haukadalsvatn, West Iceland. Journal of Paleolimnology 41, 95–115. doi:10.1007/s10933-008-9253-z.
Geirsdóttir, Á., Miller, G.H., Axford, Y., Ólafsdóttir, S., 2009b. Holocene glacier and climate history of Iceland. Quaternary Science Reviews 28, 2107–2118.
Gervais, B.R., MacDonald, G.M., Snyder, J.A., Kremenetski, C.V., 2002. Pinus sylvestris treeline development and movement on the Kola Peninsula of Russia – pollen and stomate evidence. Journal of Ecology 90, 627–638.
Gildor, H., Tziperman, E., Toggweiler, J.R., 2002. Sea ice switch mechanism and glacial–interglacial CO_2 variations. Global Biogeochemical Cycles 16. doi:10.1029/2001GB001446.
Goetcheus, V.G., Birks, H.H., 2001. Full-glacial upland tundra vegetation preserved under tephra in the Beringia National Park, Seward Peninsula, Alaska. Quaternary Science Reviews 20 (1–3), 135–147.
Goodfriend, G.A., Brigham-Grette, J., Miller, G.H., 1996. Enhanced age resolution of the marine quaternary record in the Arctic using aspartic acid racemization dating of bivalve shells. Quaternary Research 45, 176–187.
Goosse, H., Renssen, H., Timmermann, A., Bradley, R.A., 2005. Internal and forced climate variability during the last millennium – a model-data comparison using ensemble simulations. Quaternary Science Reviews 24, 1345–1360.
Gradstein, F.M., Ogg, J.G., Smith, A.G. (Eds.), 2004. A Geologic Time Scale. Cambridge University Press, Cambridge, 589 pp.
Grice, K., Klein Breteler, W.C.M., Schoten, S., Grossi, V., de Leeuw, J.W., Sinninge Damste, J.S., 1998. Effects of zooplankton herbivory on biomarker proxy records. Paleoceanography 13, 686–693.
Grove, J.M., 1988. The Little Ice Age. Methuen, London, 498 pp.
Grootes, P.M., Stuiver, M., White, J.W.C., Johnsen, S., Jouzel, J., 1993. Comparison of oxygen isotope records from the GISP2 and GRIP Greenland ice cores. Nature 366, 552–554. doi:10.1038/366552a0.
Grudd, H., Briffa, K.R., Karlén, W., Bartholin, T.S., Jones, P.D., Kromer, B., 2002. A 7400-year tree-ring chronology in northern Swedish Lapland – natural climatic variability expressed on annual to millennial timescales. The Holocene 12, 657–666.
Gudina, V.I., Kryukov, V.D., Levchuk, L.K., Sudakov, L.A., 1983. Upper-Pleistocene sediments in north-eastern Taimyr. Bulletin of Commission on Quaternary Researches 52, 90–97 (in Russian).

Hammarlund, D., Barnekow, L., Birks, H.J.B., Buchardt, B., Edwards, T.W.D., 2002. Holocene changes in atmospheric circulation recorded in the oxygen-isotope stratigraphy of lacustrine carbonates from northern Sweden. The Holocene 12, 339–351.

Hammarlund, D., Björck, S., Buchardt, B., Israelson, C., Thomsen, C.T., 2003. Rapid hydrological changes during the Holocene revealed by stable isotope records of lacustrine carbonates from Lake Igelsjön, southern Sweden. Quaternary Science Reviews 22, 353–370.

Hannon, G.E., Gaillard, M.J., 1997. The plant-macrofossil record of past lake-level changes. Journal of Paleolimnology 18, 15–28.

Hantemirov, R.M., Shiyatov, S.G., 2002. A continuous multi-millennial ring-width chronology in Yamal, northwestern Siberia. The Holocene 12 (6), 717–726.

Helmke, J.P., Bauch, H.A., 2003. Comparison of glacial and interglacial conditions between the polar and subpolar North Atlantic region over the last five climatic cycles. Paleoceanography 18 (2), 1036. doi:10.1029/2002PA000794.

Heinrich, R., Baumann, K.-H., 1994. Evolution of the Norwegian current and the Scandinavian ice sheets during the past 2.6 m.y.: evidence from ODP Leg 104 biogenic carbonate and terrigenous records. Palaeogeography, Palaeoclimatology, Palaeoecology 108, 75–94.

Herbert, T.D., 2003. Alkenone paleotemperature determinations. In: Elderfield, H., Turekian, K.K. (Eds.), Treatise in Marine Geochemistry. Elsevier, Amsterdam, pp. 391–432.

Hoffmann, G., Werner, M., Heimann, M., 1998. Water isotope module of the ECHAM atmospheric general circulation model – a study on timescales from days to several years. Journal of Geophysical Research 103, 16,871–16,896.

Holland, M.H., Bitz, C.M., Tremblay, B., 2006. Future abrupt reductions in the summer Arctic sea ice. Geophysical Research Letters 33, L23503. doi:10.1029/2006GL028024.

Hu, F.S., Shemesh, A., 2003. A biogenic-silica $\delta^{18}O$ record of climatic change during the last glacial–interglacial transition in southwestern Alaska. Quaternary Research 59, 379–385.

Hu, F.S., Ito, E., Brown, T.A., Curry, B.B., Engstrom, D.R., 2001. Pronounced climatic variations in Alaska during the last two millennia. Proceedings of the National Academy of Science 98, 10552–10556.

Huang, Y., Shuman, B., Wang, Y., Webb III, T., 2002. Hydrogen isotope ratios of palmitic acid in lacustrine sediments record late Quaternary climate variations. Geology 30, 1103–1106.

Huber, C., Leuenberger, M., Spahni, R., Flückiger, J., Schwander, J., Stocker, T.F., Johnsen, S., Landais, A., Jouzel, J., 2006. Isotope calibrated Greenland temperature record over Marine Isotope Stage 3 and its relation to CH_4. Earth and Planetary Science Letters 243 (3–4), 504–519.

Hughen, K., Overpeck, J., Anderson, R.F., Williams, K.M., 1996. The potential for palaeoclimate records from varved Arctic lake sediments: Baffin Island, Eastern Canadian Arctic. In: Kemp, A.E.S. (Ed.), Lacustrine Environments. Palaeoclimatology and Palaeoceanography from Laminated Sediments. Geological Society of London, Special Publications, vol. 116, pp. 57–71.

Hughes, M.K., Diaz, H.F., 1994. Was there a 'Medieval Warm Period' and if so, where and when? Journal of Climatic Change 265, 109–142.

Huybers, P., 2006. Early Pleistocene glacial cycles and the integrated summer insolation forcing. Science 313, 508–511.

Hyvärinen, H., 1976. Flandrian pollen deposition rates and tree-line history in northern Fennoscandia. Boreas 5 (3), 163–175.

Ilyashuk, E.A., Ilyashuk, B.P., Hammarlund, D., Larocque, I., 2005. Holocene climatic and environmental changes inferred from midge records (Diptera: Chironomidae, Chaoboridae, Ceratopogonidae) at Lake Berkut, southern Kola Peninsula, Russia. Holocene 15, 897–914.

Imbrie, J., Kipp, N.G., 1971. A new micropaleontological method for Quantitative Paleoclimatology: application to a late Pleistocene Caribbean Core. In: Turekian, K.K. (Ed.), The Late Cenozoic Glacial Age. Yale Univeristy Press, New Haven, CT, pp. 71–181.

Intergovernmental Panel on Climate Change (IPCC), 2007. Summary for policymakers. Contribution of Working Group I to the Fourth Assessment Report of the Intergovernmental Panel on Climate Change. In: Solomon, S., Qin, D., Manning, M., Chen, Z., Marquis, M., Averyt, K.B., Tignor, M., Miller, H.L. (Eds.), Climate Change 2007 – The Physical Science Basis. Cambridge University Press, Cambridge and New York, p. 18.

Iversen, J., 1944. Viscum, Hedera and Ilex as climatic indicators. A contribution to the study of past-glacial temperature climate. Geologiska Foreningens Forhandlingar 66, 463–483.

Jacoby, G.C., RD'Arrigo, D., 1995. Tree ring width and density evidence of climatic and potential forest change in Alaska. Global Biogeochemical Cycles 9 (2), 227–234.

Jakobsson, M., Macnab, R., 2006. A comparison between GEBCO sheet 5.17 and the International Bathymetric Chart of the Arctic Ocean (IBCAO) version 1.0. Marine Geophysical Researches 27 (1), 35–48.

Jansen, E., Bleil, E., Henrich, R., Kringstad, L., Slettemark, B., 1988. Paleoenvironmental changes in the Norwegian Sea and the northeast atlantic during the last 2.8 m.y.: deep sea drilling project/ocean drilling program sites 610, 642, 643 and 644. Paleoceanography 3, 563–581.

Jansen, E., Overpeck, J., Briffa, K.R., Duplessy, J.-C., Joos, F., Masson-Delmotte, V., Olago, D., Otto-Bliesner, B., Peltier, W.R., Rahmstorf, S., Ramesh, R., Raynaud, D., Rind, D., Solomina, O., Villalba, R., Zhang, D., 2007. Palaeoclimate. Contribution of Working Group I to the Fourth Assessment Report of the Intergovernmental Panel on Climate Change. In: Solomon, S., Qin, D., Manning, M., Chen, Z., Marquis, M., Averyt, K.B., Tignor, M., Miller, H.L. (Eds.), Climate Change 2007 – The Physical Science Basis. Cambridge University Press, Cambridge, United Kingdom and New York, pp. 434–497.

Jenkyns, H.C., Forster, A., Schouten, S., Sinninghe Damsté, J.S., 2004. High temperatures in the Late Cretaceous Arctic Ocean. Nature 432 (7019), 888–892.

Jennings, A.E., Knudsen, K.L., Hald, M., Hansen, C.V., Andrews, J.T., 2002. A mid-Holocene shift in Arctic sea ice variability on the East Greenland shelf. The Holocene 12, 49–58.

Johnsen, S.J., Dansgaard, W., White, J.W.C., 1989. The origin of Arctic precipitation under present and glacial conditions. Tellus 41B, 452–468.

Johnsen, S.J., Dahl-Jensen, D., Dansgaard, W., Gundestrup, N., 1995. Greenland palaeotemperatures derived from GRIP bore hole temperature and ice core isotope profiles. Tellus 47B, 624–629.

Jones, P.D., Briffa, K.R., Barnett, T.P., Tett, S.F.B., 1998. High-resolution palaeoclimatic records for the last millennium: interpretation, integration and comparison with General Circulation Model control-run temperatures. Holocene 8, 455–471.

Jouzel, J., Masson-Delmotte, V., Cattani, O., Dreyfus, G., Falourd, S., Hoffmann, G., Minster, B., Nouet, J., Barnola, J.M., Chappellaz, J., Fischer, H., Gallet, J.C., Johnsen, S., Leuenberger, M., Loulergue, L., Luethi, D., Oerter, H., Parrenin, F., Raisbeck, G., Raynaud, D., Schilt, A., Schwander, J., Selmo, E., Souchez, R., Spahni, R., Stauffer, B., Steffensen, J.P., Stenni, B., Stocker, T.F., Tison, J.L., Werner, M., Wolff, E.W., 2007. Orbital and millennial Antarctic climate variability over the past 800,000 Years. Science 317, 793–796. doi:10.1126/science.1141038.

Jouzel, J., Alley, R.B., Cuffey, K.M., Dansgaard, W., Grootes, P., Hoffmann, G., Johnsen, S.J., Koster, R.D., Peel, D., Shuman, C.A., Stievenard, M., Stuiver, M., White, J., 1997. Validity of the temperature reconstruction from water isotopes in ice cores. Journal of Geophysical Research 102 (C12), 26,471–26,487.

Kaakinen, A., Eronen, M., 2000. Holocene pollen stratigraphy indicating climatic and tree-line changes derived from a peat section at Ortino, in the Pechora lowland, northern Russia. The Holocene 10, 611–620.

Kandiano, E.S., Bauch, H.A., 2007. Phase relationship and surface water mass change in the Northeast Atlantic during Marine Isotope Stage 11 (MIS11). Quaternary Research 68 (3), 445–455.

Kaplan, J.O., Bigelow, N.H., Bartlein, P.J., Christiansen, T.R., Cramer, W., Harrison, S.P., Matveyeva, N.V., McGuire, A.D., Murray, D.F., Prentice, I.C., Razzhivin, V.Y., Smith, B., Walker, D.A., Anderson, P.M., Andreev, A.A., Brubaker, L.B., Edwards, M.E., Lozhkin, A.V., Ritchie, J.C., 2003. Climate change and arctic ecosystems II – modeling paleodata-model comparisons, and future projections. Journal of Geophysical Research 108 (D19), 8171. doi:10.1029/2002JD002559.

Kapsner, W.R., Alley, R.B., Shuman, C.A., Anandakrishnan, S., Grootes, P.M., 1995. Dominant control of atmospheric circulation on snow accumulation in central Greenland. Nature 37, 52–54.

Kaufman, D.S., 2009. An overview of late Holocene climate and environmental change inferred from Arctic lake sediment. Journal of Paleolimnology 41, 1–6. doi:10.1007/s10933-008-9259-6.

Kaufman, D.S., Brigham-Grette, J., 1993. Aminostratigraphic correlations and paleotemperature implications, Pliocene-Pleistocene high sea level deposits, northwestern Alaska. Quaternary Science Reviews 12, 21–33.

Kaufman, D.S., Ager, T.A., Anderson, N.J., Anderson, P.M., Andrews, J.T., Bartlein, P.J., Brubaker, L.B., Coats, L.L., Cwynar, L.C., Duvall, M.L., Dyke, A.S., Edwards, M.E., Eisner, W.R., Gajewski, K., Geirsdóttir, A., Hu, F.S., Jennings, A.E., Kaplan, M.R., Kerwin, M.W., Lozhkin, A.V., MacDonald, G.M., Miller, G.H., Mock, C.J., Oswald, W.W., Otto-Bliesner, B.L., Porinchu, D.F., Ruüland, K., Smol, J.P., Steig, E.J., Wolfe, B.B., 2004. Holocene thermal maximum in the western Arctic (0–180°W). Quaternary Science Reviews 23, 529–560.

Kaufman, D.S., Schneider, D.P., McKay, N.P., Ammann, C.M., Bradley, R.S., Briffa, K.R., Miller, G.H., Otto-Bliesner, B.L., Overpeck, J.T., Vinther, B.M., Arctic Lakes 2 k Project Members, 2009. Recent warming reverses long-term Arctic cooling. Science 235, 1236–1239.

Keigwin, L.D., Donnelly, J.P., Cook, M.E., Driscoll, N.W., Brigham-Grette, J., 2006. Rapid sea-level rise and Holocene climate in the Chukchi Sea. Geology 34, 861–864.

Kellogg, T.B., 1977. Paleoclimatology and paleo-oceanography of the Norwegian and Greenland seas: the last 450,000 years. Marine Micropaleontology 2, 235–249.

Kerwin, M., Overpeck, J.T., Webb, R.S., DeVernal, A., Rin, D.H., Healy, R.J., 1999. The role of oceanic forcing in mid-Holocene northern hemisphere climatic change. Paleoceanography 14, 200–210.

Kirk-Davidov, D.B., Schrag, D.P., Anderson, J.G., 2002. On the feedback of stratospheric clouds on polar climate. Geophysical Research Letters 29 (11), 1556.

Knutson, T.R., Delworth, T.L., Dixon, K.W., Held, I.M., Lu, J., Ramaswamy, V., Schwarzkopf, M.D., Stenchikov, G., Stouffer, R.J., 2006. Assessment of twentieth-century regional surface temperature trends using the GFDL CM2 coupled models. Journal of Climate 19 (9), 1624–1651.

Koç, N., Jansen, E., 1994. Response of the high-latitude Northern Hemisphere to orbital climate forcing – evidence from the Nordic Seas. Geology 22, 523–526.

Koç, N., Jansen, E., Haflidason, H., 1993. Paleooceanographic reconstruction of surface ocean conditions in the Greenland, Iceland and Norwegian Seas through the last 14 ka based on diatoms. Quaternary Science Reviews 12, 115–140.

Koerner, R.M., 2005. Mass balance of glaciers in the Queen Elizabeth Islands, Nunavut, Canada. Annals of Glaciology 42 (1), 417–423.

Koerner, R.M., Fisher, D.A., 1990. A record of Holocene summer climate from a Canadian high-Arctic ice core. Nature 343, 630–631.

Korhola, A., Olander, H., Blom, T., 2000. Cladoceran and chironomid assemblages as quantitative indicators of water depth in sub-Arctic Fennoscandian lakes. Journal of Paleolimnology 24, 43–54.
Korty, R.L., Emanuel, K.A., Scott, J.R., 2008. Tropical cyclone-induced upper-ocean mixing and climate: application to equable climates. Journal of Climate 21 (4), 638–654.
Kremenetski, C.V., Sulerzhitsky, L.D., Hantemirov, R., 1998. Holocene history of the northern range limits of some trees and shrubs in Russia. Arctic and Alpine Research 30, 317–333.
Kukla, G.J., 2000. The last interglacial. Science 287, 987–988.
Kump, L.R., Pollard, D., 2008. Amplification of Cretaceous warmth by biological cloud feedbacks. Science 11 (5873), 195. doi:10.1126/science.1153883.
Kurschner, W.M., van der Burgh, J., Visscher, H., Dilcher, D.L., 1996. Oak leaves as biosensors of late Neogene and early Pleistocene paleoatmospheric CO_2 concentrations. Marine Micropaleontology 27, 299–312.
Lamb, H.H., 1977. Climate History and the Future. Climate – Past, Present and Future, vol. 2. Metheun, London. 835pp.
Lambeck, K., Yokoyama, Y., Purcell, T., 2002. Into and out of the Last Glacial Maximum: sea-level change during oxygen isotope stages 3 and 2. Quaternary Science Reviews 21, 343–360.
Lauritzen, S.-E., 1996. Calibration of speleothem stable isotopes against historical records: a Holocene temperature curve for north Norway? In: Lauritzen, S.-E. (Ed.), Climatic Change: the Karst Record Karst Waters Institute Special Publication, vol. 2, pp. 78–80. Charles Town, West Virginia.
Lauritzen, S.-R., Lundberg, J., 1999. Calibration of the speleothem delta function: an absolute temperature record for the Holocene in northern Norway. The Holocene 9, 659–669. doi:10.1191/095968399667823929.
Lear, C.H., Rosenthal, Y., Coxall, H.K., Wilson, P.A., 2004. Late Eocene to early Miocene ice sheet dynamics and the global carbon cycle. Paleoceanography 19, PA4015. doi:10.1029/2004PA001039.
LeGrande, A.N., Schmidt, G.A., 2006. Global gridded data set of the oxygen isotopic composition in seawater. Geophysical Research Letters 33, L12604. doi:10.1029/2006GL026011.
Lemke, P., Ren, J., Alley, R.B., Allison, I., Carrasco, J., Flato, G., Fujii, Y., Kaser, G., Mote, P., Thomas, R.H., Zhang, T., 2007. Observations: changes in snow, ice and frozen ground. Contribution of Working Group I to the Fourth Assessment Report of the Intergovernmental Panel on Climate Change. In: Solomon, S., Qin, D., Manning, M., Chen, Z., Marquis, M., Averyt, K.B., Tignor, M., Miller, H.L. (Eds.), Climate Change 2007: The Physical Science Basis. Cambridge University Press, Cambridge and New York, p. 996.
Leng, M.J., Barker, P.A., 2005. A review of the oxygen isotope composition of lacustrine diatom silica for palaeoclimate reconstruction. Earth Science Reviews 75, 5–27. doi:10.1016/j.earscirev.2005.10.001.
Leng, M.J., Marshall, J.D., 2004. Palaeoclimate interpretation of stable isotope data from lake sediment archives. Quaternary Science Reviews 23, 811–831.
Letreguilly, A., Reeh, N., Huybrechts, P., 1991. The Greenland ice sheet through the Last Glacial–Interglacial cycle. Global and Planetary Change 4 (4), 385–394.
Levac, E., de Vernal, A., Blake, W.J., 2001. Sea-surface conditions in northernmost Baffin Bay during the Holocene – palynological evidence. Journal of Quaternary Science 16, 353–363.
Levy, L.B., Kaufman, D.S., Werner, A., 2003. Holocene glacier fluctuations, Waskey Lake, northeastern Ahklun Mountains, southwestern Alaska. Holocene 14, 185–193.
Lisiecki, L.E., Raymo, M.E., 2005. A Pliocene-Pleistocene stack of 57 globally distributed benthic $\delta^{18}O$ records. Paleoceanography 20, PA1003. doi:10.1029/2004PA001071.
Loutre, M.F., 2003. Clues from MIS 11 to predict the future climate – a modeling point of view. Earth and Planetary Science Letters 212 (1–2), 213–224.
Lozhkin, A.V., Anderson, P.M., 1995. The last interglaciation of northeast Siberia. Quaternary Research 43, 147–158.
Lozhkin, A.V., Anderson, P.M., 1996. A late Quaternary pollen record from Elikchan 4 Lake, northeast Siberia. Geology of the Pacific Ocean 12, 609–616.
Lozhkin, A.V., Anderson, P.M., Eisner, W.R., Ravako, L.G., Hopkins, D.M., Brubaker, L. B., Colinvaux, P.A., Miller, M.C., 1993. Late Quaternary lacustrine pollen records from southwestern Beringia. Quaternary Research 9, 314–324.
Lozhkin, A.V., Anderson, P.M., Vartanyan, S.L., Brown, T.A., Belaya, B.V., Kotov, A.N., 2001. Late Quaternary paleoenvironments and modern pollen data from Wrangel Island (Northern Chukotka). Quaternary Science Reviews 20, 217–233.
Lozhkin, A.V., Anderson, P.M., Matrosova, T.V., Minyuk, P.S., 2007. The pollen record from El'gygytgyn Lake: implications for vegetation and climate histories of northern Chukotka since the late middle Pleistocene. Journal of Paleolimnology 37 (1), 135–153.
Lubinski, D.J., Forman, S.L., Miller, G.H., 1999. Holocene glacier and climate fluctuations on Franz Josef Land, Arctic Russia, 80°N. Quaternary Science Reviews 18, 85–108.
Luckman, B.H., 2007. Dendroclimatology. In: Elias, S. (Ed.), Encyclopedia of Quaternary Science, 1, pp. 465–475.
Lüthi, D., Le Floch, M., Bereiter, B., Blunier, T., Barnola, J.-M., Siegenthaler, U., Raynaud, D., Jouzel, J., Fischer, H., Kawamura, K., Stocker, T.F., 2008. High-resolution carbon dioxide concentration record 650,000–800,000 years before present. Nature 453, 379–382.
MacDonald, G.M., Edwards, T., Moser, K., Pienitz, R., 1993. Rapid response of treeline vegetation and lakes to past climate warming. Nature 361, 243–246.
MacDonald, G.M., Gervais, B.R., Snyder, J.A., Tarasov, G.A., Borisova, O.K., 2000a. Radiocarbon dated *Pinus sylvestris* L. wood from beyond treeline on the Kola Peninsula, Russia. The Holocene 10, 143–147.
MacDonald, G.M., Velichko, A.A., Kremenetski, C.V., Borisova, O.K., Goleva, A.A., Andreev, A.A., Cwynar, L.C., Riding, R.T., Forman, S.L., Edwards, T.W.D., Aravena, R., Hammarlund, D., Szeicz, J.M., Gattaulin, V.N., 2000b. Holocene treeline history and climate change across northern Eurasia. Quaternary Research 53, 302–311.
MacDonald, G.M., Kremenetski, K.V., Beilman, D.W., 2008. Climate change and the northern Russian treeline zone. Philosophical Transactions of the Royal Society B 363, 2283–2299. doi:10.1098/rstb.2007.2200.
Mahowald, N.M., Muhs, D.R., Levis, S., Rasch, P.J., Yoshioka, M., Zender, C.S., Luo, C., 2006. Change in atmospheric mineral aerosols in response to climate: Last glacial period, preindustrial, modern, and doubled carbon dioxide climates. Journal of Geophysical Research 111, D10202. doi:10.1029/2005JD006653.
Mann, M.E., Jones, P.D., 2003. Global surface temperatures over the past two millennia. Geophysical Research Letters 30 (15), 1820. doi:10.1029/2003GL017814.
Mann, M.E., Bradley, R.S., Hughes, M.K., 1998. Global-scale temperature patterns and climate forcing over the past six centuries. Nature 392, 779–787.
Mann, M.E., Zhang, A., Hughes, M.K., Bradley, R.S., Miller, S.K., Rutherford, S., Ni, F., 2008. Proxy-based reconstructions of hemispheric and global surface temperature variations over the past two millennia. Proceedings of the National Academy of Sciences 105, 13252–13257.
Marchant, D.R., Denton, G.H., 1996. Miocene and Pliocene paleoclimate of the Dry Valleys region, southern Victoria Land: A geomorphological approach. Marine Micropaleontology 27, 253–271.
Marincovich Jr., L., Gladenkov, A.Y., 2001. New evidence for the age of Bering Strait. Quaternary Science Reviews 20 (1–3), 329–335.
Marshall, S.J., Clark, P.U., 2002. Basal temperature evolution of North American ice sheets and implications for the 100-kyr cycle. Geophysical Research Letters 29 (24), 2214.
Masson-Delmotte, V., Jouzel, J., Landais, A., Stievenard, M., Johnsen, S.J., White, J.W. C., Werner, M.A., Sveinbjornsdottir, A., Fuhrer, K., 2005. GRIP deuterium excess reveals rapid and orbital-scale changes in Greenland moisture origin. Science 309, 118–121.
Mathieu, R., Pollard, D., Cole, J.E., White, J.W.C., Webb, R.S., Thompson, S.L., 2002. Simulation of stable water isotope variations by the GENESIS GCM for modern conditions. Journal of Geophysical Research 107 (D4), 4037. doi:10.1029/2001JD900255.
Matthews Jr., J.V., Schweger, C.E., Janssens, J., 1990. The last (Koy-Yukon) interglaciation in the northern Yukon – evidence from unit 4 at Chijee's Bluff, Bluefish Basin. Geographie physique et Quaternaire 44, 341–362.
Matthiessen, J., Knies, J., Vogt, C., Stein, R., 2009. Pliocene palaeoceanography of the Arctic Ocean and subarctic seas. Philosophical Transactions of the Royal Society of London, Series A 367, 21.
Mayewski, P.A., Meeker, L.D., Twickler, M.S., Whitlow, S.I., Yang, Q., Lyons, W.B., Prentice, M., 1997. Major features and forcing of high-latitude Northern Hemisphere atmospheric circulation using a 110,000-year-long glaciochemical series. Journal of Geophysical Research 102, 26,345–26,366.
Maximova, L.N., Romanovsky, V.E., 1988. A hypothesis of the Holocene permafrost evolution. In: Proceedings of the Fifth International Conference on Permafrost, Norwegian Institute of Technology, Trondheim, Norway, 102–106.
McGhee, R., 2004. The Last Imaginary Place: a Human History of the Arctic World. Key Porter, Ontario, 296 pp.
McKenna, M.C., 1980. Eocene paleolatitude, climate and mammals of Ellesmere Island. Paleogeography, Paleoclimatology and Paleoecology 30, 349–362.
McManus, J.F., Bond, G.C., Broecker, W.S., Johnsen, S., Labeyrie, L., Higgins, S., 1994. High-resolution climate records from the North Atlantic during the last interglacial. Nature 371, 326–327.
McManus, J.F., 2004. A great grand-daddy of ice cores. Nature 429, 611–612.
Meeker, L.D., Mayewski, P.A., 2002. A 1400-year high-resolution record of atmospheric circulation over the North Atlantic and Asia. Holocene 12, 257–266.
Miller, G.H., Alley, R.B., Brigham-Grette, J., Fitzpatrick, J.J., Polyak, L., Serreze, M., White, J.W.C., 2010. Arctic Amplification: can the past constrain the future? Quaternary Science Reviews 29, 1779–1790.
Miller, G.H., Wolfe, A.P., Briner, J.P., Sauer, P.E., Nesje, A., 2005. Holocene glaciation and climate evolution of Baffin Island, Arctic Canada. Quaternary Science Reviews 24, 1703–1721.
Moberg, A., Sonechkin, D.M., Holmgren, K., Datsenko, N.M., Karlen, W., 2005. Highly variable northern hemisphere temperatures reconstructed from low- and high-resolution proxy data. Nature 433, 613–617.
Moran, K., Backman, J., Brinkhuis, H., Clemens, S.C., Cronin, T., Dickens, G.R., Eynaud, F., Gattacceca, J., Jakobsson, M., Jordan, R.W., Kaminski, M., King, J., Koç, N., Krylov, A., Martinez, N., Matthiessen, J., McInroy, D., Moore, T.C., Onodera, J., O'Regan, A.M., Pälike, H., Rea, B., Rio, D., Sakamoto, T., Smith, D.C., Stein, R., St. John, K., Suto, I., Suzuki, N., Takahashi, K., Watanabe, M., Yamamoto, M., Farrell, J., Frank, M., Kubik, P., Jokat, W., Kristoffersen, Y., 2006. The Cenozoic palaeoenvironment of the Arctic Ocean. Nature 441, 601–605.
Muller, P.J., Kirst, G., Ruhland, G., von Storch, I., Rossell-Mele, A., 1998. Calibration of the alkenone paleotemperature index $U^{K'}_{37}$ based on core-tops from the eastern South Atlantic and the global ocean (60°N–60°S). Geochimica et Cosmochimica Acta 62, 1757–1772.
National Research Council, 2006. Surface Temperature Reconstructions for the Last 2,000 Years. National Academic Press, Washington, DC. 160pp.
Naurzbaev, M.M., Vaganov, E.A., Sidorova, O.V., Schweingruber, F.H., 2002. Summer temperatures in eastern Taimyr inferred from a 2427-year late-Holocene tree-ring chronology and earlier floating series. The Holocene 12, 727–736.

Nelson, R.E., Carter, L.D., 1991. Preliminary interpretation of vegetation and paleoclimate in northern Alaska during the late Pliocene Colvillian marine transgression. In: Bradley, D.C., Ford, A.B. (Eds.), Geologic Studies in Alaska, U.S. Geological Survey Bulletin 1999, pp. 219–222.
Nesje, A., Matthews, J.A., Dahl, S.O., Berrisford, M.S., Andersson, C., 2001. Holocene glacier fluctuations of Flatebreen and winter precipitation changes in the Jostedalsbreen region, western Norway, based on glaciolacustrine records. The Holocene 11, 267–280.
Nesje, A., Bakke, J., Dahl, S.O., Lie, O., Matthews, J.A., 2008. Norwegian mountain glaciers in the past, present and future. Global and Planetary Change 60, 10–27.
Nørgaard-Pedersen, N., Spielhagen, R.F., Thiede, J., Kassens, H., 1998. Central Arctic surface ocean environment during the past 80,000 years. Paleoceanography 13, 193–204.
Nørgaard-Pedersen, N., Spielhagen, R.F., Erlenkeuser, H., Grootes, P.M., Heinemeier, J., Knies, J., 2003. The Arctic Ocean during the Last Glacial Maximum – Atlantic and polar domains of surface water mass distribution and ice cover. Paleoceanography 18, 8-1–8-19.
Nørgaard-Pedersen, N., Mikkelsen, N., Kristoffersen, Y., 2007a. Arctic Ocean record of last two glacial-interglacial cycles off North Greenland/Ellesmere Island – implications for glacial history. Marine Geology 244, 93–108.
Nørgaard-Pedersen, N., Mikkelsen, N., Lassen, S.J., Kristoffersen, Y., Sheldon, E., 2007b. Reduced sea ice concentrations in the Arctic Ocean during the last interglacial period revealed by sediment cores off northern Greenland. Paleoceanography 22, PA1218. doi:10.1029/2006PA001283.
Nürnberg, D., Tiedemann, R., 2004. Environmental changes in the Sea of Okhotsk during the last 1.1 million years. Paleoceanography 19, PA4011.
O'Brien, S.R., Mayewski, P.A., Meeker, L.D., Meese, D.A., Twickler, M.S., Whitlow, S.I., 1995. Complexity of Holocene climate as reconstructed from a Greenland ice core. Science 270, 1962–1964.
Ogilvie, A.E.J., Jónsson, T., 2001. "Little Ice Age" research: a perspective from Iceland. Climate Change 48, 9–52.
Olson, S.L., Hearty, P.J., 2009. A sustained +21 m sea-level highstand during MIS 11 (400ka): direct fossil and sedimentary evidence from Bermuda. Quaternary Science Reviews 28, 271–285.
Oswald, W.W., Brubaker, L.B., Hu, F.S., Kling, G.W., 2003. Holocene pollen records from the central Arctic Foothills, northern Alaska – testing the role of substrate in the response of tundra to climate change. Journal of Ecology 91, 1034–1048.
Otto-Bliesner, B.L., Marshall, S.J., Overpeck, J.T., Miller, G.H., Hu, A., CAPE Last Interglacial Project members, 2006. Simulating Arctic climate warmth and icefield retreat in the Last Interglaciation. Science 311, 1751–1753. doi:10.1126/science.1120808.
Overpeck, J., Hughen, K., Hardy, D., Bradley, R., Case, R., Douglas, M., Finney, B., Gajewski, K., Jacoby, G., Jennings, A., Lamoureux, S., Lasca, A., MacDonald, G., Moore, J., Retelle, M., Smith, S., Wolfe, A., Zielinski, G., 1997. Arctic environmental changes of the last four centuries. Science 278, 1251–1256.
Pagani, M., Liu, Z., LaRiviere, J., Ravelo, A.C., 2010. High Earth-system climate sensitivity determined from Pliocene carbon dioxide concentrations. Nature Geoscience 3, 27–30.
Pienitz, R., Smol, J.P., Last, W.M., Leavitt, P.R., Cumming, B.F., 2000. Multi-proxy Holocene palaeoclimatic record from a saline lake in the Canadian Subarctic. The Holocene 10 (6), 673–686. doi:10.1191/09596830094935.
Pienitz, R., Douglas, M.S.V., Smol, J.P. (Eds.), 2004. Long-Term Environmental Change in Arctic and Antarctic Lakes. Springer, Dordrecht, Germany, p. 579.
Peixoto, J.P., Oort, A.H., 1992. Physics of Climate. American Institute of Physics, New York, 520 pp.
Pisaric, M.F.J., MacDonald, G.M., Velichko, A.A., Cwynar, L.C., 2001. The late-glacial and post-glacial vegetation history of the northwestern limits of Beringia, from pollen, stomates and tree stump evidence. Quaternary Science Reviews 20, 235–245.
Polyak, L., Alley, R.B., Andrews, J.T., Brigham-Grette, J., Darby, D., Dyke, A., Fitzpatrick, J.J., Funder, S., Holland, M., Jennings, A., Miller, G.H., Savelle, J., Serreze, M., White, J.W.C., Wolff, E., 2010. History of Sea Ice in the Arctic. Quaternary Science Reviews 29, 1757–1778.
Polyak, L., Curry, W.B., Darby, D.A., Bischof, J., Cronin, T.M., 2004. Contrasting glacial/interglacial regimes in the western Arctic Ocean as exemplified by a sedimentary record from the Mendeleev Ridge. Paleogeography, Paleoclimatology and Paleoecology 203, 73–93.
Porter, S.C., Denton, G.H., 1967. Chronology of neoglaciation. American Journal of Science 165, 177–210.
Poulsen, C.J., Barron, E.J., Peterson, W.H., Wilson, P.A., 1999. A reinterpretation of mid-Cretaceous shallow marine temperatures through model-data comparison. Paleoceanography 14 (6), 679–697.
Prahl, F.G., Muelhausen, L.A., Zahnle, D.L., 1988. Further evaluation of long-chain alkenones as indicators of paleoceanographic conditions. Geochimica et Cosmochimica Acta 52, 2303–2310.
Prahl, F.G., de Lange, G.J., Lyle, M., Sparrow, M.A., 1989. Post-depositional stability of long-chain alkenones under contrasting redox conditions. Nature 341, 434–437.
Prentice, I.C., Webb III, T., 1998. BIOME 6000 – reconstructing global mid-Holocene vegetation patterns from palaeoecological records. Journal of Biogeography 25, 997–1005.
Rasmussen, S.O., Andersen, K.K., Svensson, A.M., Steffensen, J.P., Vinther, B.M., Clausen, H.B., Siggaard-Andersen, M.-L., Johnsen, S.J., Larsen, L.B., Dahl-Jensen, D., Bigler, M., Röthlisberger, R., Fischer, H., Goto-Azuma, K., Hansson, M. E., Ruth, U., 2006. A new Greenland ice core chronology for the last glacial termination. Journal of Geophysical Research 111, D06102. doi:10.1029/2005JD006079.
Raymo, M.E., 1994. The initiation of northern hemisphere glaciation. Annual Review of Earth and Planetary Sciences 22, 353–383. doi:10.1146/annurev.ea.22.050194.002033.
Raymo, M.E., 1997. The timing of major climate terminations. Paleoceanography 12, 577–585.
Raymo, M.E., Oppo, D.W., Curry, W., 1997. The mid-Pleistocene climate transition: a deep sea carbon isotopic perspective. Paleoceanography 12, 546–559.
Raymo, M.E., Lisiecki, L.E., Nisancioglu, K.H., 2006. Plio-Pleistocene ice volume, Antarctic climate, and the global $\delta^{18}O$ record. Science 313, 492–495.
Raymo, M.E., Grant, B., Horowitz, M., Rau, G.H., 1996. Mid-Pliocene warmth: stronger greenhouse and stronger conveyor. Marine Micropaleontology 27, 313–326.
Renssen, H., Goosse, H., Fichefet, T., Brovkin, V., Dresschaert, E., Wolk, F., 2005. Simulating the Holocene climate evolution at northern high latitudes using a coupled atmosphere–sea ice–ocean–vegetation model. Climate Dynamics 24, 23–43.
Reyes, A.V., Wiles, G.C., Smith, D.J., Barclay, D.J., Allen, S., Jackson, S., Larocque, S., Laxton, S., Lewis, D., Calkin, P.E., Clauge, J.J., 2006. Expansion of alpine glaciers in Pacific North America in the first millennium A.D. Geology 34, 57–60.
Ritchie, J.C., Cwynar, L.C., Spear, R.W., 1983. Evidence from northwest Canada for an early Holocene Milankovitch thermal maximum. Nature 305, 126–128.
Robinson, M.M., 2009. New quantitative evidence of extreme warmth in the Pliocene Arctic. Stratigraphy 6, 265–275.
Roe, G.H., Allen, M.R., 1999. A comparison of competing explanations for the 100,000-yr ice age cycle. Geophysical Research Letters 26 (15), 2259–2262.
Rosell-Mele, A., Eglinton, G., Pflaumann, U., Sarnthein, M., 1995. Atlantic core top calibration of the U^{k}_{37} index as a sea-surface temperature indicator. Geochimica et Cosmochimica Acta 59, 3099–3107.
Royer, D.L., 2006. CO_2-forced climate thresholds during the Phanerozoic. Geochimica et Cosmochimica Acta 70 (23), 5665–5675.
Royer, D.L., Berner, R.A., Park, J., 2007. Climate sensitivity constrained by CO_2 concentrations over the past 420 million years. Nature 446, 530–532.
Ruddiman, W.F., 2003. Insolation, ice sheets and greenhouse gases. Quaternary Science Reviews 22, 1597.
Ruddiman, W.F., 2006. Ice-driven CO_2 feedback on ice volume. Climate of the Past 2, 43–55.
Ruddiman, W.F., Shackleton, N.J., McIntyre, A., 1986. North Atlantic sea-surface temperatures for the last 1.1 million years. In: Summerhayes, C.P., Shackleton, N. J. (Eds.), North Atlantic Paleoceanography. Geological Society of London, Special Publication, vol. 21, pp. 155–173.
Salvigsen, O., 2002. Radiocarbon-dated *Mytilus edulis* and *Modiolus modiolus* from northern Svalbard: climatic implications. Norsk Geografisk Tidsskrift 56, 56–61.
Salvigsen, O., Forman, S.L., Miller, G.H., 1992. Thermophilous mollusks on Svalbard during the Holocene and their paleoclimatic implications. Polar Research 11, 1–10.
Salzmann, U., Haywood, A.M., Lunt, D.J., Valdes, P.J., Hill, D.J., 2008. A new global biome reconstruction and data-model comparison for the Middle Pliocene. Global Ecology and Biogeography 17, 432–447.
Sauer, P.E., Miller, G.H., Overpeck, J.T., 2001. Oxygen isotope ratios of organic matter in Arctic lakes as a paleoclimate proxy – field and laboratory investigations. Journal of Paleolimnology 25, 43–64.
Schiff, C.J., Kaufman, D.S., Wolfe, A.P., Dodd, J., Sharp, Z., 2008. Late Holocene storm-trajectory changes inferred from the oxygen isotope composition of lake diatoms, south Alaska. Journal of Paleolimnology 41, 189–208.
Schindler, D.W., Smol, J.P., 2006. Cumulative effects of climate warming and other human activities on freshwaters of Arctic and subarctic North America. Ambio 35, 160–168.
Schmidt, G.A., LeGrande, A.N., Hoffman, G., 2007. Water isotope expressions of intrinsic and forced variability in a coupled ocean–atmosphere model. Journal of Geophysical Research 112, D10103. doi:10.1029/2006JD007781.
Schneider, K.B., Faro, B., 1975. Effects of sea ice on sea otters (*Enhydra lutris*). Journal of Mammalogy 56, 91–101.
Schouten, S., Hopmans, E.C., Damsté, J.S.S., 2004. The effect of maturity and depositional redox conditions on archaeal tetraether lipid palaeothermometry. Organic Geochemistry 35 (5), 567–571.
Schrag, D.P., Adkins, J.F., McIntyre, K., Alexander, J.L., Hodell, D.A., Charles, C.D., JMcManus, F., 2002. The oxygen isotopic composition of seawater during the Last Glacial Maximum. Quaternary Science Reviews 21 (1–3), 331–342.
Schulz, H., von Rad, U., Erlenkeuser, H., 1998. Correlation between Arabian Sea and Greenland climate oscillations of the past 110,000 years. Nature 393, 54–57.
Scott, D.B., Mudie, P.J., Baki, V., MacKinnon, K.D., Cole, F.E., 1989. Biostratigraphy and late Cenozoic paleoceanography of the Arctic Ocean – foraminiferal, lithostratigraphic, and isotopic evidence. Geological Society of America Bulletin 101, 260–277.
Seppä, H., 1996. Post-glacial dynamics of vegetation and tree-lines in the far north of Fennoscandia. Fennia 174, 1–96.
Seppä, H., Birks, H.J.B., 2001. July mean temperature and annual precipitation trends during the Holocene in the Fennoscandian tree-line area – pollen-based climate reconstructions. The Holocene 11, 527–539.
Seppä, H., Birks, H.J.B., 2002. Holocene climate reconstructions from the Fennoscandian tree-line area based on pollen data from Toskaljavri. Quaternary Research 57, 191–199.
Seppä, H., Hammarlund, D., 2000. Pollen-stratigraphical evidence of Holocene hydrological change in northern Fennoscandia supported by independent isotopic data. Journal of Paleolimnology 24 (1), 69–79.

Seppä, H., Cwynar, L.C., MacDonald, G.M., 2003. Post-glacial vegetation reconstruction and a possible 8200 cal. yr BP event from the low arctic of continental Nunavut, Canada. Journal of Quaternary Science 18, 621–629.
Seppä, H., Birks, H.J.B., Odland, A., Poska, A., Veski, S., 2004. A modern pollen-climate calibration set from northern Europe – developing and testing a tool for palaeoclimatological reconstructions. Journal of Biogeography 31, 251–267.
Serreze, M.C., Francis, J.A., 2006. The Arctic amplification debate. Climatic Change 76, 241–264.
Severinghaus, J.P., Brook, E.J., 1999. Abrupt climate change at the end of the last glacial period inferred from trapped air in polar ice. Science 286, 930–934.
Severinghaus, J.P., Sowers, T., Brook, E.J., Alley, R.B., Bender, M.L., 1998. Timing of abrupt climate change at the end of the Younger Dryas interval from thermally fractionated gases in polar ice. Nature 391 (6663), 141–146.
Sewall, J.O., Sloan, L.C., 2001. Equable Paleogene climates: the result of a stable, positive Arctic oscillation? Geophysical Research Letters 28 (19), 3693–3695.
Sewall, J.O., Sloan, L.C., 2004. Disappearing Arctic sea ice reduces available water in the American west. Geophysical Research Letters 31. doi:10.1029/2003GL019133.
Shackleton, N.J., 1967. Oxygen isotope analyses and paleotemperatures reassesssed. Nature 215, 15–17.
Shackleton, N.J., 1974. Attainment of isotopic equilibrium between ocean water and the benthonic foraminifera genus Uvigerina – isotopic changes in the ocean during the last glacial. Colloques International du CNRS 219, 203–209.
Shellito, C.J., Sloan, L.C., Huber, M., 2003. Climate model sensitivity to atmospheric CO_2 levels in the early-middle Paleogene. Palaeogeography, Palaeoclimatology, Palaeoecology 193, 113–123.
Shemesh, A., Rosqvist, G., Riett-Shati, M., Rubensdotter, L., Bigler, C., Yam, R., Karlén, W., 2001. Holocene climate change in Swedish Lapland inferred from an oxygen-isotope record of lacustrine biogenic silica. The Holocene 11, 447–454.
Shindell, D.T., Schmidt, G.A., Mann, M.E., Rind, D., Waple, A., 2001. Solar forcing of regional climate change during the Maunder Minimum. Science 294, 2149–2152.
Shuman, C.A., Alley, R.B., Anandakrishnan, S., White, J.W.C., Grootes, P.M., Stearns, C. R., 1995. Temperature and accumulation at the Greenland Summit: comparison of high-resolution isotope profiles and satellite passive microwave brightness temperature trends. Journal of Geophysical Research 100 (D5), 9165–9177.
Siegenthaler, U., Stocker, T.F., Monnin, E., Lüthi, E., Schwander, J., Stauffer, B., Raynaud, D., Barnola, J.M., Fischer, H., Masson-Delmotte, V., Jouzel, J., 2005. Stable carbon cycle–climate relationship during the late Pleistocene. Science 310, 1313–1317. doi:10.1126/science.1120130.
Sloan, L.C., Barron, E.J., 1992. A comparison of Eocene climate model results to quantified paleoclimatic interpretations. Palaeogeography, Palaeoclimatology, Palaeoecology 93 (3–4), 183–202.
Sloan, L.C., Pollard, D., 1998. Polar stratospheric clouds: a high latitude warming mechanism in an ancient greenhouse world. Geophysical Research Letters 25 (18), 3517–3520.
Sluijs, A., Schouten, S., Pagani, M., Woltering, M., Brinkhuis, H., Damste, J.S.S., Dickens, G.R., Huber, M., Reichart, G.J., Stein, R., Matthiessen, J., Lourens, L.J., Pedentchouk, N., Backman, J., Moran, K., 2006. Subtropical arctic ocean temperatures during the Palaeocene/Eocene thermal maximum. Nature 441, 610–613.
Sluijs, A., Rohl, U., Schouten, S., Brumsack, H.J., Sangiorgi, F., Damste, J.S.S., Brinkhuis, H., 2008. Arctic late Paleocene-early Eocene paleoenvironments with special emphasis on the Paleocene-Eocene thermal maximum (Lomonosov Ridge, Integrated Ocean Drilling Program Expedition 302). Paleoceanography 23 (1), PA1S11.
Smol, J.P., 2008. Pollution of Lakes and Rivers – A Paleoenvironmental Perspective, second ed. Blackwell Publishing, Oxford, U.K., 280 pp.
Smol, J.P., Cumming, B.F., 2000. Tracking long-term changes in climate using algal indicators in lake sediments. Journal of Phycology 36, 986–1011.
Smol, J.P., Douglas, M.S.V., 2007a. Crossing the final ecological threshold in high Arctic ponds. Proceedings of the National Academy of Sciences 104, 12,395–12,397.
Smol, J.P., Douglas, M.S.V., 2007b. From controversy to consensus: making the case for recent climatic change in the Arctic using lake sediments. Frontiers in Ecology and the Environment 5, 466–474.
Smol, J.P., Wolfe, A.P., Birks, H.J.B., Douglas, M.S.V., Jones, V.J., Korhola, A., Pienitz, R., Rühland, K., Sorvari, S., Antoniades, D., Brooks, S.J., Fallu, M.-A., Hughes, M., Keatley, B.E., Laing, T.E., Michelutti, N., Nazarova, L., Nyman, M., Paterson, A.M., Perren, B., Quinlan, R., Rautio, M., Saulnier-Talbot, É., Siitonen, S., Solovieva, N., Weckström, J., 2005. Climate-driven regime shifts in the biological communities of arctic lakes. Proceedings of the National Academy of Sciences 102, 4397–4402.
Solovieva, N., Tarasov, P.E., MacDonald, G.M., 2005. Quantitative reconstruction of Holocene climate from the Chuna Lake pollen record, Kola Peninsula, northwest Russia. The Holocene 15, 141–148.
Sowers, T., Bender, M., Raynaud, D., 1989. Elemental and isotopic composition of occluded O_2 and N_2 in polar ice. Journal of Geophysical Research-Atmospheres 94 (D4), 5137–5150.
Spencer, M.K., Alley, R.B., Fitzpatrick, J.J., 2006. Developing a bubble number–density paleoclimatic indicator for glacier ice. Journal of Glaciology 52 (178), 358–364.
Spielhagen, R.F., Erlenkeuser, H., 1994. Stable oxygen and carbon isotopes in planktic foraminifers from Arctic Ocean surface sediments – reflection of the low salinity surface water layer. Marine Geology 119 (3/4), 227–250.
Spielhagen, R.F., Baumann, K.-H., Erlenkeuser, H., Nowaczyk, N.R., Nørgaard-Pedersen, N., Vogt, C., Weiel, D., 2004. Arctic Ocean deep-sea record of northern Eurasian ice sheet history. Quaternary Science Reviews 23 (11–13), 1455–1483.
Spielhagen, R.F., Erlenkeuser, H., Siegert, C., 2005. History of freshwater runoff across the Laptev Sea (Arctic) during the last deglaciation. Global and Planetary Change 48 (1–3), 187–207.
Stanton-Frazee, C., Warnke, D.A., Venz, K., Hodell, D.A., 1999. The stage 11 problem as seen from ODP site 982. In: Poore, R.Z., Burckle, L., Droxler, A., McNulty, W.E. (Eds.), Marine Oxygen Isotope Stage 11 and Associated Terrestrial Records. U.S. Geological Survey, p. 75. Open-file Report 99-312.
Stein, R., Nam, S.I., Schubert, C., Vogt, C., Fütterer, D., Heinemeier, J., 1994. The last deglaciation event in the eastern central Arctic Ocean. Science 264, 692–696.
Stötter, J., Wastl, M., Caseldine, C., Häberle, T., 1999. Holocene palaeoclimatic reconstruction in Northern Iceland – approaches and results. Quaternary Science Reviews 18, 457–474.
Stroeve, J.C., Serreze, M., Drobot, S., Gearheard, S., Holland, M., Maslanik, J., Meier, W., Scambos, T., 2008. Arctic sea ice extent plummets in 2007. EOS, Transactions of the American Geophysical Union 89, 13–14.
Svendsen, J.I., Mangerud, J., 1997. Holocene glacial and climatic variations on Spitsbergen, Svalbard. The Holocene 7, 45–57.
Taylor, K.C., Mayewski, P.A., Alley, R.B., Brook, E.J., Gow, A.J., Grootes, P.M., Meese, D. A., Saltzman, E.S., Severinghaus, J.P., Twickler, M.S., White, J.W.C., Whitlow, S., Zielinski, G.A., 1997. The Holocene/Younger Dryas transition recorded at Summit Greenland. Science 278, 825–827.
Teece, M.A., Getliff, J.M., Leftley, J.W., Parkes, R.J., Maxwell, J.R., 1998. Microbial degradation of the marine prymnesiophyte *Emiliania huxleyi* under oxic and anoxic conditions as a model for early diagenesis – long chain alkadienes, alkenones and alkyl alkenoates. Organic Geochemistry 29, 863–880.
Toggweiler, J.R., 2008. Origin of the 100,000-year timescale in Antarctic temperatures and atmospheric CO_2. Paleoceanography 23, PA2211. doi:10.1029/2006PA001405.
Tripati, A., Eagle, R., Morton, A., Dowdeswell, J., Atkinson, K., Bahé, Y., Dawber, C., Khadun, E., Shaw, R., Shorttle, O., Thanabalasundaram, L., 2008. Evidence for glaciation in the Northern Hemisphere back to 44 Ma from ice-rafted debris in the Greenland Sea. Earth and Planetary Science Letters 265, 112–122.
Tripati, A.K., Roberts, C.D., Eagle, R.A., 2009. Coupling of CO_2 and ice sheet stability over major climate transitions of the last 20 Million years. Science 326, 1394–1397.
Troitsky, S.L., 1964. Osnoviye zakonomernosti izmeneniya sostava fauny po razrezam morskikh meshmorennykh sloev ust-eniseyskoy vpadiny i nishnepechorskoy depressii. Akademia NAUK SSSR, Trudy instituta geologii i geofiziki 9, 48–65 (in Russian).
Vassiljev, J., 1998. The simulated response of lakes to changes in annual and seasonal precipitation – implication for Holocene lake-level changes in northern Europe. Climate Dynamics 14, 791–801.
Vassiljev, J., Harrison, S.P., Guiot, J., 1998. Simulating the Holocene lake-level record of Lake Bysjon, southern Sweden. Quaternary Research 49, 62–71.
Velichko, A.A., Andreev, A.A., Klimanov, V.A., 1997. Climate and vegetation dynamics in the tundra and forest zone during the Late Glacial and Holocene. Quaternary International 41/42, 71–96.
Vinther, B.M., Clausen, H.B., Johnsen, S.J., Rasmussen, S.O., Andersen, K.K., Buchardt, S.L., Dahl-Jensen, D., Seierstad, I.K., Siggaard-Andersen, M.-L., Steffensen, J.P., Svensson, A.M., Olsen, J., Heinemeier, J., 2006. A synchronized dating of three Greenland ice cores throughout the Holocene. Journal of Geophysical Research 111, D13102. doi:10.1029/2005JD006921.
Vinther, B.M., Clausen, H.B., Fisher, D.A., Koerner, R.M., Johnsen, S.J., Andersen, K.K., Dahl-Jensen, D., Rasmussen, S.O., Steffensen, J.P., Svensson, A.M., 2008. Synchronizing ice cores from the Renland and Agassiz ice caps to the Greenland Ice Core Chronology. Journal of Geophysical Research 113, D08115. doi:10.1029/2007JD009143.
Wang, Y.J., Cheng, H., Edwards, R.L., An, Z.S., Wu, J.Y., Shen, C.-C., Dorale, J.A., 2001. A high-resolution absolute-dated late Pleistocene monsoon record from Hulu Cave, China. Science 294, 2345–2348.
Weijers, J.W.H., Schouten, S., Sluijs, A., Brinkhuis, H., Damste, J.S.S., 2007. Warm arctic continents during the Palaeocene-Eocene thermal maximum. Earth and Planetary Science Letters 261 (1–2), 230–238.
Werner, M., Mikolajewicz, U., Heimann, M., Hoffmann, G., 2000. Borehole versus isotope temperatures on Greenland – Seasonality does matter. Geophysical Research Letters 27, 723–726.
White, J.M., Ager, T.A., Adam, D.P., Leopold, E.B., Liu, G., Jetté, H., Schweger, C.E., 1997. An 18-million-year record of vegetation and climate change in northwestern Canada and Alaska: tectonic and global climatic correlates. Palaeogeography, Paleoclimatology, Palaeoecology 130, 293–306.
White, J.W.C., Alley, R.B., Brigham-Grette, J., Fitzpatrick, J.J., Jennings, A., Johnsen, S., Miller, G.H., Nerem, S., Polyak, L., 2010. Past Rates of climate change in the Arctic. Quaternary Science Reviews 29, 1716–1727.
Whitlock, C., Dawson, M.R., 1990. Pollen and vertebrates of the early Neogene Haughton Formation, Devon Island, Arctic Canada. Arctic 43 (4), 324–330.
Wiles, G.C., Barclay, D.J., Calkin, P.E., Lowell, T.V., 2008. Century to millennial-scale temperature variations for the last two thousand years indicated from glacial geologic records of Southern Alaska. Global and Planetary Change 60, 15–125.
Willerslev, E., Cappellini, E., Boomsma, W., Nielsen, R., Hebsgaard, M.B., Brand, T.B., Hofreiter, M., Bunce, M., Poinar, H.N., Dahl-Jensen, D., Johnsen, S., Steffensen, J.P., Bennike, O., Schwenninger, J.L., Nathan, R., Armitage, S., de Hoog, C.J.,

Alfimov, V., Christi, M., Beer, J., Muscheler, R., Barker, J., Sharp, M., Penkman, K.E. H., Haile, J., Taberlet, P., Bilbert, M.T.P., Casoli, A., Campani, E., Collins, M.J., 2007. Ancient biomolecules from deep ice cores reveal a forested Southern Greenland. Science 317, 111–114.

Williams, C.J., Johnson, A.H., LePage, B.A., Vann, D.R., Sweda, T., 2003. Reconstruction of tertiary metasequoia forests II. Structure, biomass and productivity of Eocene floodplain forests in the Canadian Arctic. Paleobiology 29 (2), 271–292.

Wohlfarth, B., Lemdahl, G., Olsson, S., Persson, T., Snowball, I., Ising, J., Jones, V., 1995. Early Holocene environment on Bjornoya (Svalbard) inferred from multidisciplinary lake sediment studies. Polar Research 14, 253–275.

Wohlfahrt, J., Harrison, S.P., Braconnot, P., 2004. Synergistic feedbacks between ocean and vegetation on mid- and high-latitude climates during the Holocene. Climate Dynamics 22, 223–238.

Wolfe, B.B., Edwards, T.W.D., Aravena, R., MacDonald, G., 1996. Rapid Holocene hydrologic change along boreal tree-line revealed by $\delta^{13}C$ and $\delta^{18}O$ in organic lake sediments, Northwest Territories, Canada. Journal of Paleolimnology 15, 171–181.

Wolfe, B.B., Edwards, T.W.D., Aravena, R., Forman, S.L., Warner, B.G., Velichko, A.A., MacDonald, G., 2000. Holocene paleohydrology and paleoclimate at treeline, north-central Russia, inferred from oxygen isotope records in lake sediment cellulose. Quaternary Research 53, 319–329.

Wolfe, J.A., 1997. Relations of environmental change to angiosperm evolution during the Late Cretaceous and Tertiary. In: Iwatsuki, K., Raven, P.H. (Eds.), Evolution and Diversification of Land Plants. Springer-Verlag, Tokyo, pp. 269–290.

Wuchter, C., Schouten, S., Coolen, M.J.L., Damsté, J.S.S., 2004. Temperature-dependent variation in the distribution of tetraether membrane lipids of marine Crenarchaeota – implications for TEX86 paleothermometry. Paleoceanography 19 (4), PA4028.

Wuchter, W., Schouten, S., Wakeham, S.G., Sinninghe Damsté, J.S., 2005. Temporal and spatial variation in tetraether membrane lipids of marine *Crenarchaeota* in particulate organic matter: implications for TEX86 paleothermometry. Paleoceanography 20, PA3013.

Zachos, J., Pagani, M., Sloan, L., Thomas, E., Billups, K., 2001. Trends, rhythms, and aberrations in global climate 65 Ma to present. Science 292 (5517), 686–693.

Zachos, J.C., Dickens, G.R., Zeebe, R.E., 2008. An early Cenozoic perspective on greenhouse warming and carbon-cycle dynamics. Nature 451 (7176), 279–283.

Zazula, G.D., Froese, D.G., Schweger, C.E., Mathewes, R.W., Beaudoin, A.B., Telka, A. M., Harington, C.R., Westgate, J.A., 2003. Ice-age steppe vegetation in east Beringia – tiny plant fossils indicate how this frozen region once sustained huge herds of mammals. Nature 423, 603–613.